Emulators and their applications in low-energy nuclear physics

Alberto J. Garcia

PhD defense 2023

The Ohio State University

Summary of major contributions

- **Wave-function-based emulation for nucleon-nucleon scattering in momentum space**
  - ajg, C. Drischler, R. J. Furnstahl, J. A. Melendez, and X. Zhang, Phys. Rev. C **107**, 054001 (2023), arXiv:2301.05093

- **BUQEYE Guide to Projection-Based Emulators in Nuclear Physics**
  - C. Drischler, J. A. Melendez, R. J. Furnstahl, ajg, and X. Zhang, Front. Phys. **10**, 92931 (2023), arXiv:2212.04912

- **Model reduction methods for nuclear emulators**
  - J. A. Melendez, C. Drischler, R. J. Furnstahl, ajg, and X. Zhang, J. Phys. G **49**, 102001 (2022), arXiv:2203.05528

- **Fast & accurate emulation of two-body scattering observables without wave functions**
  - J. A. Melendez, C. Drischler, ajg, R. J. Furnstahl, and X. Zhang, Phys. Lett. B **821**, 136608 (2021), arXiv:2106.15608

- **Efficient emulators for scattering using eigenvector continuation**
  - R. J. Furnstahl, ajg, P. J. Millican, and X. Zhang, Phys. Lett. B **809**, 135719 (2020), arXiv:2007.03635

+ publicly available python codes to reproduce results!

The nuclear landscape

*H. Schatz, J. Phys. G **43**, 064001 (2016)*

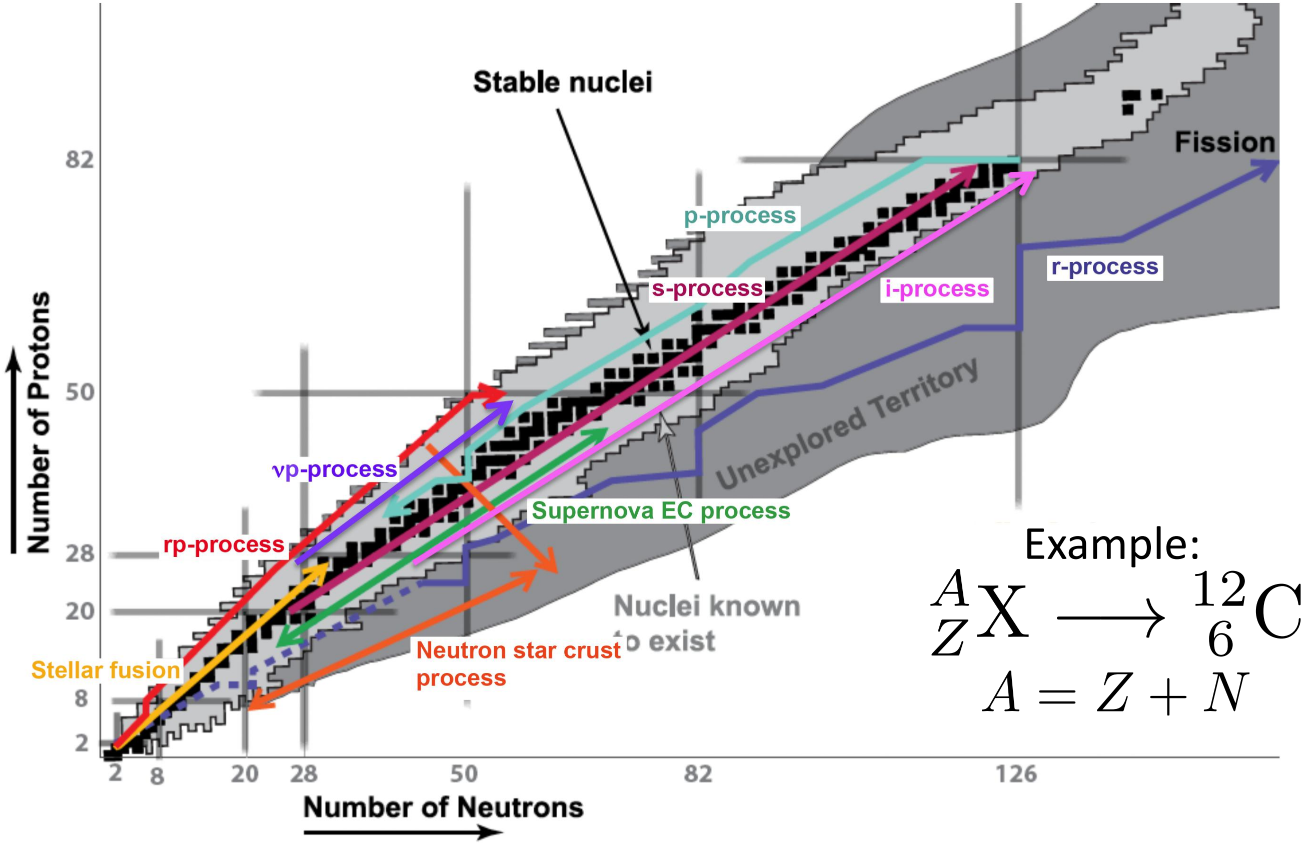

Example:

$$ {}^{A}_{Z}\mathrm{X} \longrightarrow {}^{12}_{6}\mathrm{C} $$

$$ A = Z + N $$

- Schematic overview of the nuclear processes on the nuclear chart
- Nuclei are arranged by proton number Z and neutron number N

- The black squares represent stable nuclei
- The light gray region represent nuclei known to exist
- The dark gray region represent nuclei that are believed to exist but have not been measured experimentally

Four questions provided by the Long Range Plan for Nuclear Science:

1. How did visible matter come into being and how does it evolve?
2. How does subatomic matter organize itself and what phenomena emerge?
3. Are the fundamental interactions that are basic to the structure of matter fully understood?
4. How can the knowledge and technical progress provided by nuclear physics best be used to benefit society?

Degrees of freedom

Nuclear Science Advisory Committee, arXiv:0809.3137 (2007)

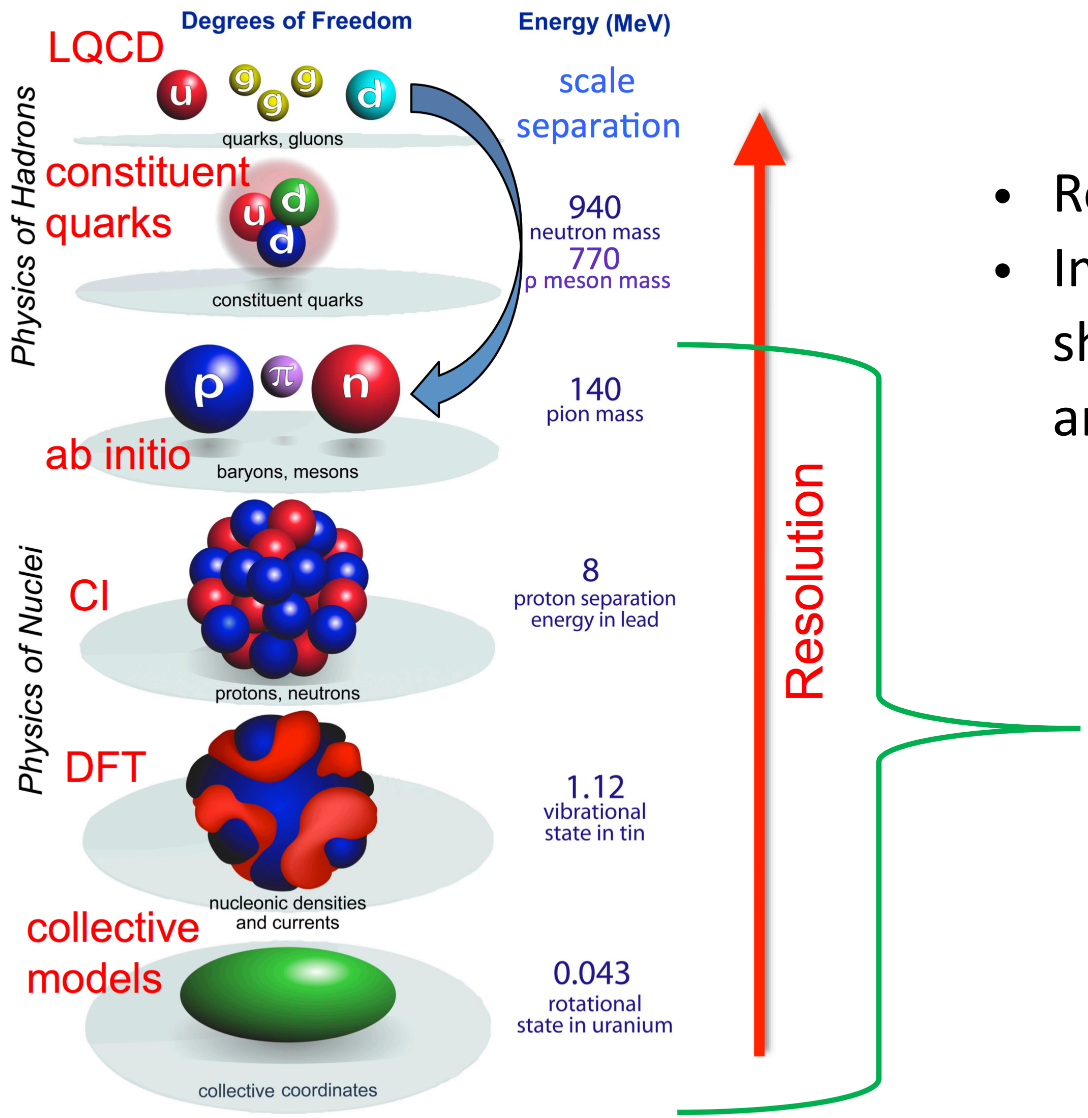

- Resolution scales in nuclear physics.
- Images of the different degrees of freedom are shown while their corresponding energy scales are given in purple on the right.

Focus of low-energy nuclear physics!

Effective field theory (EFT)

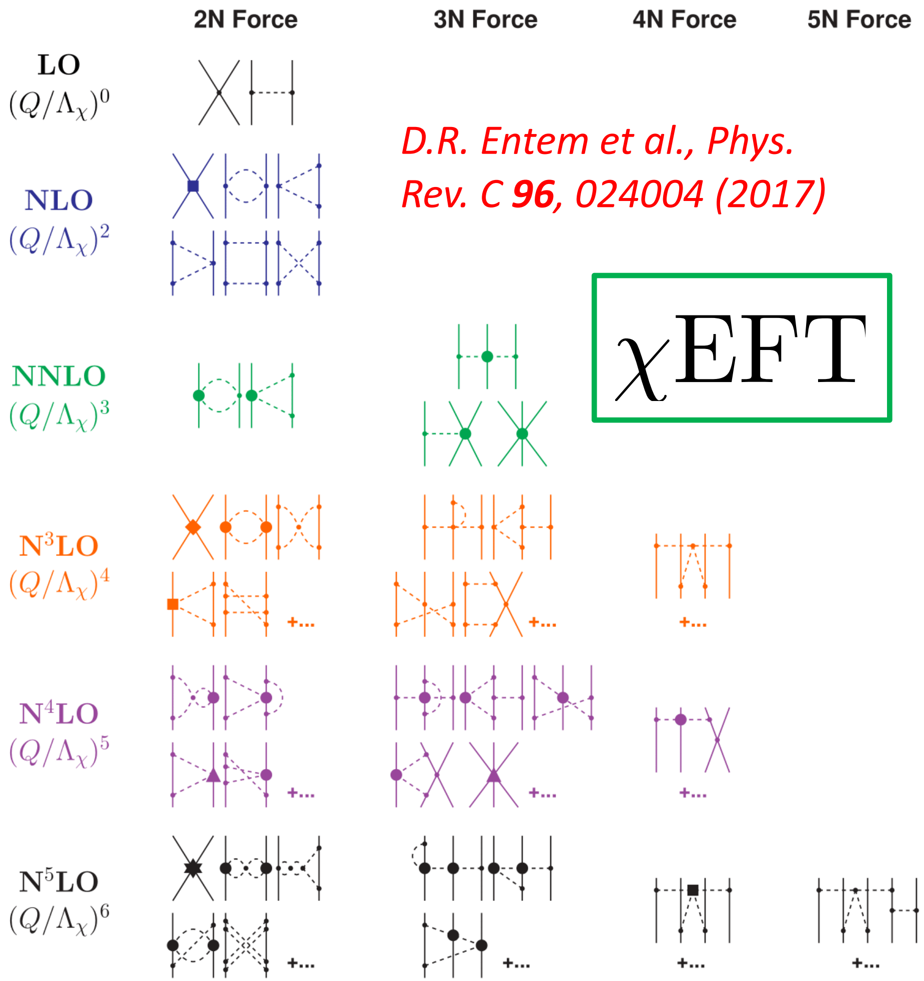

D.R. Entem et al., Phys. Rev. C ***96****, 024004 (2017)*

χEFT

J. Holt, Phys. Rept. ***621****, 2-75 (2016)*

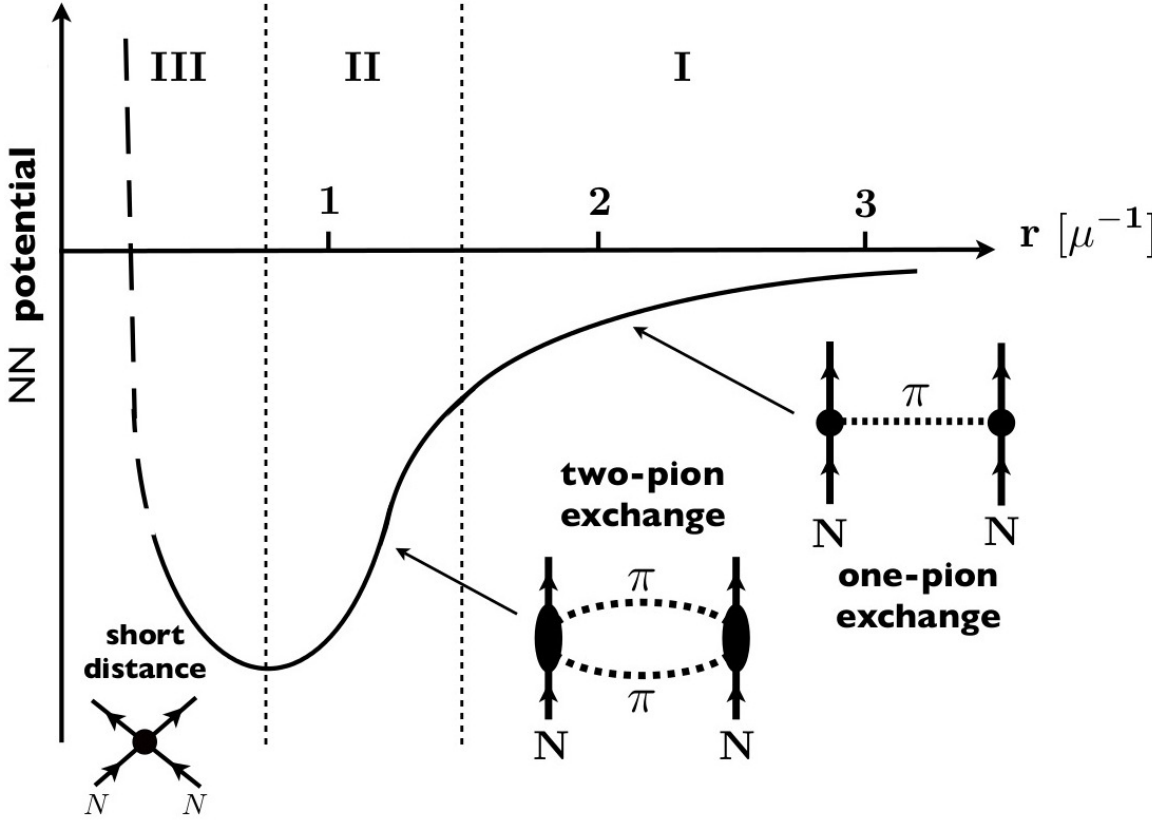

- An overview of the order-by-order nucleon-nucleon (NN) interactions contained in the chiral expansion organized by chiral order and number of interacting nucleons

- Different interactions associated with the nucleon-nucleon (NN) interaction

Effective field theory (EFT)

*J. Holt, Phys. Rept. **621**, 2-75 (2016)*

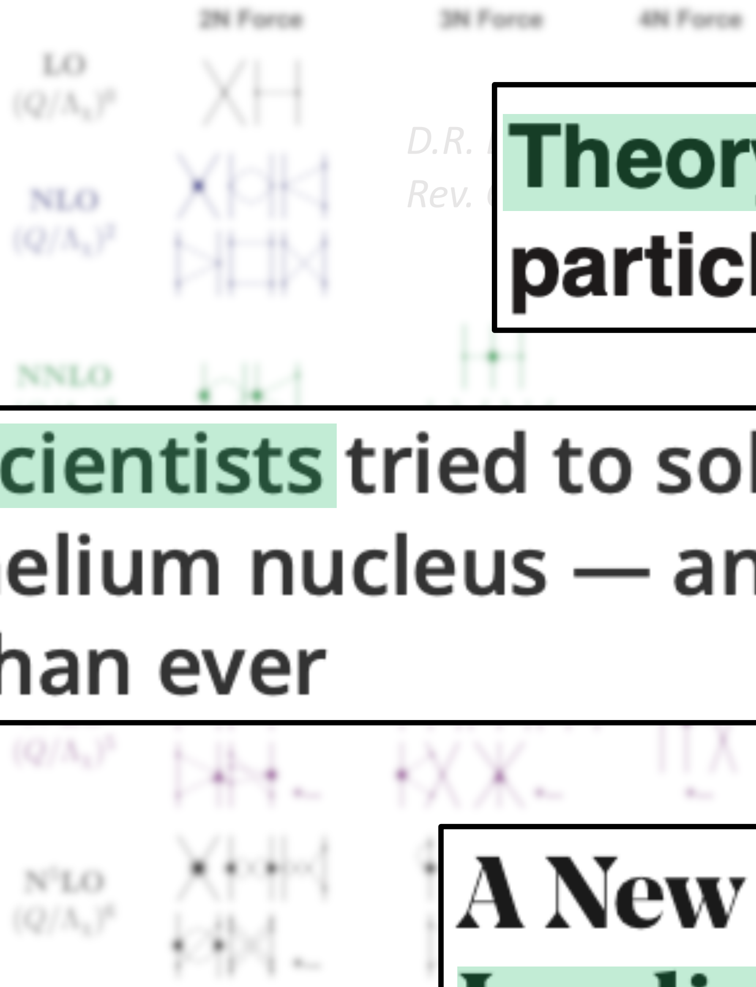

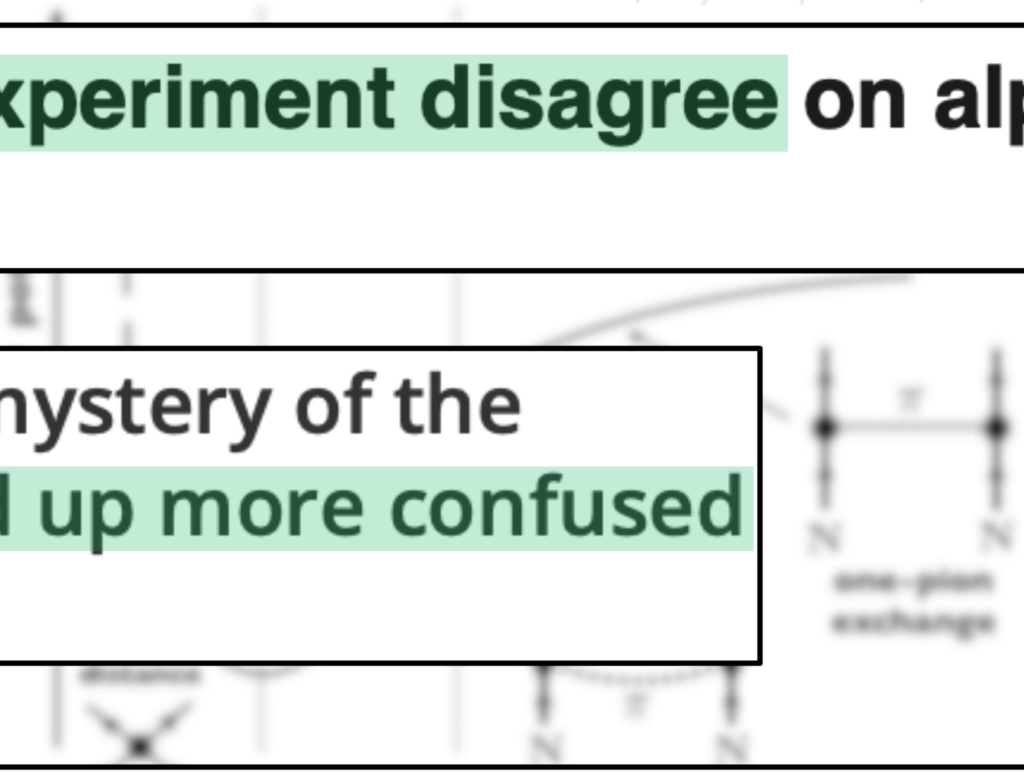

Theory and experiment disagree on alpha particles

Scientists tried to solve the mystery of the helium nucleus — and ended up more confused than ever

A New Experiment Casts Doubt on the Leading Theory of the Nucleus

- An overview of the c… contained in the chiral expansion organized by chiral order and number of interacting nucleons.

Alberto Garcia

Effective field theory (EFT)

J. Holt, Phys. Rept. ***621****, 2-75 (2016)*

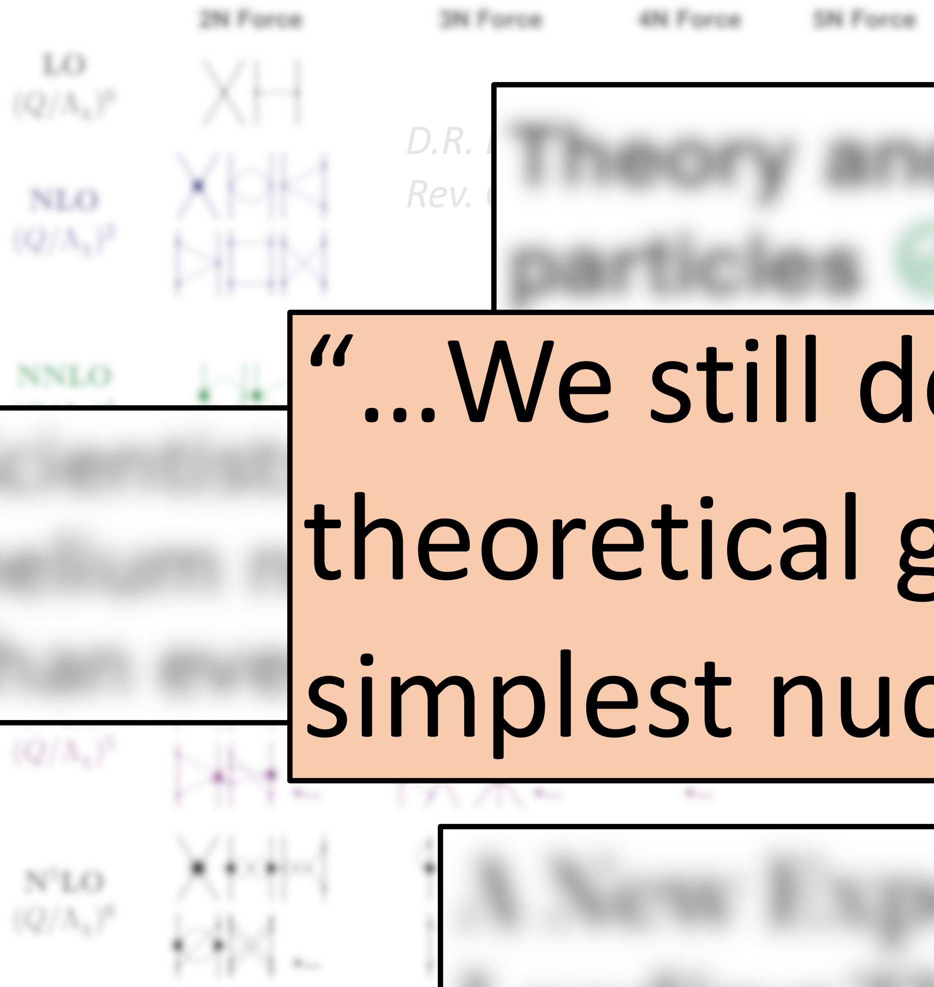

D.R.
Rev.

Theory and experiment disagree on alpha particles

“…We still don’t have a solid theoretical grasp of even the simplest nuclear systems.”

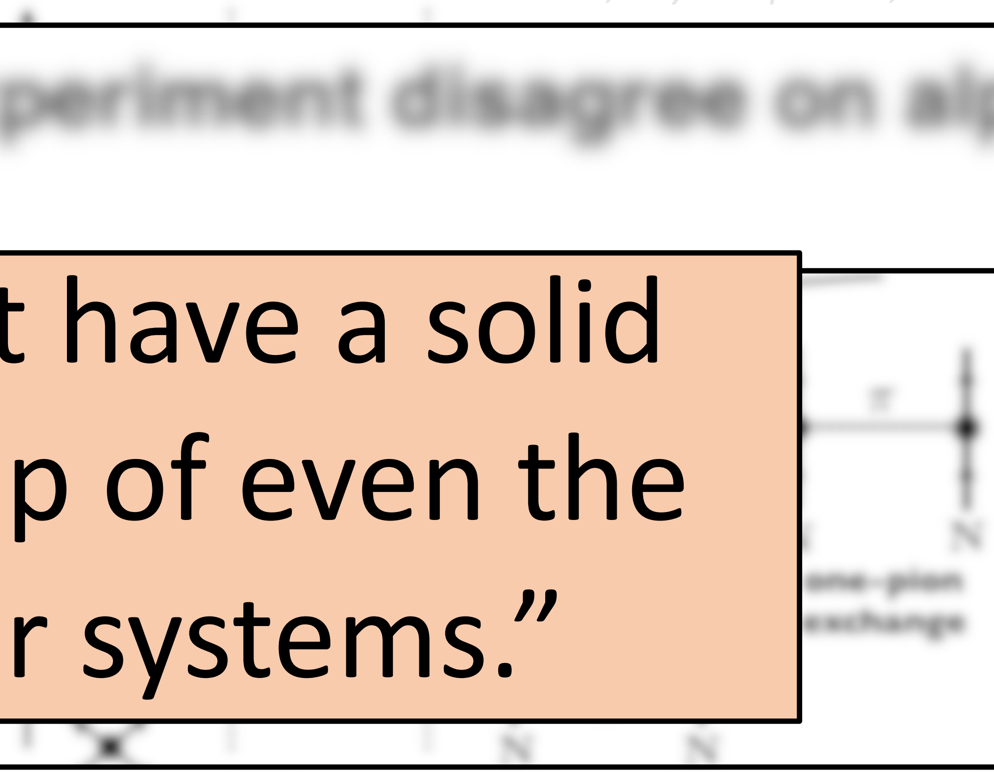

A New Experiment Casts Doubt on the Leading Theory of the Nucleus

- An overview of the c… contained in the chiral expansion organized by chiral order and number of interacting nucleons.

Effective field theory (EFT)

S. Kegel et al., Phys. Rev. Lett. ***130****, 152502 (2023)*

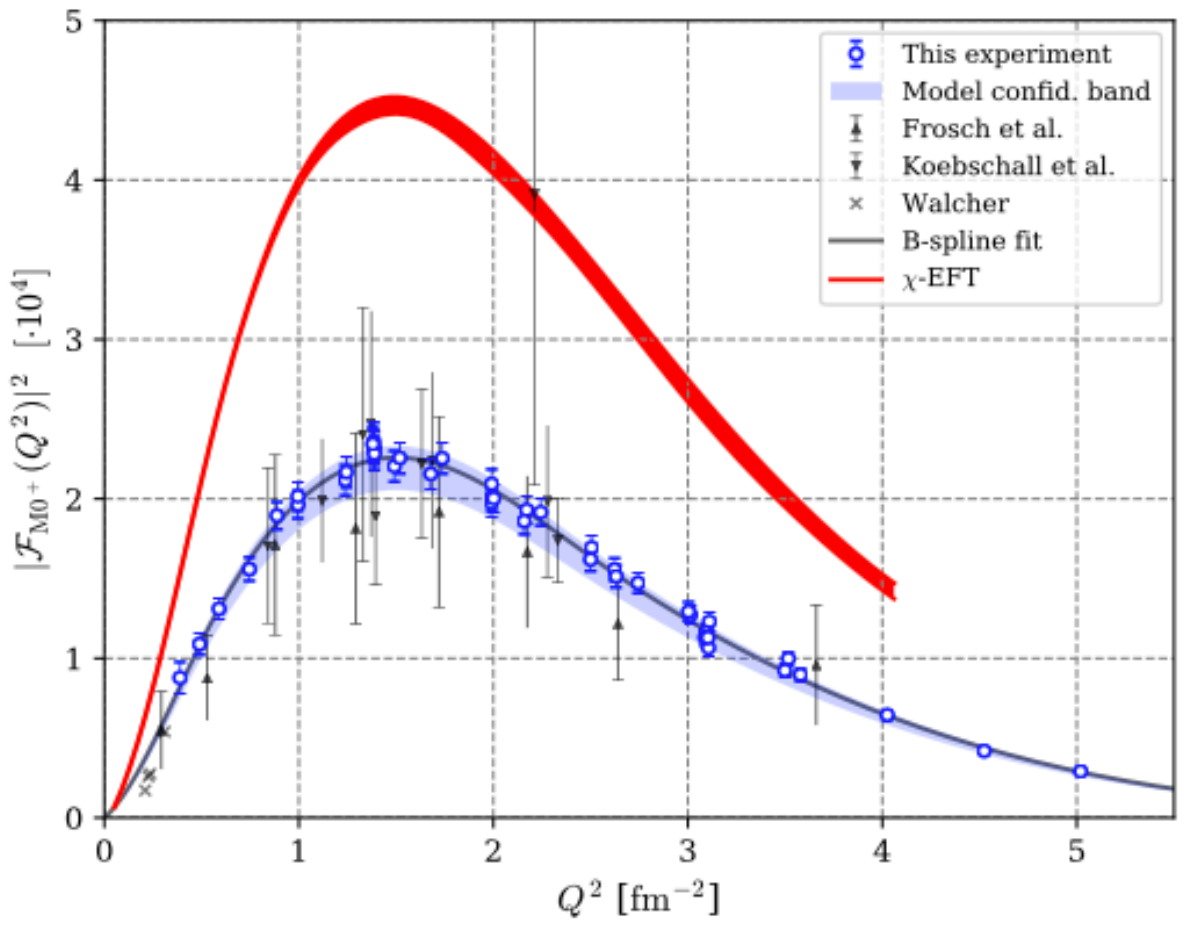

FIG. 3. Monopole transition form factor as a function of Q^2, in comparison to previous data [26–28] and χEFT prediction [12] (see text for details).

Alberto Garcia

Effective field theory (EFT)

N. Michel et al., arXiv:2306.05192 (2023)

...hys. Rept. *621*, 2-75 (2016)

Moral: Theories need error bars!

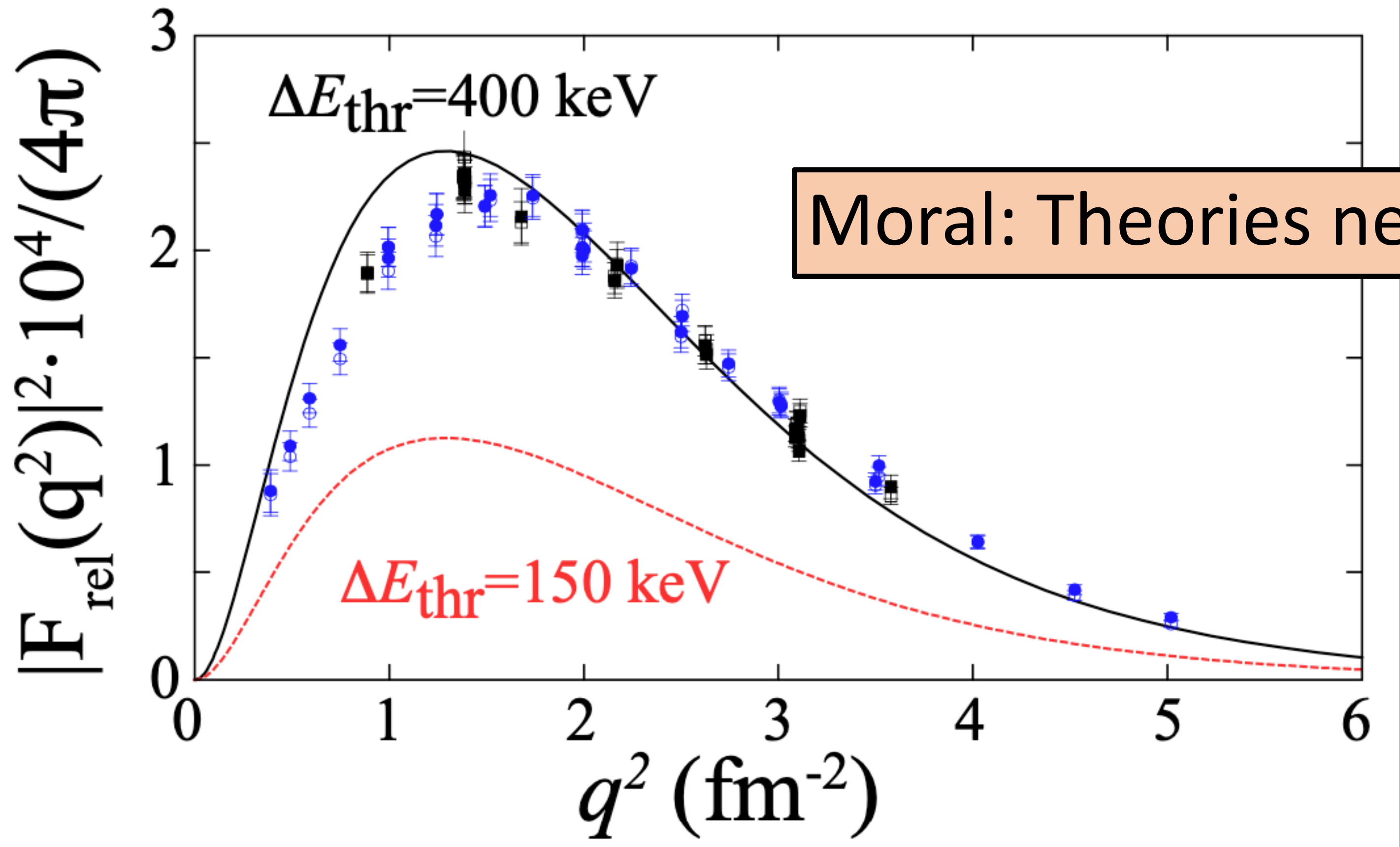

FIG. 2. Monopole transition form factor $|F_{\rm rel}(q^2)|^2$ for the excitation of the ground state 0_1^+ to the excited 0_2^+ state of ^{4}He as a function of q^2 for the two values of $\Delta E_{\rm thr}$. For the experimental data, see Ref. [16].

- An overview of ... contained in th... order and num...

Emulators

S. Wesolowski et al., J. Phys. G **46**, 045102 (2019)

- Full sampling for Bayesian UQ and experimental design can be expensive using direct calculations (high-fidelity system/simulator)
- Must solve high-fidelity system for many sets of parameters
- Inexpensive: sample from a previously trained low-dimensional surrogate model (emulator)

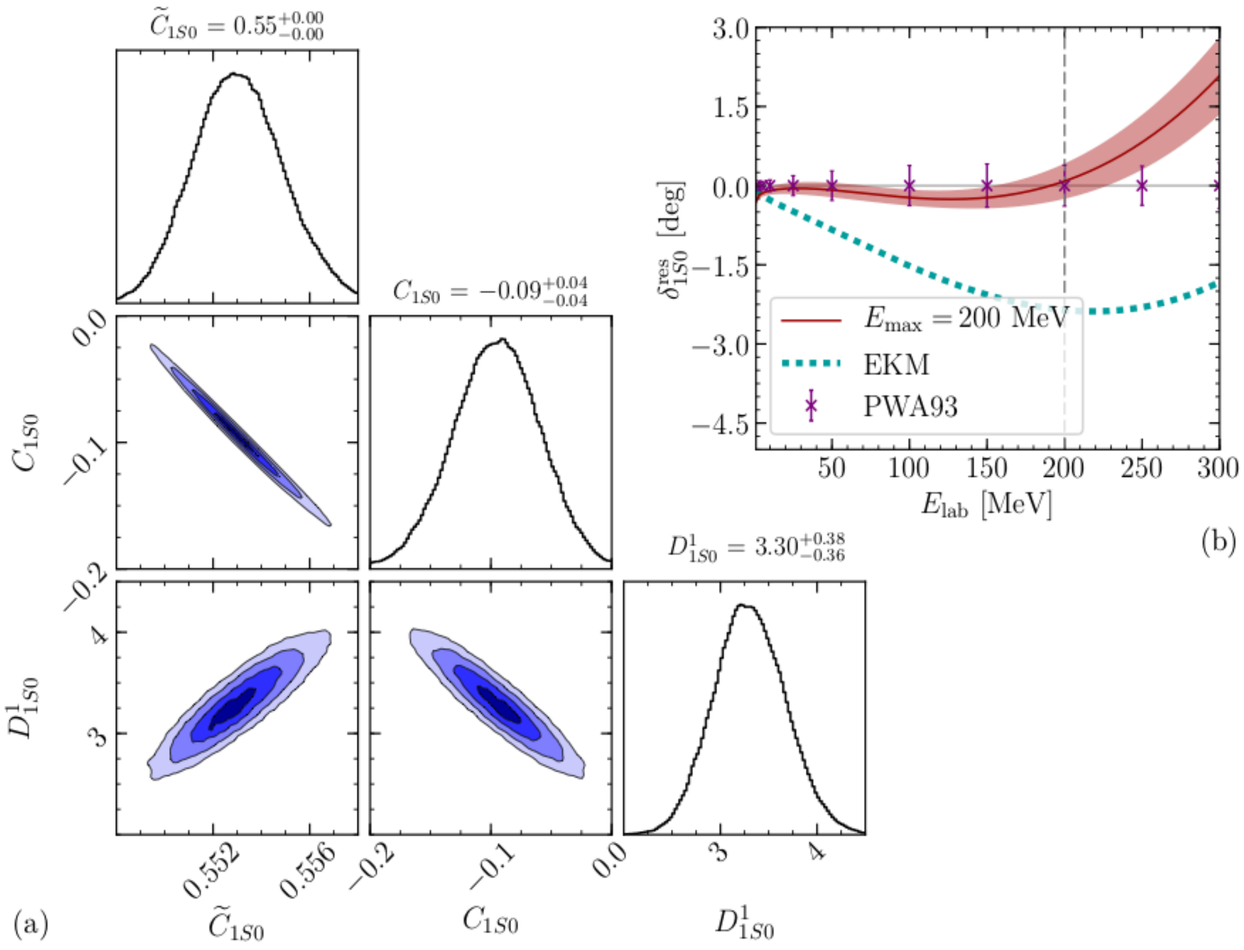

- Full two-dimensional posterior PDF of LECs at N3LO for the semilocal EKM (Epelbaum-Krebs- Meißner) potential in the 1S0 channel

Projection-based emulation

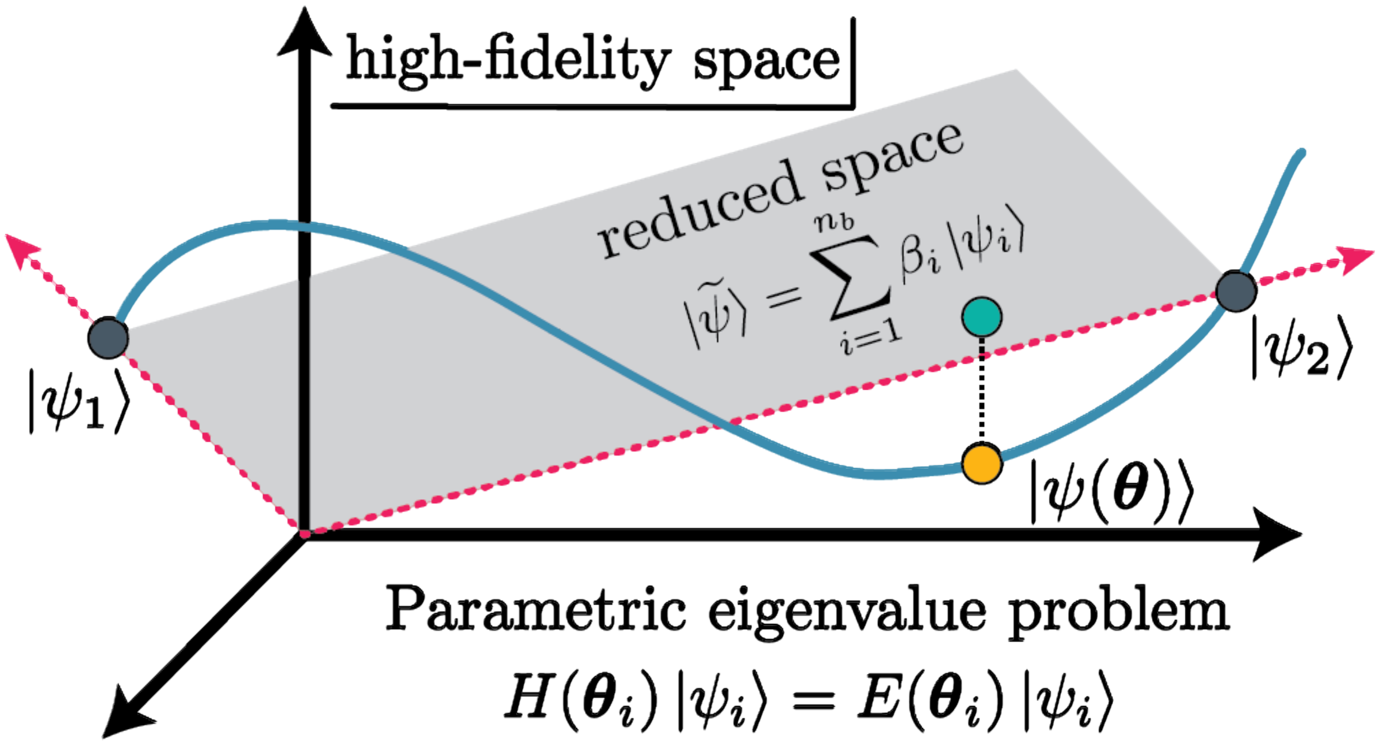

- Subspace projection for projection-based emulation

C. Drischler, ajg et al., Front. Phys. ***10*** *92931 (2023)*

- Blue curve represents high-fidelity trajectory, and the orange dot represents the high-fidelity solution
- Two high-fidelity snapshots
- Gray area represents subspace
- Turquoise dot represents emulator prediction with the residual between emulator and high-fidelity solution given by the dotted line
- Also known as Reduced basis method (RBM)

Constructing a reduced-order model (ROM)

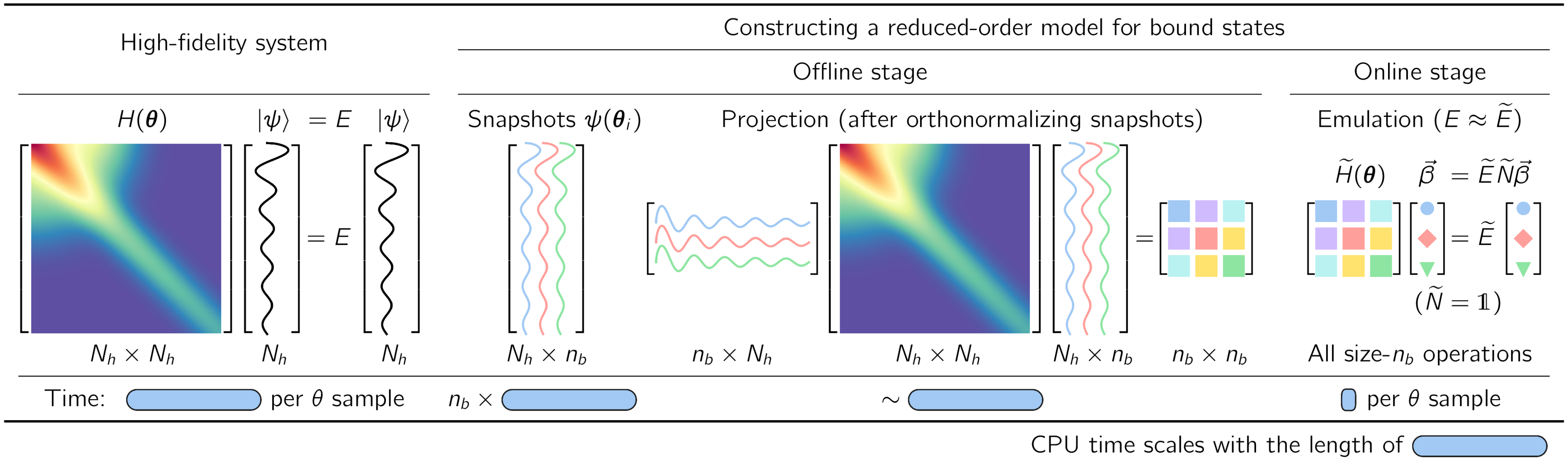

- Offline stage (pre-calculate):
  - Parameter set is chosen (using a greedy algorithm, Latin-hypercube sampling, etc.)
  - Construct basis using snapshots from high-fidelity system (simulator)
  - Project high-fidelity system to small-space using snapshots
- Online stage:
  - Make many predictions fast & accurately
  - Take advantage of affine dependence → $V(\boldsymbol{\theta}) = V^0 + \boldsymbol{\theta} \cdot \boldsymbol{V}^1$

C. Drischler, ajg et al., Front. Phys. ***10*** *92931 (2023)*

Alberto Garcia

Eigen-emulators

Schrödinger equation:

$$H(\boldsymbol{\theta})|\psi(\boldsymbol{\theta})\rangle = E(\boldsymbol{\theta})|\psi(\boldsymbol{\theta})\rangle$$

→ Training set:

$$\{(\boldsymbol{\theta})_i\}$$

C. Drischler, ajg, et al., Front. Phys. **10** 92931 (2023)

J.A. Melendez, ajg, et al., J. Phys. G **49**, 102001 (2022)

Variational approach (Rayleigh-Ritz):

$$\mathcal{E}[\widetilde{\psi}] = \langle\widetilde{\psi}|H(\boldsymbol{\theta})|\widetilde{\psi}\rangle - \widetilde{E}(\boldsymbol{\theta})(\langle\widetilde{\psi}|\widetilde{\psi}\rangle - 1)$$

Can also use Galerkin formalism!

Implementation:

$$|\widetilde{\psi}\rangle = \sum_{i=1}^{n_\mathrm{b}} \beta_i|\psi_i\rangle \equiv X\vec{\beta},$$

Snapshots

Basis weights

$$X = \big[|\psi_1\rangle\ |\psi_2\rangle\ \cdots\ |\psi_{n_\mathrm{b}}\rangle\big],$$

$$\delta\mathcal{E}[\widetilde{\psi}] = 0$$

→ Reduced-order equations:

$$\widetilde{H}(\boldsymbol{\theta})\vec{\beta}_\star(\boldsymbol{\theta}) = \widetilde{E}(\boldsymbol{\theta})\widetilde{N}\vec{\beta}_\star(\boldsymbol{\theta})$$

$$[\widetilde{H}(\boldsymbol{\theta})]_{ij} = \langle\psi_i|H(\boldsymbol{\theta})|\psi_j\rangle,\ [\widetilde{N}]_{ij} = \langle\psi_i|\psi_j\rangle$$

→ Linear algebra in small-space!

Anharmonic oscillator potential

C. Drischler, ajg et al., Front. Phys. ***10*** *92931 (2023)*

$$V(r,\boldsymbol{\theta}) = V_{\mathrm{HO}}(r) + \sum_{n=1}^{3} \boldsymbol{\theta}^{(n)} \exp(-r^2/\sigma_n^2)$$

Non-affine!

Affine!

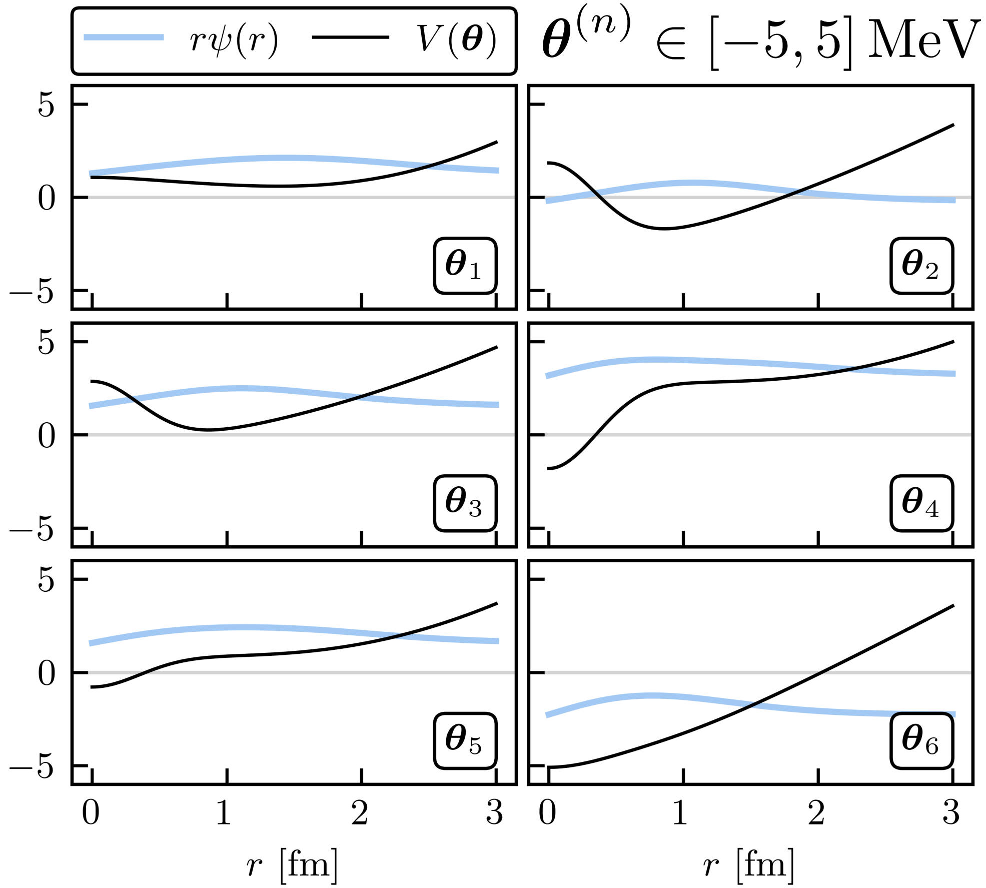

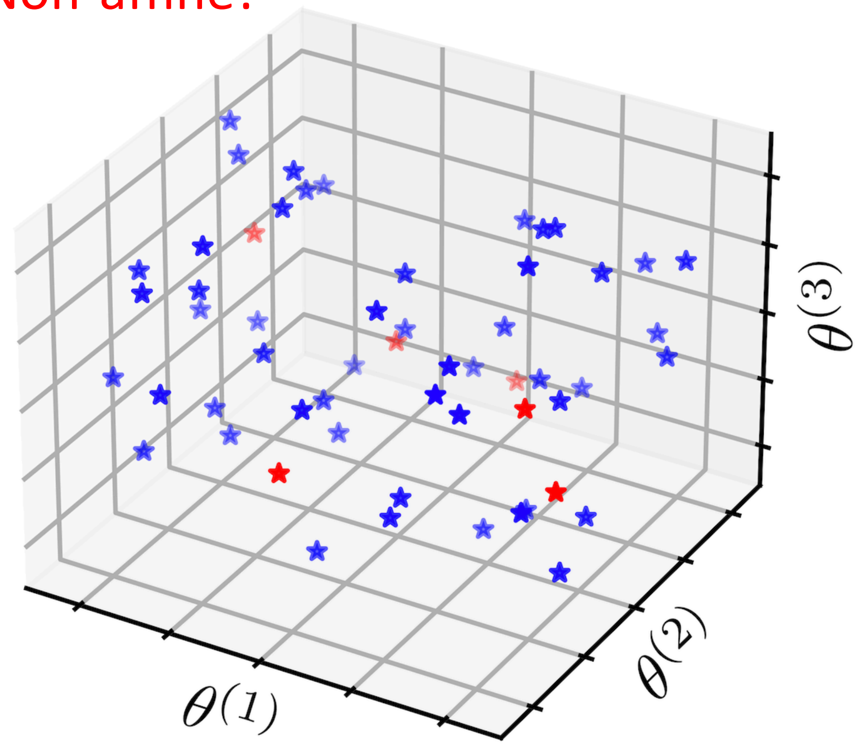

- Solve: a particle with zero angular momentum within a 3D anharmonic oscillator potential
- Compare versus other methods (i.e., harmonic oscillator basis and Gaussian process)

Alberto Garcia

Wave functions

C. Drischler, ajg et al., Front. Phys. ***10*** *92931 (2023)*

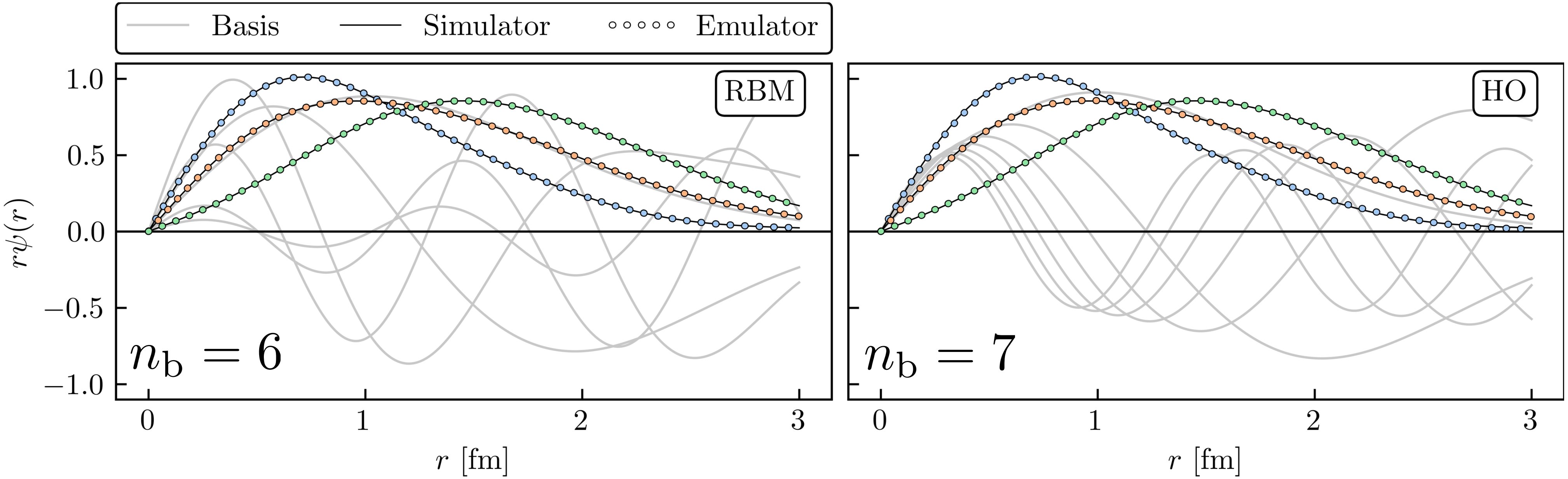

- Emulation of the ground state wave functions
- Basis used to train the emulators given in gray
- Three validation parameter sets denoted by colored dots
- High-fidelity solutions are denoted by the black curves

Wave functions

*C. Drischler, ajg et al., Front. Phys. **10** 92931 (2023)*

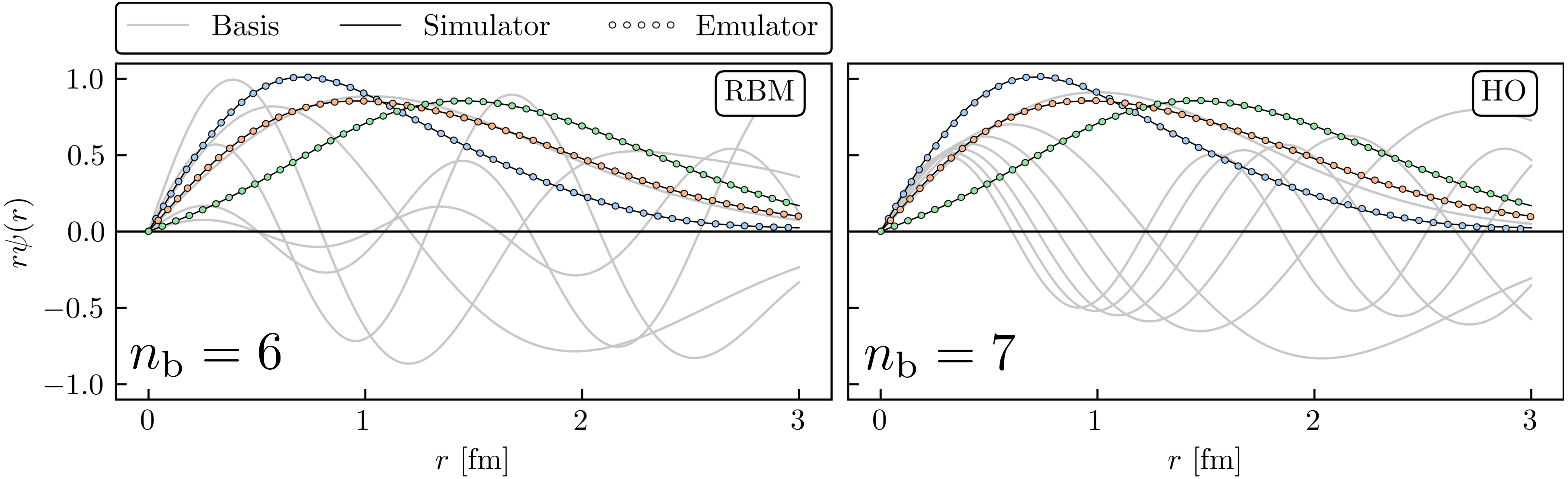

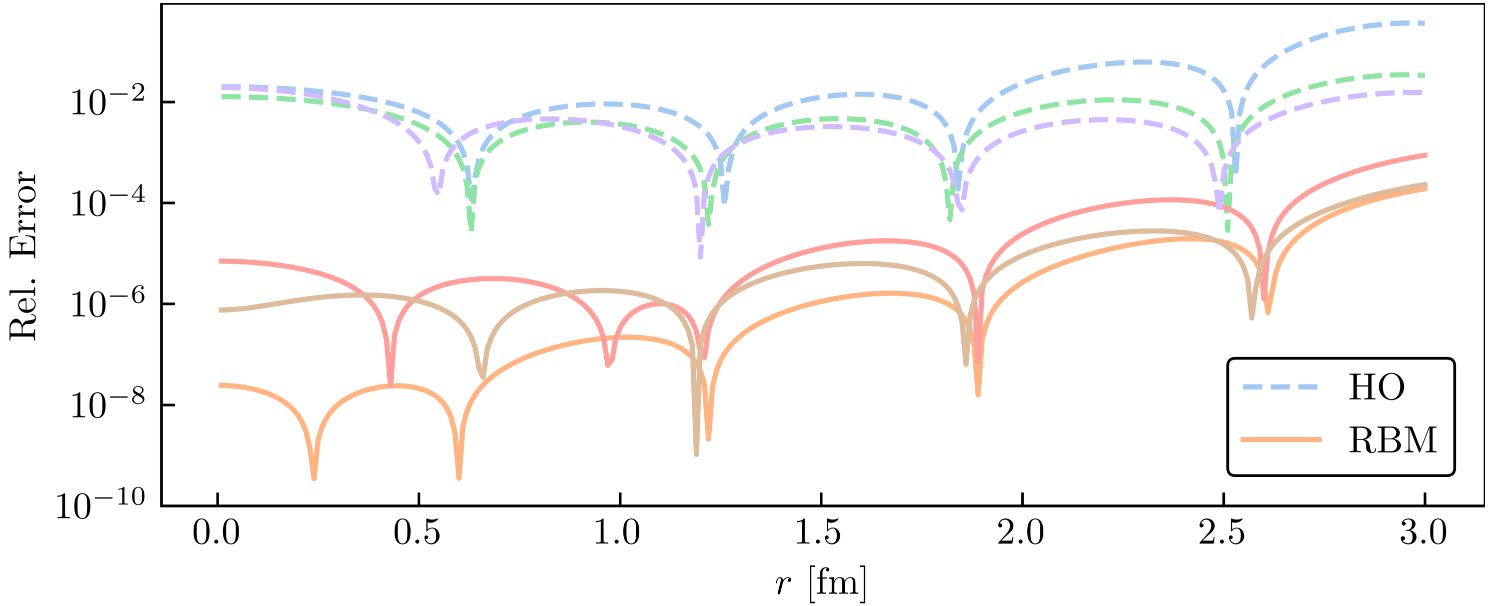

Alberto Garcia

Observables

C. Drischler, ajg et al., *Front. Phys.* **10** 92931 (2023)

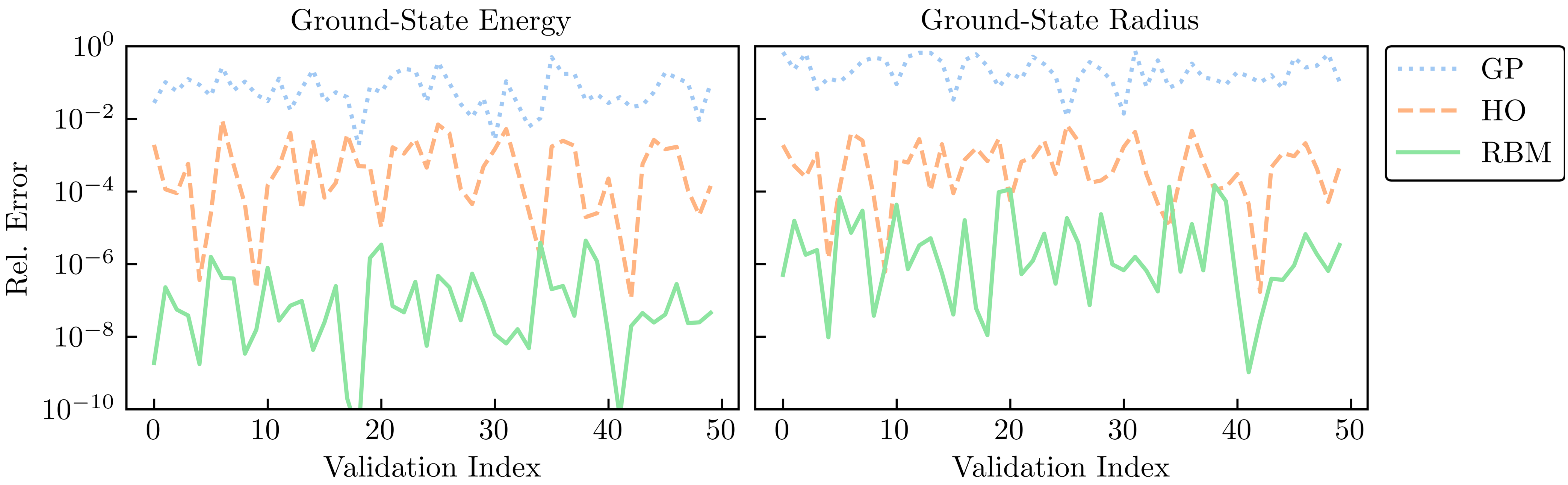

- Emulate observables

$$\langle\psi(\boldsymbol{\theta})|O(\boldsymbol{\theta})|\psi(\boldsymbol{\theta})\rangle \approx \vec{\beta}_\star^\dagger \widetilde{O} \vec{\beta}_\star$$

- Plotted for each validation parameter set
- Calculated three different way:
  - Reduced basis method (RBM) emulator
  - Harmonic oscillator (HO) basis
  - Gaussian process (GP)

Alberto Garcia

Scattering RBM example

*R.J. Furnstahl, ajg et al., Phys. Lett. B **809**, 135719 (2020)*

- Minnesota potential: approximation of nuclear interaction between neutron and proton
- Proof-of-principle for the application of RBM for scattering problems

$$V_{^1S_0}(r) = V_{0R} e^{-\kappa_R r^2} + V_{0s} e^{-\kappa_s r^2} \quad \text{with} \quad \kappa_R = 1.487\,\text{fm}^{-2}, \kappa_s = 0.465\,\text{fm}^{-2}$$

Affine!

$$\boldsymbol{\theta} = \{V_{0R}, V_{0s}\} \xrightarrow{\text{"physical"}} \{200\,\text{MeV}, -178\,\text{MeV}\}$$

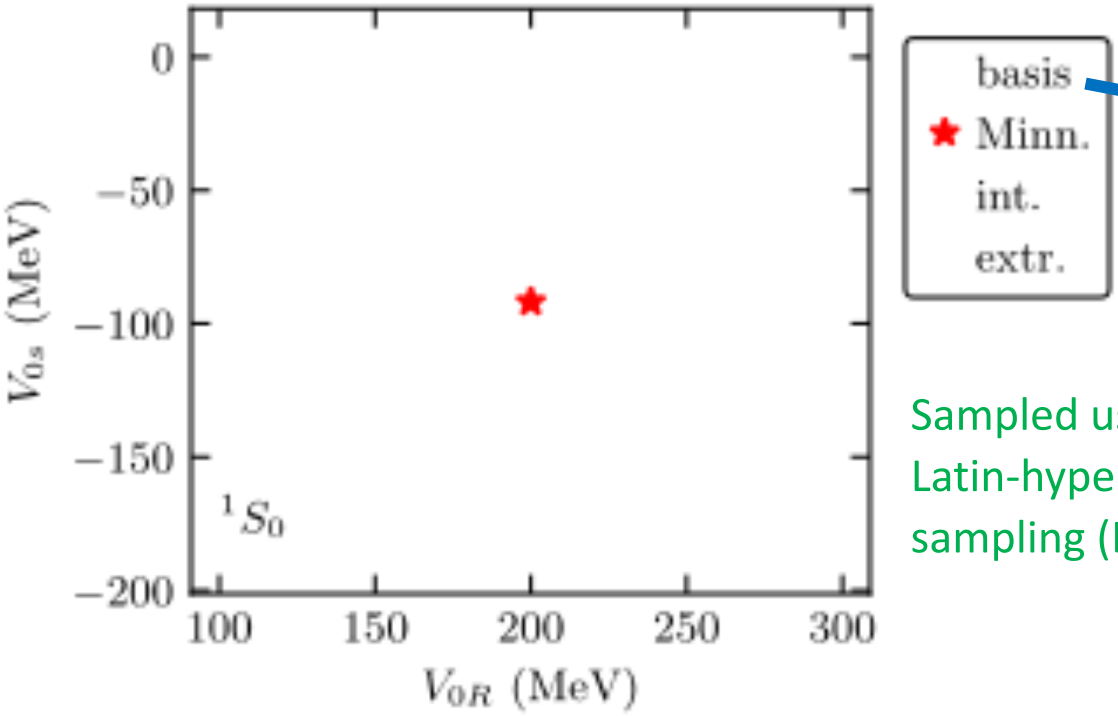

Sampled using Latin-hypercube sampling (LHS)

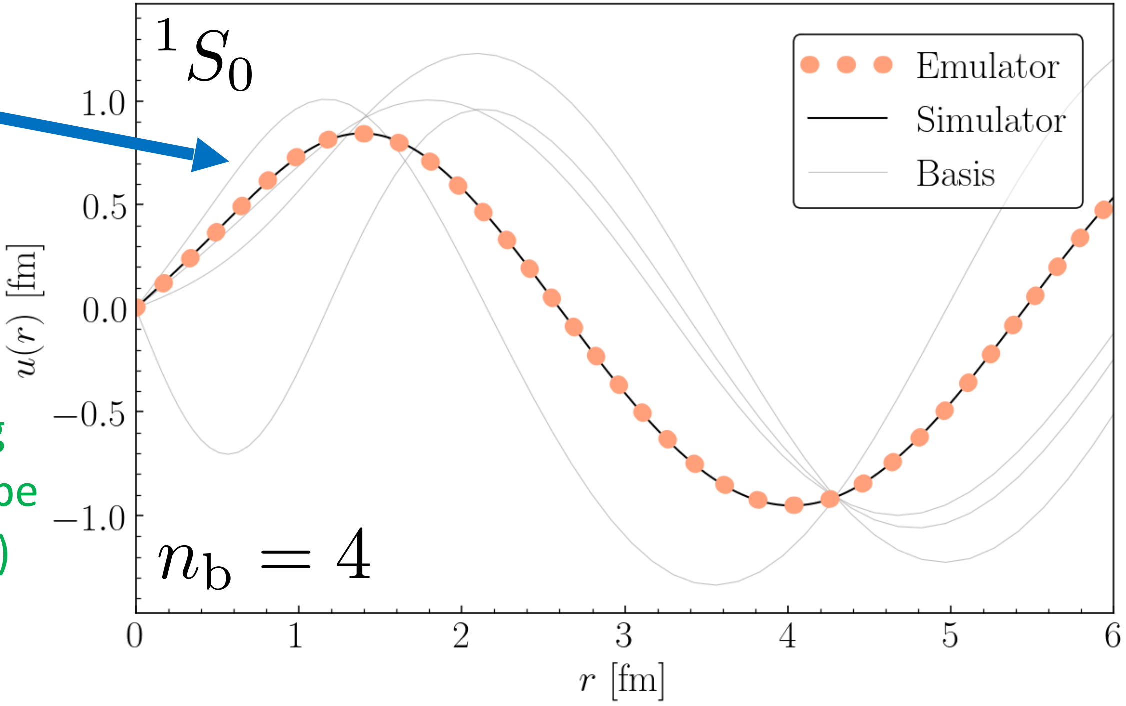

Alberto Garcia

Scattering RBM example

R.J. Furnstahl, ajg et al., Phys. Lett. B **809**, 135719 (2020)

- Minnesota potential: approximation of nuclear interaction between neutron and proton
- Proof-of-principle for the application of RBM for scattering problems

$$V_{^1S_0}(r) = V_{0R}e^{-\kappa_R r^2} + V_{0s}e^{-\kappa_s r^2} \quad \text{with} \quad \kappa_R = 1.487\,\text{fm}^{-2}, \kappa_s = 0.465\,\text{fm}^{-2}$$

Affine!

$$\boldsymbol{\theta} = \{V_{0R}, V_{0s}\} \xrightarrow{\text{“physical”}} \{200\,\text{MeV}, -178\,\text{MeV}\}$$

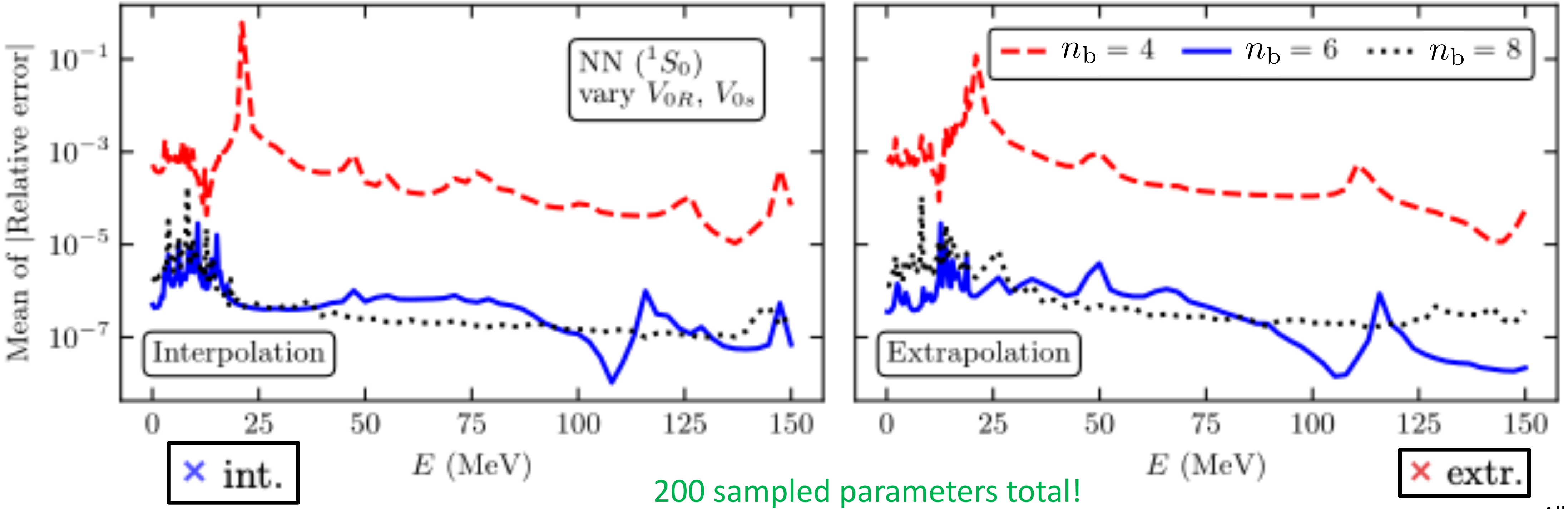

200 sampled parameters total!

Alberto Garcia

Total cross section emulation

*ajg et al., Phys. Rev. C **107**, 054001 (2023)*

- Partial waves up to $j = 20$
- Number of parameters → 25
- Used LHS to sample 500 parameter sets in an interval of [-5, 5]

- Errors negligible compared to other uncertainties
- Speed is highly implementation-dependent!
- Consistent for $\Lambda = 400 - 550\,\mathrm{MeV}$

- Kohn anomalies mitigated!

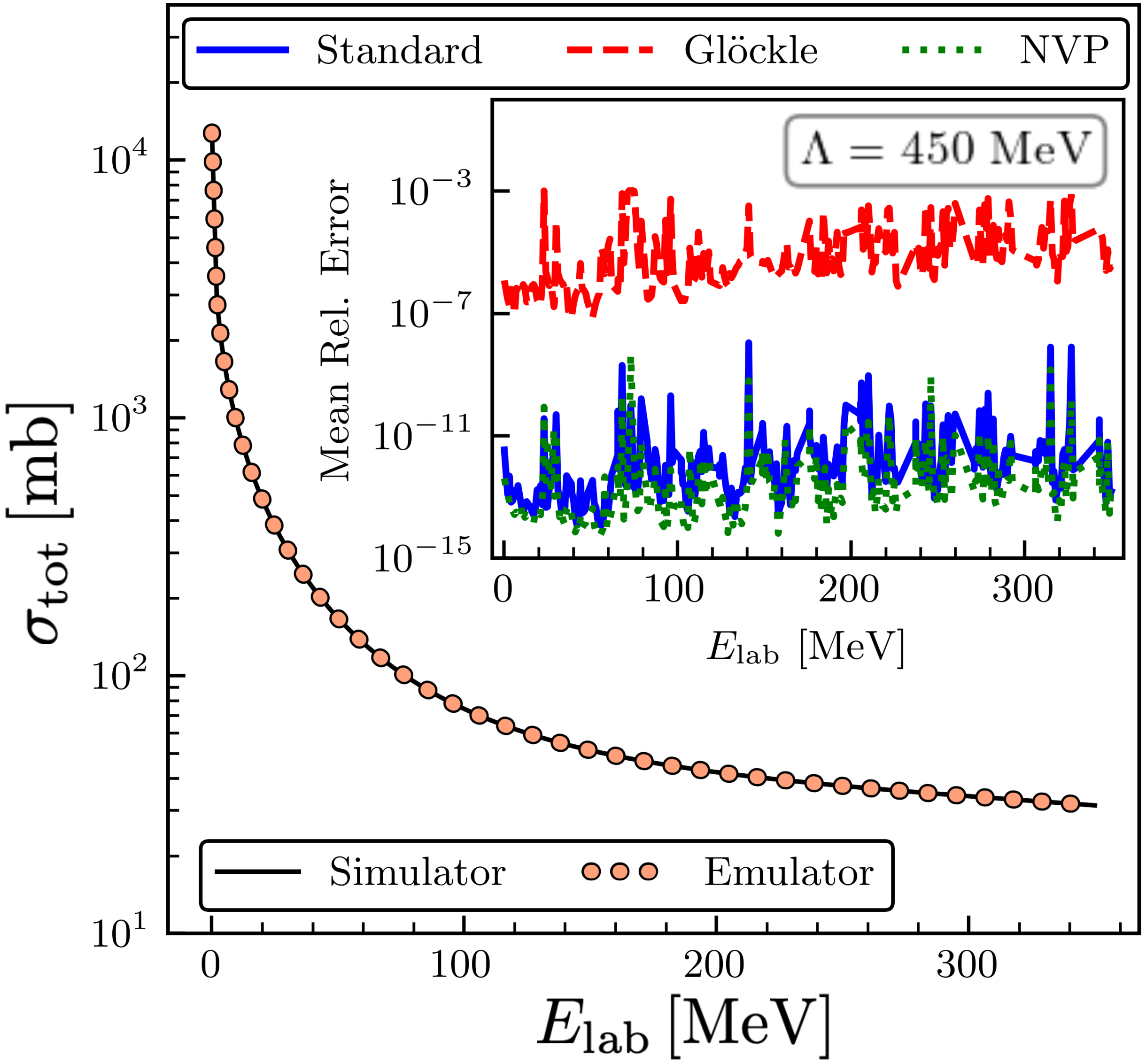

Emulation of other observables

ajg et al., Phys. Rev. C ***107**, 054001 (2023)*

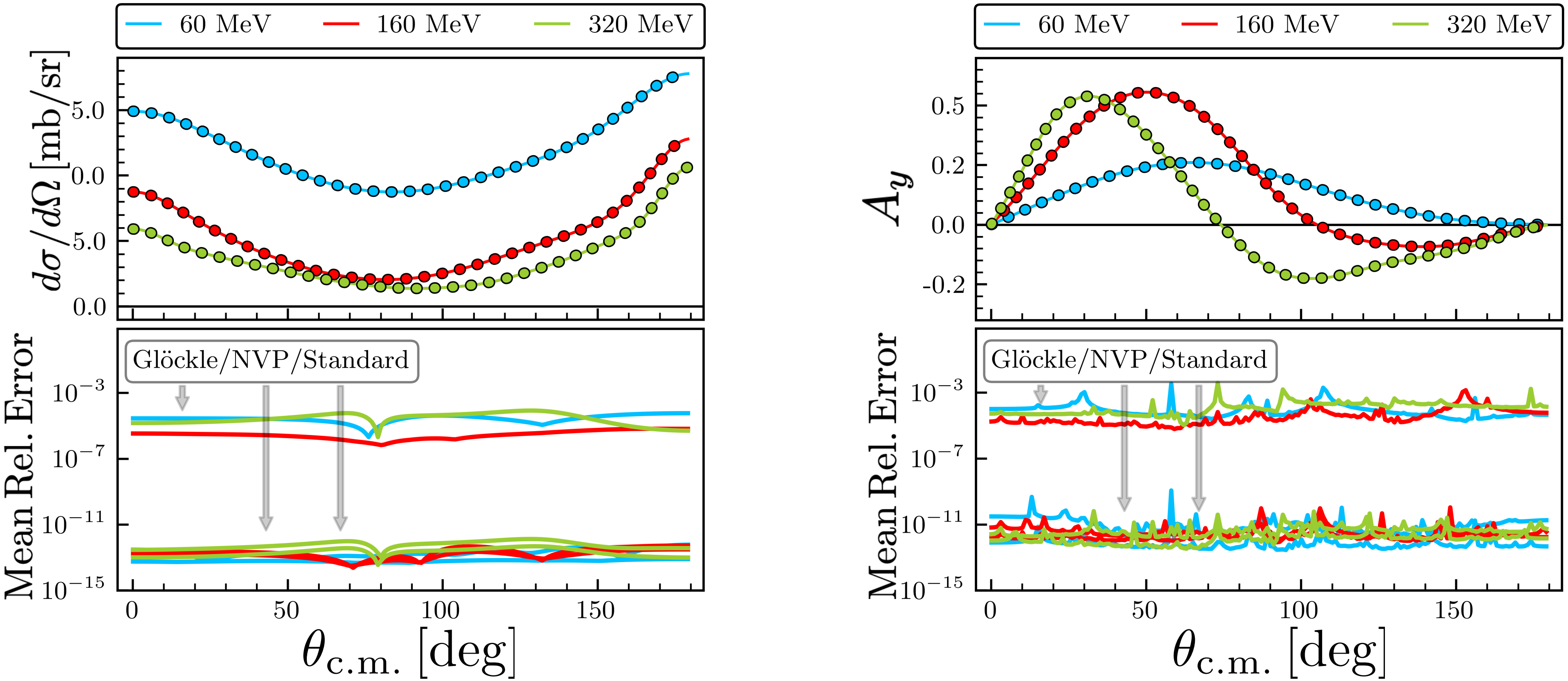

- Differential cross section: probability of observing a scattered particle in a specific quantum state per solid angle
- Analyzing power: changes in polarization of the beam or target nuclei

Different methods to construct emulators

	Variational Principle		Galerkin Projection Information			
	Name	Functional for K	Strong Form	Trial Basis	Test Basis	Constrained?
(KVP)	Kohn (λ)	$\widetilde{K}_E + \langle\widetilde{\psi}\|H - E\|\widetilde{\psi}\rangle$	$H\,\|\psi\rangle = E\,\|\psi\rangle$	$\|\psi_i\rangle$	$\langle\psi_i\|$	Yes
(KVP)	Kohn (No λ)	$\langle\widetilde{\chi}\|H - E\|\widetilde{\chi}\rangle + \langle\phi\|V\|\widetilde{\chi}\rangle$ $+ \langle\phi\|H - E\|\phi\rangle + \langle\widetilde{\chi}\|V\|\phi\rangle$	$[E - H]\,\|\chi\rangle = V\,\|\phi\rangle$	$\|\chi_i\rangle$	$\langle\chi_i\|$	No
(SVP)	Schwinger	$\langle\widetilde{\psi}\|V\|\phi\rangle + \langle\phi\|V\|\widetilde{\psi}\rangle$ $- \langle\widetilde{\psi}\|V - VG_0V\|\widetilde{\psi}\rangle$	$\|\psi\rangle = \|\phi\rangle + G_0V\,\|\psi\rangle$	$\|\psi_i\rangle$	$\langle\psi_i\|$	No
(NVP)	Newton	$V + VG_0\widetilde{K} + \widetilde{K}G_0V$ $-\widetilde{K}G_0\widetilde{K} + \widetilde{K}G_0VG_0\widetilde{K}$	$K = V + VG_0K$	K_i	K_i	No

- Two-body scattering emulators can be constructed using different formulations
  - Variational methods
  - Coordinate space and momentum space
- All variational methods have Galerkin counterparts

C. Drischler, ajg, et al., Front. Phys. ***10*** *92931 (2023)*

Alberto Garcia

Reduced-order model (ROM) for scattering w/ KVP

Hamiltonian:

$$\widehat{H}(\boldsymbol{\theta}) = \widehat{T} + \widehat{V}(\boldsymbol{\theta})$$

Training set:

$$\{(\boldsymbol{\theta})_i\}$$

K-matrix formulation:

$$K_s(E) = \tan\delta_s(E)$$

$$E = k_0^2/2\mu$$

Generalized Kohn variational principle (KVP):

$$\mathcal{L}^{ss'}[\widetilde{\psi}] = \widetilde{L}^{ss'}(E) - \frac{2\mu k_0}{\det \boldsymbol{u}}\langle\widetilde{\psi}^s|\widehat{H}(\boldsymbol{\theta}) - E|\widetilde{\psi}^{s'}\rangle$$

$$\mathcal{L}^{ss'}[\psi + \delta\psi] = L_E^{ss'} + \mathcal{O}(\delta L^2)$$

*R.J. Furnstahl, ajg et al., Phys. Lett. B **809**, 135719 (2020)*
*C. Drischler, ajg et al., Front. Phys. **10** 92931 (2023)*
*ajg et al., Phys. Rev. C **107**, 054001 (2023)*

Implementation:

$$|\widetilde{\psi}^s\rangle \equiv \sum_{i=1}^{n_\mathrm{b}} \beta_i |\psi_i^s\rangle$$

Snapshots

Basis weights

Reduced-order equations:

$$\mathcal{L}^{ss'}[\vec{\beta}] = \beta_i L_{E,i}^{ss'} - \frac{1}{2}\beta_i \Delta\widetilde{U}_{ij}^{ss'}\beta_j$$

$$\Delta\widetilde{U}_{ij}^{ss'}(\boldsymbol{\theta}) = \frac{2\mu k_0}{\det \boldsymbol{u}}\left[\langle\psi_i^s|\widehat{V}(\boldsymbol{\theta}) - \widehat{V}_j|\psi_j^{s'}\rangle + (i \leftrightarrow j)\right]$$

Linear algebra in small-space!

Alberto Garcia

Reduced-order model (ROM) for scattering w/ NVP

LS equation:

$$K(\boldsymbol{\theta}) = V(\boldsymbol{\theta}) + V(\boldsymbol{\theta})G_0(E)K(\boldsymbol{\theta})$$

→ Training set: $\{(\boldsymbol{\theta})_i\}$

K-matrix formulation:

$$K_s(E) = \tan\delta_s(E)$$

$$E = k_0^2/2\mu$$

Newton variational principle (NVP):

$$\mathcal{K}[\widetilde{K}] = V + VG_0\widetilde{K} + \widetilde{K}G_0K - \widetilde{K}G_0\widetilde{K} + \widetilde{K}G_0VG_0\widetilde{K}$$

$$\mathcal{K}[K + \delta K] = K + \mathcal{O}(\delta K^2)$$

Implementation:

$$\widetilde{K}(\vec{\beta}) = \sum_{i=1}^{n_\mathrm{b}} \beta_i K_i$$

Snapshots (K_i); Basis weights (β_i)

Reduced-order equations:

$$\langle\phi'|\mathcal{K}(\boldsymbol{\theta}, \vec{\beta})|\phi\rangle \approx \langle\phi'|V(\boldsymbol{\theta})|\phi\rangle + \frac{1}{2}\vec{m}^T M^{-1}(\boldsymbol{\theta})\vec{m}$$

→ Linear algebra in small-space!

J.A. Melendez, ajg et al., Phys. Lett. B ***821****, 136608 (2021)*

Emulating multiple boundary conditions w/ KVP

- Examples of **u** matrices

$$\boldsymbol{u}_K = \begin{pmatrix} 1 & 0 \\ 0 & 1 \end{pmatrix}, \; \boldsymbol{u}_{K^{-1}} = \begin{pmatrix} 0 & 1 \\ 1 & 0 \end{pmatrix}, \; \boldsymbol{u}_T = \begin{pmatrix} 1 & 0 \\ i & 1 \end{pmatrix}$$

1. Rescale functional quantities

$$\Delta\tilde{U}^{(\boldsymbol{u}')} = C'^{-1}(L_i)C'^{-1}(L_j)\frac{\det \boldsymbol{u}}{\det \boldsymbol{u}'}\Delta\tilde{U}^{(\boldsymbol{u})} \qquad C'(L) = \frac{\det \boldsymbol{u}}{\det \boldsymbol{u}'}\frac{u'_{11} - u'_{10}K(L)}{u_{11} - u_{10}K(L)}$$

$$L'(L) = \frac{-u'_{01} + u'_{00}K(L)}{u'_{11} - u'_{10}K(L)}$$

2. Convert back into K-matrix form

Method from: Drischler et al., Phys. Lett. B ***823***, *136777 (2021)*

Alberto Garcia

Mitigating Kohn anomalies w/ KVP

1. Relative residuals between the emulator predictions of all the KVPs

$$\gamma_{\text{rel}}(L_1, L_2) = \max\left\{\left|\frac{S(L_1)}{S(L_2)} - 1\right|, \left|\frac{S(L_2)}{S(L_1)} - 1\right|\right\}$$

2. Apply relative consistency check

$$\gamma_{\text{rel}} < \epsilon_{\text{rel}} = 10^{-1}$$

3. Estimate S matrix

$$[S]^{(\text{mixed})}_{\text{KVP}} = \sum_{(\text{L}_1,\text{L}_2)\in\mathcal{P}} \omega(L_1, L_2)\frac{S(L_1) + S(L_2)}{2}, \quad \omega(L_1, L_2) = \frac{\gamma_{\text{rel}}(L_1, L_2)^{-1}}{\sum_{(\text{L}'_1,\text{L}'_2)\in\mathcal{P}} \gamma_{\text{rel}}(L'_1, L'_2)^{-1}}$$

Method from: Drischler et al., Phys. Lett. B ***823****, 136777 (2021)*

Anomalies example

- Kohn anomalies mitigated!
- Mesh-induced spikes in high-fidelity LS equation detected and removed

*ajg et al., Phys. Rev. C **107**, 054001 (2023)*

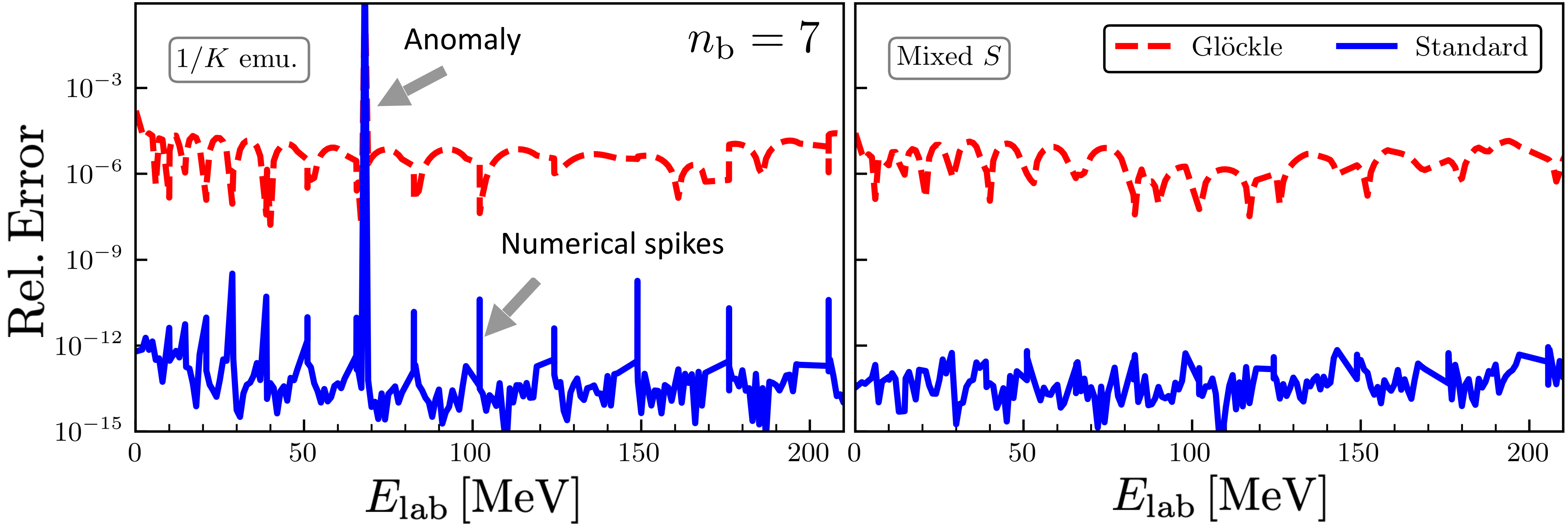

Emulators Summary and Outlook

- Developed and applied first RBM emulator for scattering applications using KVP and coordinate-space wave functions
- Developed first RBM emulator using scattering matrices as the trial basis and applied it to state-of-the-art chiral EFT potential for the prediction of the total cross section
- Extended coordinate space emulator to momentum space, developed the methodology for coupled-channel emulation, and applied it to the prediction of spin observables
- Provided documented code and guides for the nuclear physics community
- Interactions: local, nonlocal, k-space, r-space, complex, Coulomb, chiral EFT

- Application of emulators and Bayesian methods to NN uncertainty quantification (already being used!)
- Apply active-learning for effectively choosing training points
- Hyper-reduction methods for non-affine structures
- Extension of emulators to three-body scattering and emulation across different energies
- Connection between RBM emulators, reaction models, and experiments at new-generation rare-isotope facilities

Neural networks

- Artificial neural networks (ANNs) are used to identify patterns in a dataset
- Composed of input, output, and hidden layer(s)
- Fall under data-driven methods
- Goal: develop ANN emulators for applications to nuclear systems

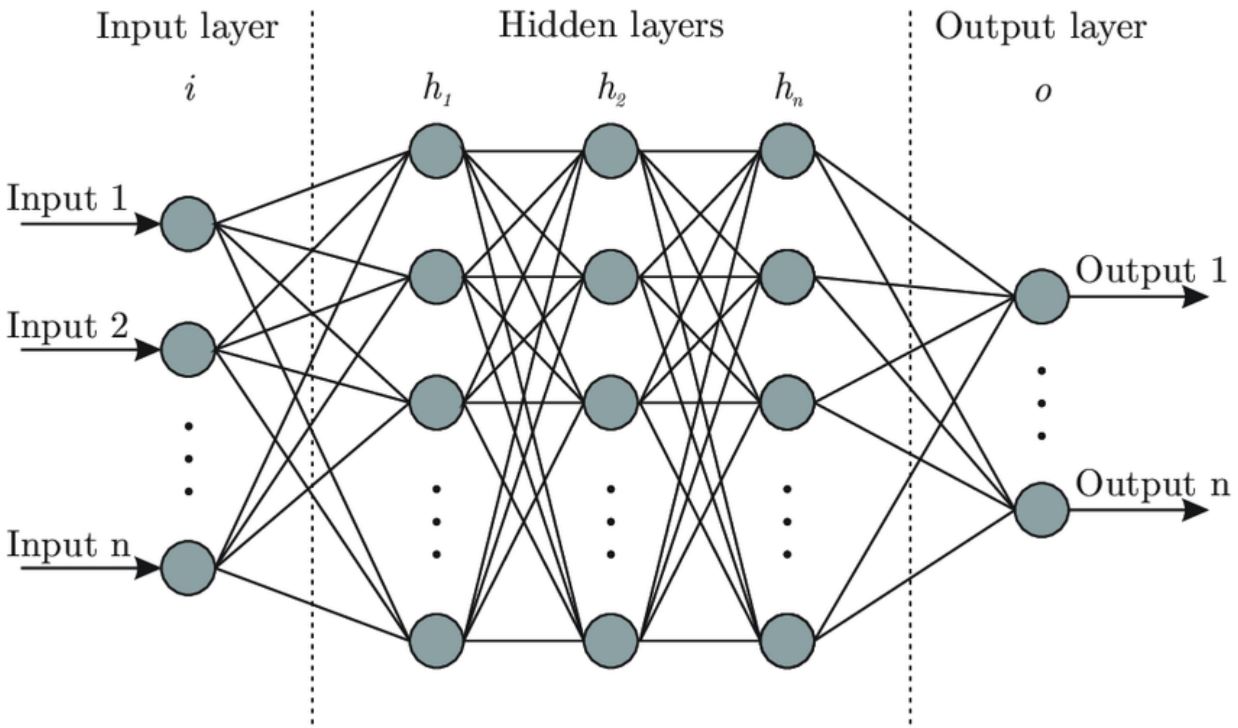

Applications of ANNs

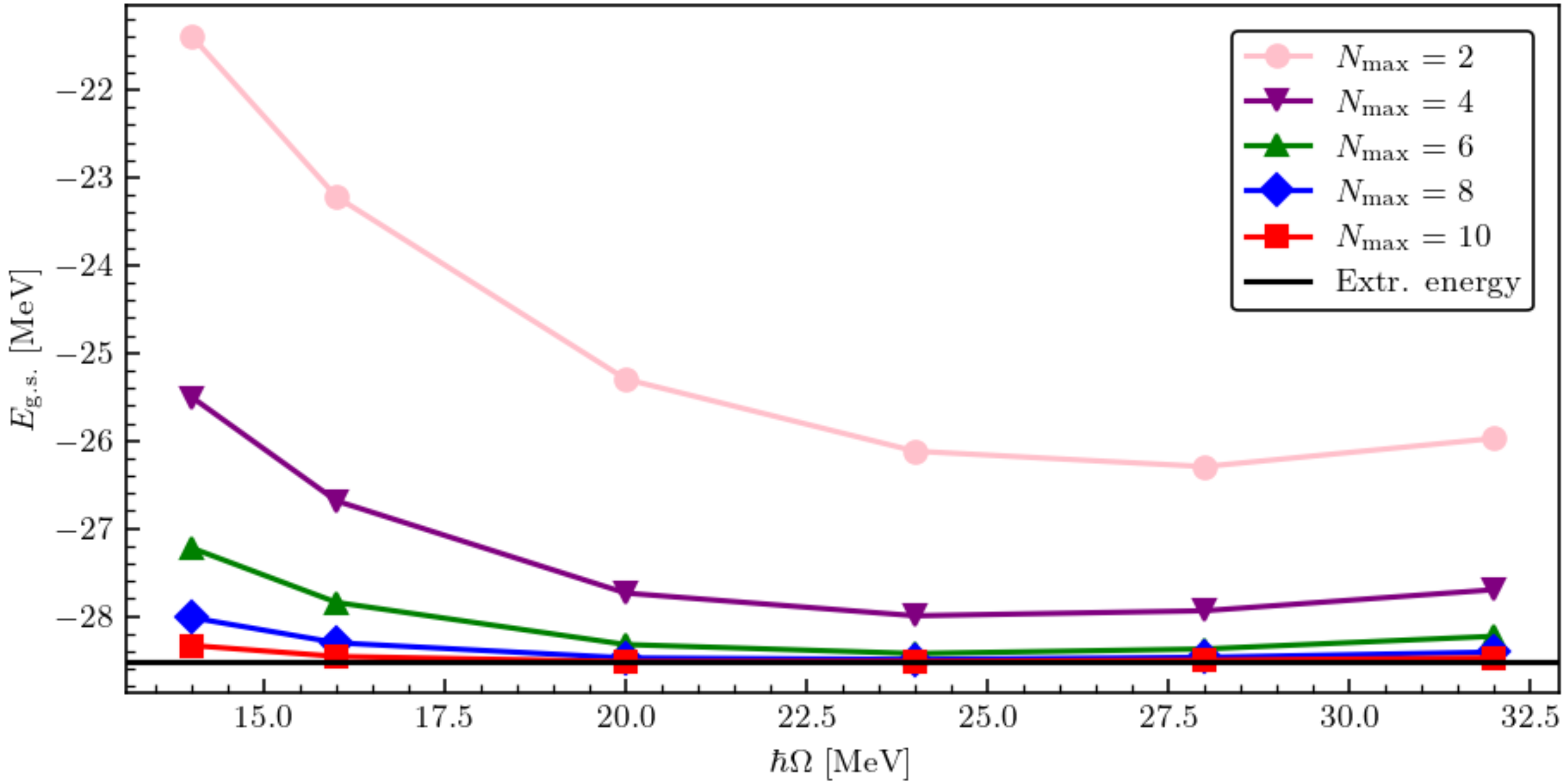

- No-core shell model (NCSM): monotonic convergence pattern displayed by the observables at fixed $\hbar\Omega$ due to the problem being variational → lower bound
- Calculations are performed in a harmonic oscillator (HO) basis and truncated to a finite model space of size $N_{\max}$

Alberto Garcia

Results

- Train 1000 ANNs with three nuclei (plus synthetic data):

$$^{2}\mathrm{H},\ ^{3}\mathrm{H},\ ^{4}\mathrm{He}$$

- Sample data set composed of three values of $\hbar\Omega$ and four consecutive values of $N_{\max}$
- Extrapolate to hard-to-calculate nuclei:

$$^{6}\mathrm{Li},\ ^{12}\mathrm{C},\ ^{16}\mathrm{O}$$

- Training: ABS method

$$d_{\mathrm{ABS}}^{N_{\max}} = (E_{\hbar\Omega_1}^{N_{\max}-6}, E_{\hbar\Omega_1}^{N_{\max}-4}, E_{\hbar\Omega_1}^{N_{\max}-2}, E_{\hbar\Omega_1}^{N_{\max}},\\ E_{\hbar\Omega_2}^{N_{\max}-6}, E_{\hbar\Omega_2}^{N_{\max}-4}, E_{\hbar\Omega_2}^{N_{\max}-2}, E_{\hbar\Omega_2}^{N_{\max}},\\ E_{\hbar\Omega_3}^{N_{\max}-6}, E_{\hbar\Omega_3}^{N_{\max}-4}, E_{\hbar\Omega_3}^{N_{\max}-2}, E_{\hbar\Omega_3}^{N_{\max}})$$

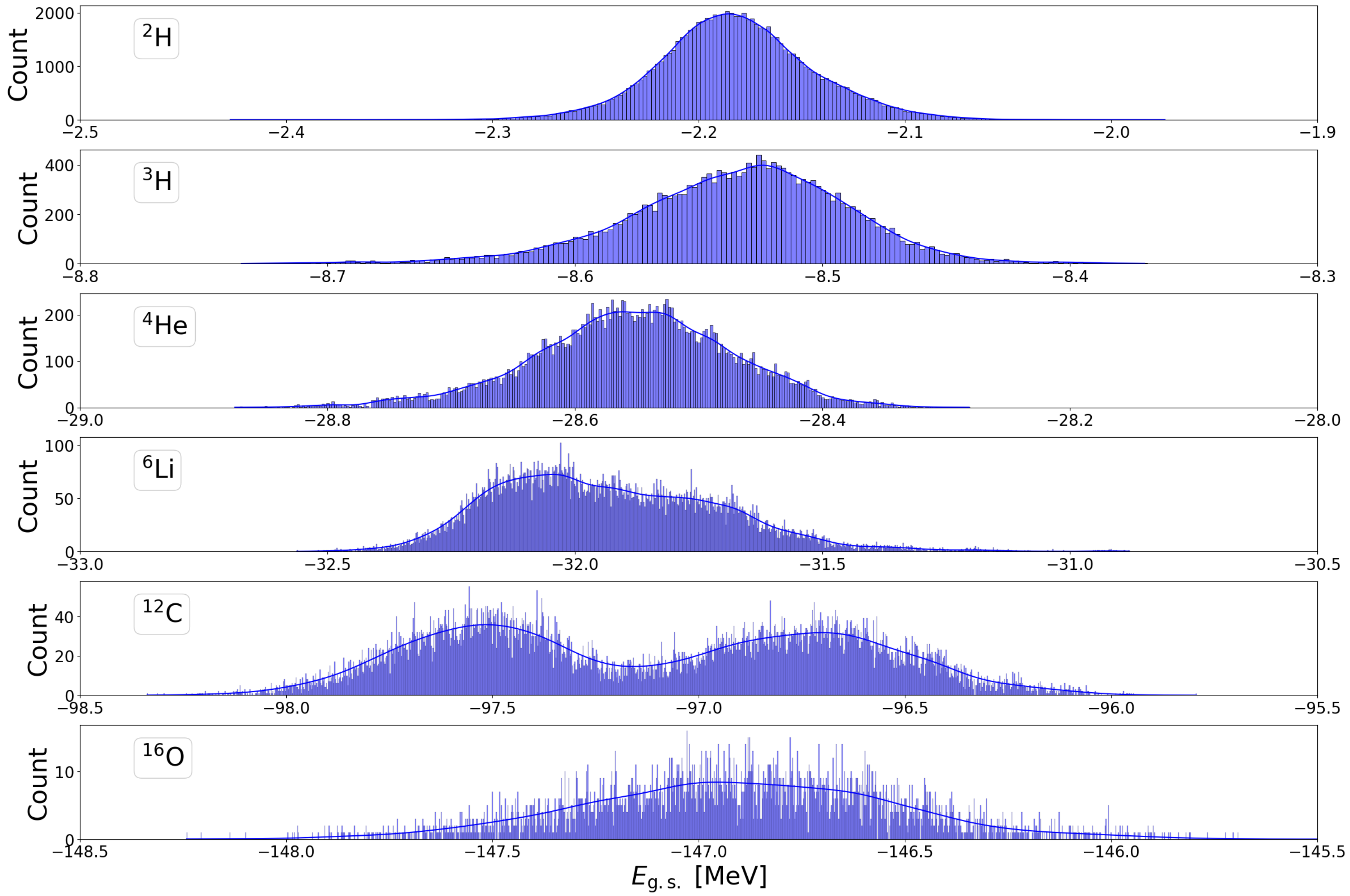

Alberto Garcia

Results

- Train 1000 ANNs with three nuclei (plus synthetic data):

$$^{2}\mathrm{H}, {}^{3}\mathrm{H}, {}^{4}\mathrm{He}$$

- Sample data set composed of three values of $\hbar\Omega$ and four consecutive values of $N_{\max}$
- Extrapolate to hard-to-calculate nuclei:

$$^{6}\mathrm{Li}, {}^{12}\mathrm{C}, {}^{16}\mathrm{O}$$

- Training: DIFF method

$$d_{\mathrm{DIFF}}^{N_{\max}} = (\Delta E_{\hbar\Omega_1}^{N_{\max}-4}, \Delta E_{\hbar\Omega_1}^{N_{\max}-2}, \Delta E_{\hbar\Omega_1}^{N_{\max}}, \Delta E_{\hbar\Omega_2}^{N_{\max}-4}, \Delta E_{\hbar\Omega_2}^{N_{\max}-2}, \Delta E_{\hbar\Omega_2}^{N_{\max}}, \Delta E_{\hbar\Omega_3}^{N_{\max}-4}, \Delta E_{\hbar\Omega_3}^{N_{\max}-2}, \Delta E_{\hbar\Omega_3}^{N_{\max}})$$

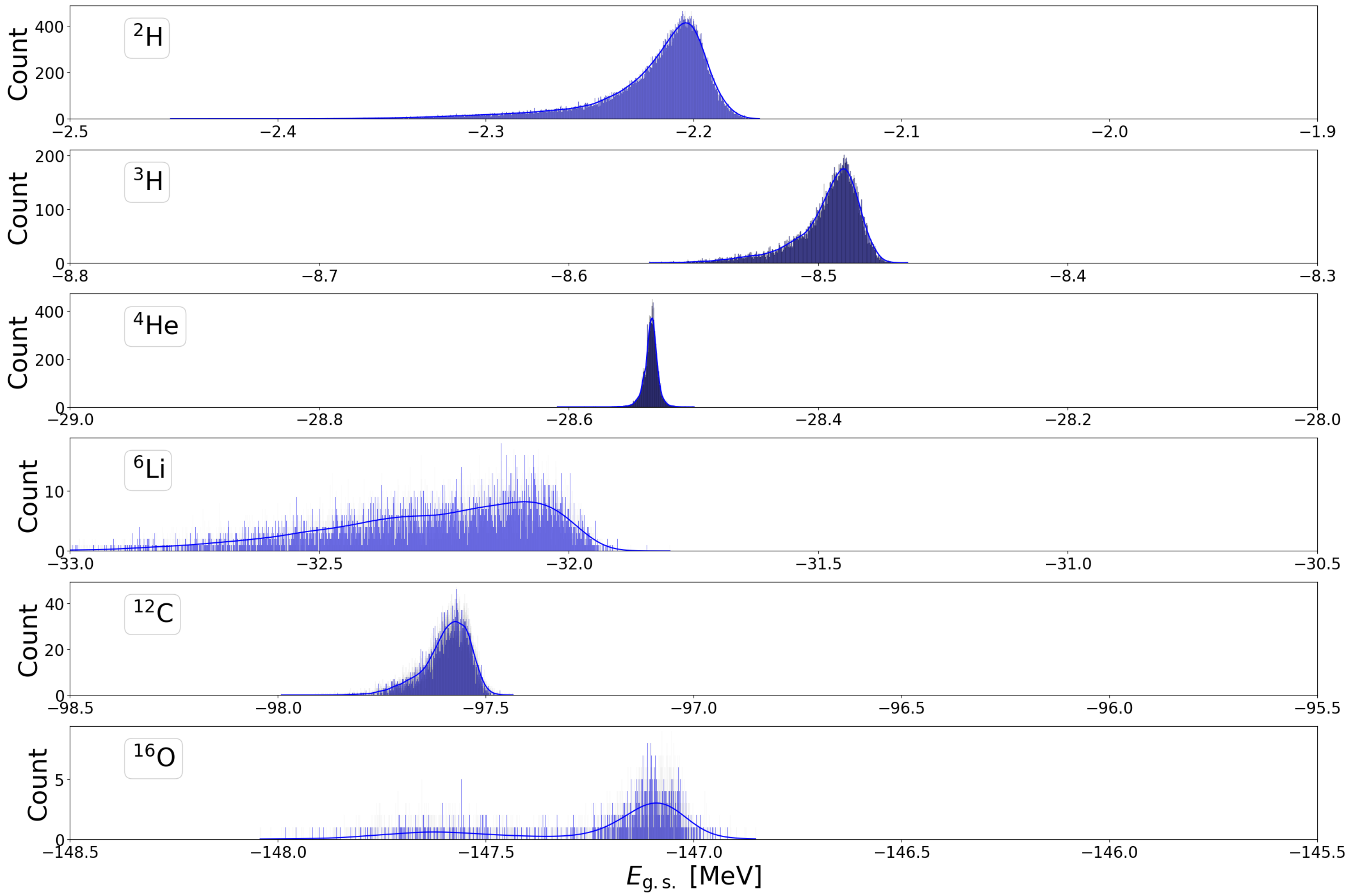

Alberto Garcia

Statistics

Nuclei	Avg. $E_{\text{g.s.}}^{\text{ABS}}$	Avg. $E_{\text{g.s.}}^{\text{DIFF}}$	Extrap.	Conv. result
^{2}H	-2.182 ± 0.037	-2.220 ± 0.030	-2.183 ± 0.091	-2.200
^{3}H	-8.534 ± 0.045	-8.496 ± 0.013	-8.473 ± 0.010	-8.481
^{4}He	-28.554 ± 0.081	-28.534 ± 0.006	-28.525 ± 0.009	-28.524
^{6}Li	-31.933 ± 0.223	-32.281 ± 0.221	-32.098 ± 0.317	—
^{12}C	-97.120 ± 0.470	-97.595 ± 0.057	-97.43 ± 0.44	—
^{16}O	-146.906 ± 0.375	-147.237 ± 0.241	-147.28 ± 1.86	—

- Average ground state binding energies and standard deviations (in MeV) for different nuclei obtained from evaluating 1000 ANNs using the ABS and DIFF method

Statistics

Nuclei	Avg. $E^{ABS}_{g.s.}$	Avg. $E^{DIFF}_{g.s.}$	Extrap.	Conv. result
^2H	-2.182 ± 0.037	-2.220 ± 0.030	-2.183 ± 0.091	-2.200
^3H	-8.534 ± 0.045	-8.496 ± 0.013	-8.473 ± 0.010	-8.481
^4He	-28.554 ± 0.081	-28.534 ± 0.006	-28.525 ± 0.009	-28.524
^6Li	-31.933 ± 0.223	-32.281 ± 0.221	-32.098 ± 0.317	—
^{12}C	-97.120 ± 0.470	-97.595 ± 0.057	-97.43 ± 0.44	—
^{16}O	-146.906 ± 0.375	-147.237 ± 0.241	-147.28 ± 1.86	—

- Average ground state binding energies and standard deviations (in MeV) for different nuclei obtained from evaluating 1000 ANNs using the ABS and DIFF method
- Overall, DIFF method works best

Training ANNs in IR/UV-convergence regions

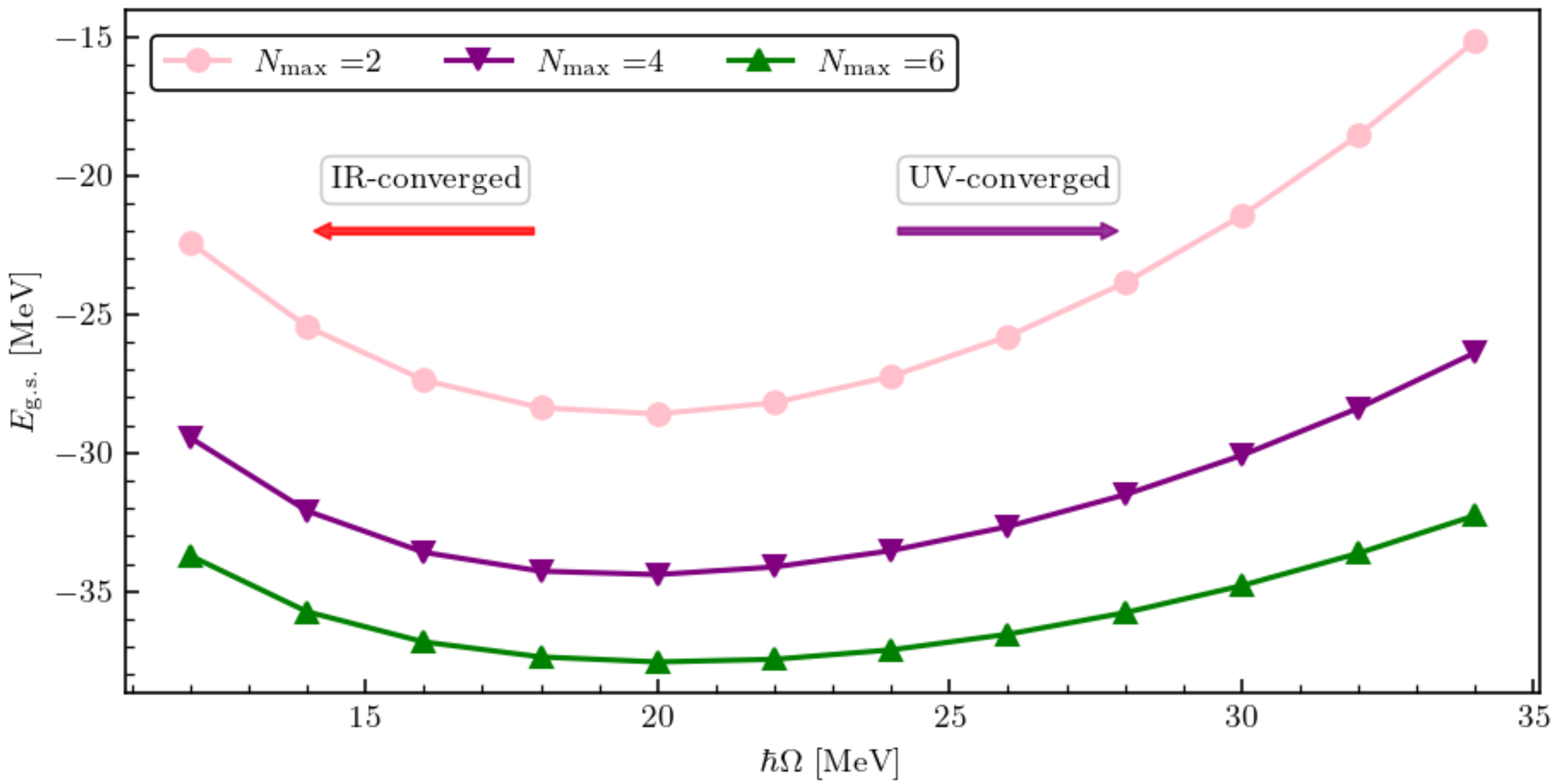

- Investigate these regions with ANNs to see if correlations between nuclear observables that can be attributed to UV errors are detected
- Enable better extrapolations in the region where the IR truncation errors are converged

Results

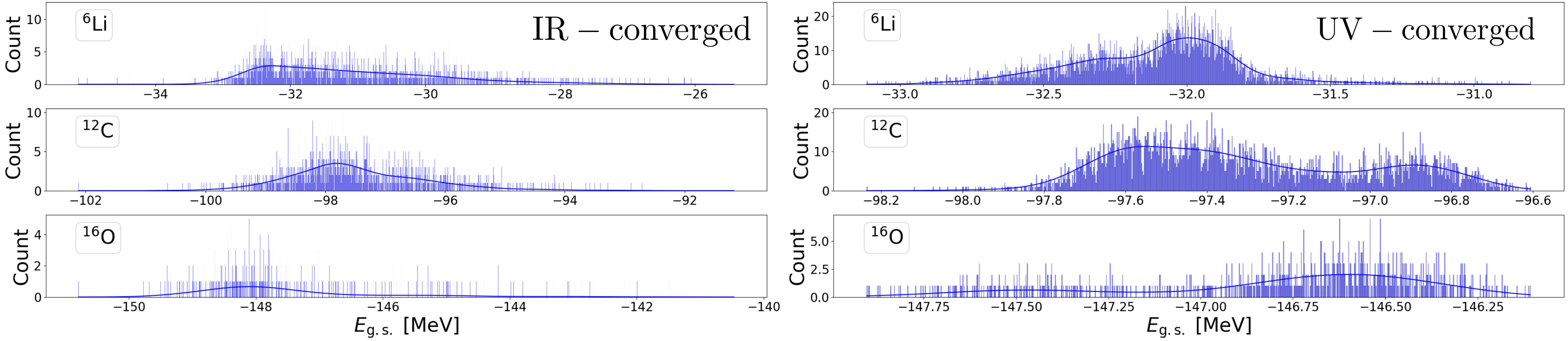

	IR-converged		UV-converged		Full spectrum
Nuclei	Avg. $E^{\text{ABS}}_{\text{g.s.}}$	Avg. $E^{\text{DIFF}}_{\text{g.s.}}$	Avg. $E^{\text{ABS}}_{\text{g.s.}}$	Avg. $E^{\text{DIFF}}_{\text{g.s.}}$	Avg. $E^{\text{DIFF}}_{\text{g.s.}}$
^{2}H	-2.063 ± 0.210	-2.374 ± 0.107	-2.172 ± 0.081	-2.233 ± 0.050	-2.220 ± 0.030
^{3}H	-8.466 ± 0.141	-8.616 ± 0.084	-8.469 ± 0.058	-8.495 ± 0.026	-8.496 ± 0.013
^{4}He	-28.727 ± 0.178	-28.700 ± 0.128	-28.544 ± 0.039	-28.543 ± 0.032	-28.534 ± 0.006
^{6}Li	-31.094 ± 1.338	-32.762 ± 0.374	-32.108 ± 0.295	-32.306 ± 0.238	-32.281 ± 0.221
^{12}C	-97.444 ± 1.173	-97.726 ± 0.262	-97.310 ± 0.301	-97.691 ± 0.089	-97.595 ± 0.057
^{16}O	-147.470 ± 1.510	-147.206 ± 0.259	-146.806 ± 0.414	-147.381 ± 0.192	-147.237 ± 0.241

Alberto Garcia

Summary and Outlook

- Constructed a universal neural network that was trained on ground state binding energies two different way using easy-to-calculate nuclei
- Extrapolated to heavier, hard-to-converge systems
- Conducted preliminary studies of the IR and UV errors-dominated regions using neural networks
- Investigated how the accuracy of the predictions vary with varying network architecture

- Neural networks may help help detect correlations between observables of different nuclei, which can be used as an extrapolation tool to study nuclei along the proton and neutron drip lines
- Neural networks may be analyzed from first-principles using an effective-theory-motivated approach

Summary of major contributions

- **Wave-function-based emulation for nucleon-nucleon scattering in momentum space**
  - ajg, C. Drischler, R. J. Furnstahl, J. A. Melendez, and X. Zhang, Phys. Rev. C **107**, 054001 (2023), arXiv:2301.05093
- **BUQEYE Guide to Projection-Based Emulators in Nuclear Physics**
  - C. Drischler, J. A. Melendez, R. J. Furnstahl, ajg, and X. Zhang, Front. Phys. **10**, 92931 (2023), arXiv:2212.04912
- **Model reduction methods for nuclear emulators**
  - J. A. Melendez, C. Drischler, R. J. Furnstahl, ajg, and X. Zhang, J. Phys. G **49**, 102001 (2022), arXiv:2203.05528
- **Fast & accurate emulation of two-body scattering observables without wave functions**
  - J. A. Melendez, C. Drischler, ajg, R. J. Furnstahl, and X. Zhang, Phys. Lett. B **821**, 136608 (2021), arXiv:2106.15608
- **Efficient emulators for scattering using eigenvector continuation**
  - R. J. Furnstahl, ajg, P. J. Millican, and X. Zhang, Phys. Lett. B **809**, 135719 (2020), arXiv:2007.03635

+ publicly available python codes to reproduce results!

Thank you!

Extra slides

Model order reduction (MOR)

- Constructing a reduced-order model (ROM)

*C. Drischler, ajg et al., Front. Phys. **10** 92931 (2023)*

*J.A. Melendez ajg et al., J. Phys. G **49**, 102001 (2022)*

- Reduction schemes:
  - Data-driven: interpolate output of high-fidelity model w/o understanding → non-intrusive
  - Examples: Gaussian processes, neural networks
  - Model-driven: derive reduced-order equations from high-fidelity equations → intrusive
  - Examples: physics-based, respects underlying structure

- Reduced Basis method (RBM):
  - Sub-class of model-driven scheme
  - Different methods to choose parameter sets
  - A basis is constructed out of snapshots
  - RBM model is built from a global basis projection

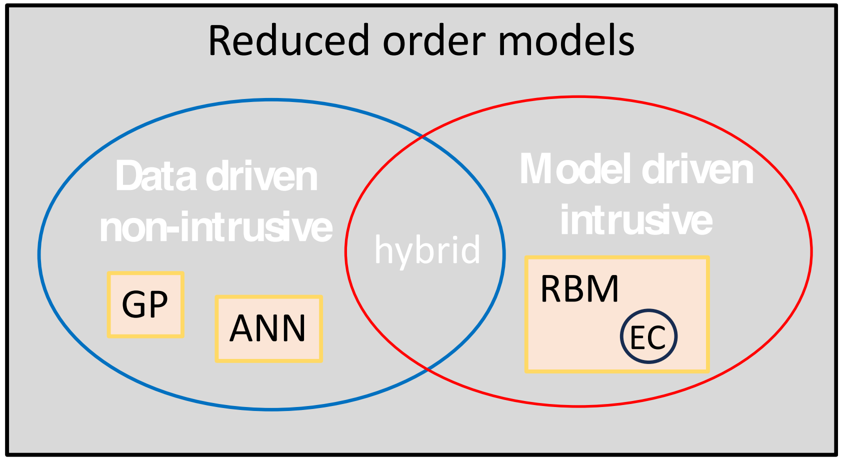

Alberto Garcia

Eigen-emulators

Schrödinger equation (weak form):

$$\langle\zeta|H(\boldsymbol{\theta}) - E(\boldsymbol{\theta})|\psi\rangle = 0, \quad \forall\, \langle\zeta|$$

→ Training set:

$$\{(\boldsymbol{\theta})_i\}$$

$$|\widetilde{\psi}\rangle = \sum_{i=1}^{n_\mathrm{b}} \beta_i|\psi_i\rangle \equiv X\vec{\beta},$$

$$X = \big[|\psi_1\rangle\ |\psi_2\rangle\ \cdots\ |\psi_{n_\mathrm{b}}\rangle\big],$$

C. Drischler, ajg, et al., Front. Phys. ***10*** *92931 (2023)*

J.A. Melendez, ajg, et al., J. Phys. G ***49****, 102001 (2022)*

Galerkin approach:

$$\langle\zeta|H(\boldsymbol{\theta}) - \widetilde{E}(\boldsymbol{\theta})|\widetilde{\psi}\rangle = 0, \quad \forall\, \langle\zeta| \in \mathcal{Z}$$

Choose:

$$\langle\zeta_i| = \langle\psi_i|\ (\mathrm{Ritz}) \rightarrow \langle\psi_i|H - \widetilde{E}|\widetilde{\psi}\rangle = 0 \quad \forall \quad i \in [1, n_\mathrm{b}]$$

- Produces same set of reduced-order equations as with variational approach!

More general:

$$\langle\zeta_i| \neq \langle\psi_i|\ (\mathrm{Petrov-Galerkin})$$

Scattering emulators

*J.A. Melendez, ajg et al., J. Phys. G **49**, 102001 (2022)*

- We want to find the solution of a time-independent differential equation such that

$$
\begin{aligned}
D(\psi;\boldsymbol{\theta}) &= 0 \quad \text{in } \Omega \\
B(\psi;\boldsymbol{\theta}) &= 0 \quad \text{in } \Gamma
\end{aligned}
$$

where Γ is the boundary and Ω the domain

- Some examples:

$$[-\nabla^2\psi = g(\theta)]_\Omega$$

$$[\frac{\partial\psi}{\partial n} = f(\theta)]_\Gamma$$

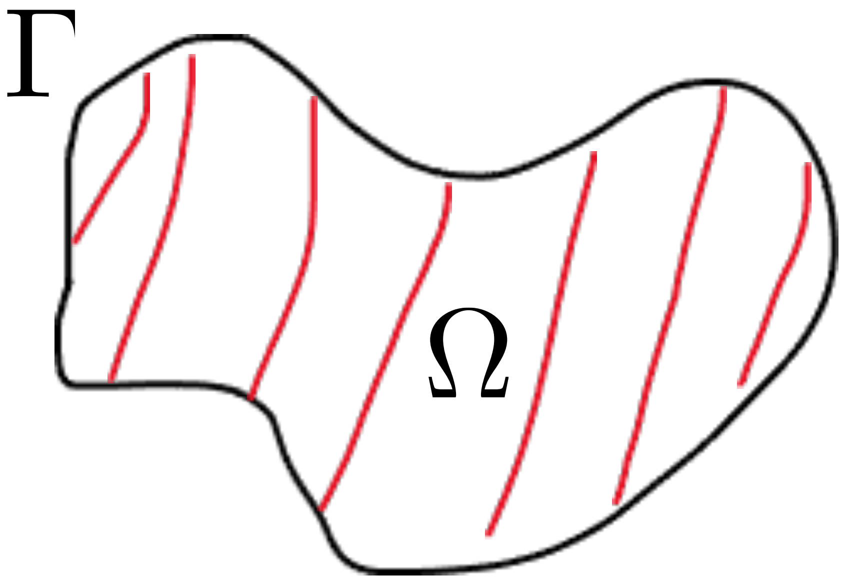

Different methods to construct emulators

J.A. Melendez, ajg et al., J. Phys. G **49**, 102001 (2022)

- Variational method → stationary functional

$$\mathcal{S}[\psi] = \int_\Omega d\Omega F[\psi] + \int_\Gamma d\Gamma G[\psi]$$

$$\text{Trial basis}: \ |\widetilde{\psi}\rangle = \sum_{i=1}^{n_\mathrm{b}} \beta_i |\psi_i\rangle$$

$$\delta\mathcal{S} = \sum_{i=1}^{n_\mathrm{b}} \frac{\partial \mathcal{S}}{\partial \beta_i}\delta\beta_i = 0 \longrightarrow \delta\mathcal{S} = A\vec{\beta}_\star + \vec{b} = 0$$

- Galerkin projection → use weak form

$$\int_\Omega d\Omega\, \zeta D(\psi) + \int_\Gamma d\Gamma\, \bar{\zeta} B(\psi) = 0$$

$$\text{Reduce dimension}: \ |\psi\rangle \to |\widetilde{\psi}\rangle = \sum_{i=1}^{n_\mathrm{b}} \beta_i |\psi_i\rangle$$

$$\text{Test bases}: \begin{cases} |\zeta\rangle = \sum_{i=1}^{n_\mathrm{b}} \delta\beta_i |\zeta_i\rangle \\ |\bar{\zeta}\rangle = \sum_{i=1}^{n_\mathrm{b}} \delta\beta_i |\bar{\zeta}_i\rangle \end{cases}$$

$$D(\psi;\boldsymbol{\theta}) = 0 \quad \text{in } \Omega$$
$$B(\psi;\boldsymbol{\theta}) = 0 \quad \text{in } \Gamma$$

$$\delta\beta_i \Big[\int_\Omega d\Omega\, \zeta_i D(\widetilde{\psi}) + \int_\Gamma d\Gamma\, \bar{\zeta}_i B(\widetilde{\psi}) \Big] = 0$$

Variational vs. Galerkin approach

J.A. Melendez, ajg et al., J. Phys. G **49**, 102001 (2022)

- Example: Poisson equation with Neumann BCs

$$[-\nabla^2\psi = g(\theta)]_\Omega \qquad [\frac{\partial\psi}{\partial n} = f(\theta)]_\Gamma$$

$$|\widetilde{\psi}\rangle = \sum_{i=1}^{n_\mathrm{b}} \beta_i |\psi_i\rangle \equiv X\vec{\beta},$$

$$X = [|\psi_1\rangle \; |\psi_2\rangle \; \cdots \; |\psi_{n_\mathrm{b}}\rangle],$$

Variational approach

$$\mathcal{S}[\psi] = \int_\Omega d\Omega \Big(\frac{1}{2}\nabla\psi\cdot\nabla\psi - g\psi\Big) - \int_\Gamma d\Gamma\, f\psi$$

$$\delta\mathcal{S}[\psi] = \int_\Omega d\Omega\, \delta\psi \underbrace{\Big(-\nabla^2\psi - g\Big)}_{\text{Poisson eq}} - \int_\Gamma d\Gamma\, \delta\psi \underbrace{\Big(\frac{\partial\psi}{\partial n} - f\Big)}_{\text{BCs}}$$

If $\delta\mathcal{S} = 0 \longrightarrow$ Poisson eq, BCs

$$\delta\mathcal{S}[\widetilde{\psi}] = \sum_{i=1}^{n_\mathrm{b}} \frac{\partial\mathcal{S}}{\partial\beta_i}\delta\beta_i = 0 \longrightarrow \delta\mathcal{S} = \widetilde{A}\vec{\beta}_\star - (\vec{g} + \vec{f}) = 0$$

where

$$\widetilde{A}_{ij} = \int_\Omega \nabla\psi_i\cdot\nabla\psi_j \qquad g_i = \int_\Omega g(\boldsymbol{\theta})\psi_i \quad f_i = \int_\Gamma f(\boldsymbol{\theta})\psi_i$$

Galerkin approach

$$\int_\Omega d\Omega\, \zeta\Big(-\nabla^2\psi - g\Big) + \int_\Gamma d\Gamma\, \zeta\Big(\frac{\partial\psi}{\partial n} - f\Big) = 0$$

$$\int_\Omega d\Omega\, \Big(\nabla\zeta\cdot\nabla\psi - g\zeta\Big) - \int_\Gamma d\Gamma\, f\zeta = 0$$

Assert holds for:

$$\psi \to \widetilde{\psi} = X\vec{\beta}, \qquad \zeta = \sum_{i=1}^{n_\mathrm{b}} \delta\beta_i\psi_i$$

$$\delta\beta_i\Big[\int_\Omega d\Omega\, (\underbrace{\nabla\psi_i\cdot\nabla\psi_j}_{\widetilde{A}_{ij}}\beta_j - \underbrace{g\psi_i}_{g_i}) - \int_\Gamma d\Gamma\, \underbrace{f\psi_i}_{f_i}\Big] = 0$$

Alberto Garcia

Deriving Poisson eqs from functional

- Apply Green's identity

$$\int_\Omega d\Omega \, [\psi \nabla^2 \varphi + \nabla\psi \cdot \nabla\varphi] = \int_\Gamma d\Gamma \, \psi(\nabla\varphi \cdot \hat{n})$$

1) $$\mathcal{S}[\psi] = \int_\Omega d\Omega \Big(\frac{1}{2}\nabla\psi \cdot \nabla\psi - g\psi\Big) - \int_\Gamma d\Gamma f\psi$$

2) $$\delta\mathcal{S} = \int_\Omega d\Omega \, (\nabla\psi \cdot \nabla(\delta\psi) - g\delta\psi) - \int_\Gamma d\Gamma \, f\delta\psi$$

3) $$\int_\Omega d\Omega \, [\nabla\psi \cdot \nabla(\delta\psi)] = \int_\Gamma d\Gamma \, \delta\psi(\nabla\psi \cdot \hat{n}) - \int_\Omega d\Omega \, (\delta\psi \nabla^2 \varphi)$$

4) $$\delta\mathcal{S}[\psi] = \int_\Omega d\Omega \, \delta\psi \Big(-\nabla^2\psi - g\Big) - \int_\Gamma d\Gamma \, \delta\psi \left(\frac{\partial\psi}{\partial n} - f\right)$$

Deriving emulator equation: Variational

$$\mathcal{S}[\widetilde{\psi}] = \int_{\Omega} d\Omega \Big(\frac{1}{2} \nabla \widetilde{\psi} \cdot \nabla \widetilde{\psi} - g \widetilde{\psi} \Big) - \int_{\Gamma} d\Gamma f \widetilde{\psi}$$

1) $$A = \frac{1}{2} \nabla \widetilde{\psi} \cdot \nabla \widetilde{\psi} = \frac{1}{2} \beta_j \nabla \psi_j \cdot \beta_k \nabla \psi_k$$

2) $$\frac{\delta A}{\delta \beta_i} = \frac{1}{2} \delta_{ij} \nabla \psi_j \cdot (\beta_k \nabla \psi_k) + \frac{1}{2} (\beta_j \nabla \psi_j) \cdot \delta_{ik} \nabla \psi_k = (\nabla \psi_i \cdot \nabla \psi_j) \beta_i$$

3) $$\delta \mathcal{S}[\widetilde{\psi}] = \delta \beta_i \Big[\int_{\Omega} d\Omega \, (\nabla \psi_i \cdot \nabla \psi_j) \beta_j - \int_{\Omega} d\Omega \, g \psi_i - \int_{\Gamma} d\Gamma \, f \psi_i \Big] = 0$$

Alberto Garcia

Deriving emulator equation: Galerkin

$$\int_\Omega d\Omega\, \zeta D(\psi) + \int_\Gamma d\Gamma\, \bar{\zeta} B(\psi) = 0$$

1) $$\int_\Omega d\Omega\, \zeta\left(-\nabla^2\psi - g\right) + \int_\Gamma d\Gamma\, \zeta\left(\frac{\partial\psi}{\partial n} - f\right) = 0$$

Apply Green's identity!

2) $$\int_\Omega d\Omega\, \zeta\nabla^2\psi = -\int_\Omega d\Omega\, \nabla\zeta\cdot\nabla\psi + \int_\Gamma d\Gamma\, \zeta(\nabla\psi\cdot\hat{n})$$

3) $$\int_\Omega d\Omega\left(\nabla\zeta\cdot\nabla\psi - g\zeta\right) - \int_\Gamma d\Gamma\, f\zeta = 0$$

4) Assert holds for:

$$\psi \to \widetilde{\psi} = X\vec{\beta}, \qquad \zeta = \sum_{i=1}^{n_\mathrm{b}} \delta\beta_i\psi_i \;\longrightarrow\; \delta\beta_i\Big[\int_\Omega d\Omega\,(\underbrace{\nabla\psi_i\cdot\nabla\psi_j}_{\widetilde{A}_{ij}}\beta_j - \underbrace{g\psi_i}_{g_i}) - \int_\Gamma d\Gamma\,\underbrace{f\psi_i}_{f_i}\Big] = 0$$

Alberto Garcia

Unconstrained KVP emulator

$$H|\psi\rangle = E|\psi\rangle \quad \rightarrow \quad |\psi\rangle = |\phi\rangle + |\chi\rangle$$

$$(E - H)(|\phi\rangle + |\chi\rangle) = 0 \longrightarrow (E - H)|\chi\rangle = (H - E)|\phi\rangle$$

$$(H - E)|\phi\rangle = (T + V - E)|\phi\rangle = V|\phi\rangle$$

$$(E - H)|\chi\rangle = V|\phi\rangle$$

since

$$(T - E)|\phi\rangle = 0$$

Alberto Garcia

Unconstrained KVP emulator

$$\delta\mathcal{K} = 0$$

$$\delta_{ik}\langle\chi_k|H-E|\chi_j\rangle\beta_j + \delta_{ij}\beta_k\langle\chi_k|H-E|\chi_j\rangle + \delta_{ij}\langle\phi|V|\chi_j\rangle + \delta_{ij}\langle\chi_j|V|\phi\rangle = 0$$

$$2\langle\chi_i|H-E|\chi_j\rangle\beta_j + 2\langle\chi_i|V|\phi\rangle = 0$$

$$\langle\chi_i|E-H|\chi_j\rangle\beta_j = \langle\chi_i|V|\phi\rangle$$

$$\begin{aligned}\langle\chi_i|E-H|\chi_j\rangle &= [E-(T+V)+V_j-V_j]|\chi_j\rangle \\ &= [E-H_j]|\chi_j\rangle + [V_j-V]|\chi_j\rangle\end{aligned}$$

$$\text{since} \quad H_j|\chi_j\rangle = (T+V_j)|\chi_j\rangle$$

$$\begin{aligned}[E-H_j]|\chi_j\rangle &= [E-T-V_j](|\psi_j\rangle - |\phi_j\rangle) \\ &= [E-T-V_j]|\psi_j\rangle - (E-T)|\phi_j\rangle + V_j|\phi_j\rangle \\ &= V_j|\phi_j\rangle\end{aligned}$$

$$[E-H]|\chi_j\rangle = V_j|\phi_j\rangle + [V_j-V]|\chi_j\rangle$$

Alberto Garcia

Comparison between emulators

C. Drischler, ajg et al., Front. Phys. **10** 92931 (2023)

- Yamaguchi potential for $\ell = 0$

$$V_\ell = \sum_{ij}^{n} |\nu_i^\ell\rangle \Lambda_{ij} \langle \nu_j^\ell| \qquad \{\Lambda_{00}, \Lambda_{01}, \Lambda_{11}\} \in [-50, 50]\,\mathrm{MeV}$$

- Has an exact (mesh-independent) answer!

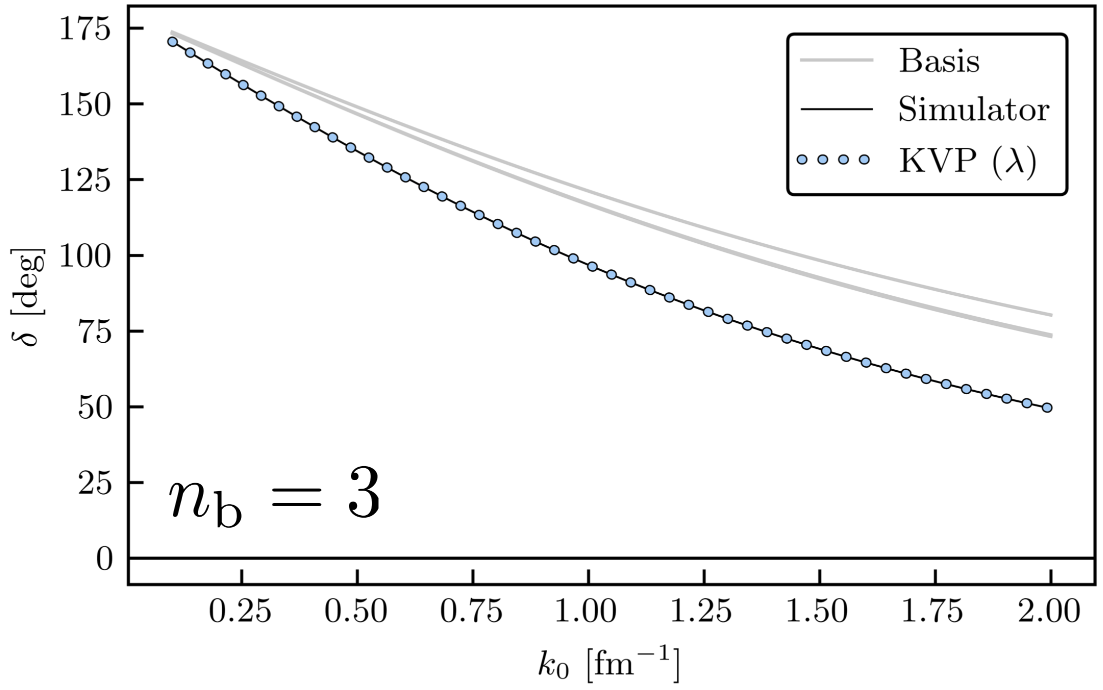

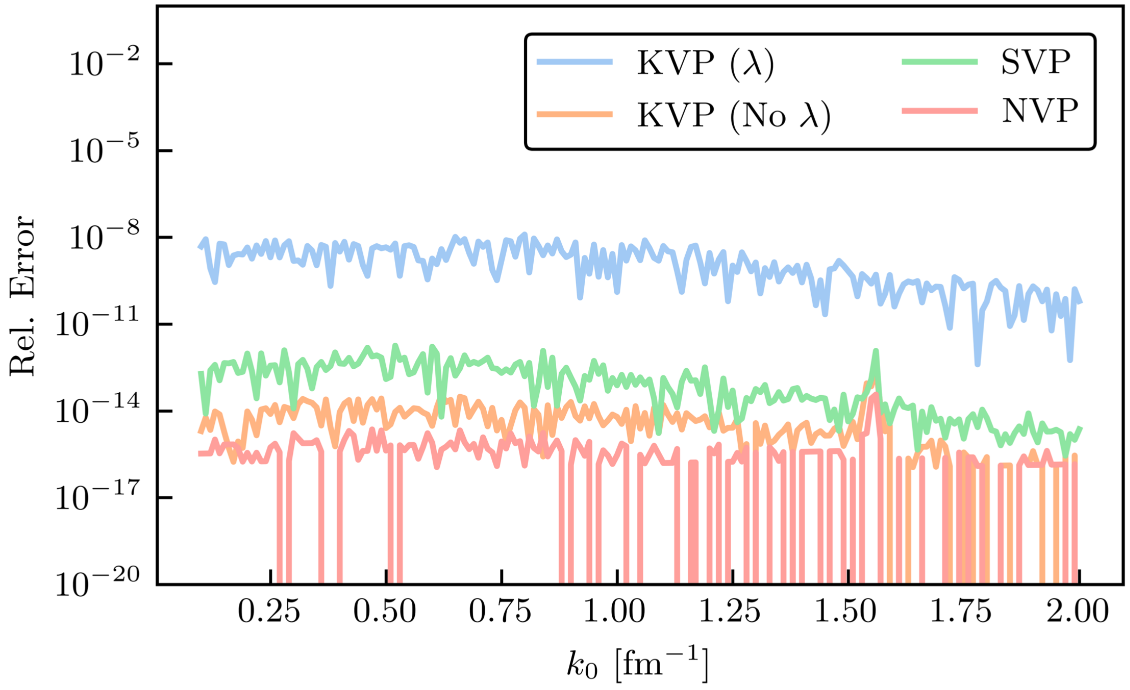

Comparison between emulators

C. Drischler ajg, et al., Front. Phys. **10** 92931 (2023)

- Yamaguchi potential for $\ell = 0$

$$V_\ell = \sum_{ij}^{n} |\nu_i^\ell\rangle \Lambda_{ij} \langle \nu_j^\ell| \qquad \{\Lambda_{00}, \Lambda_{01}, \Lambda_{11}\} \in [-50, 50]\,\mathrm{MeV}$$

- Has an exact (mesh-independent) answer!

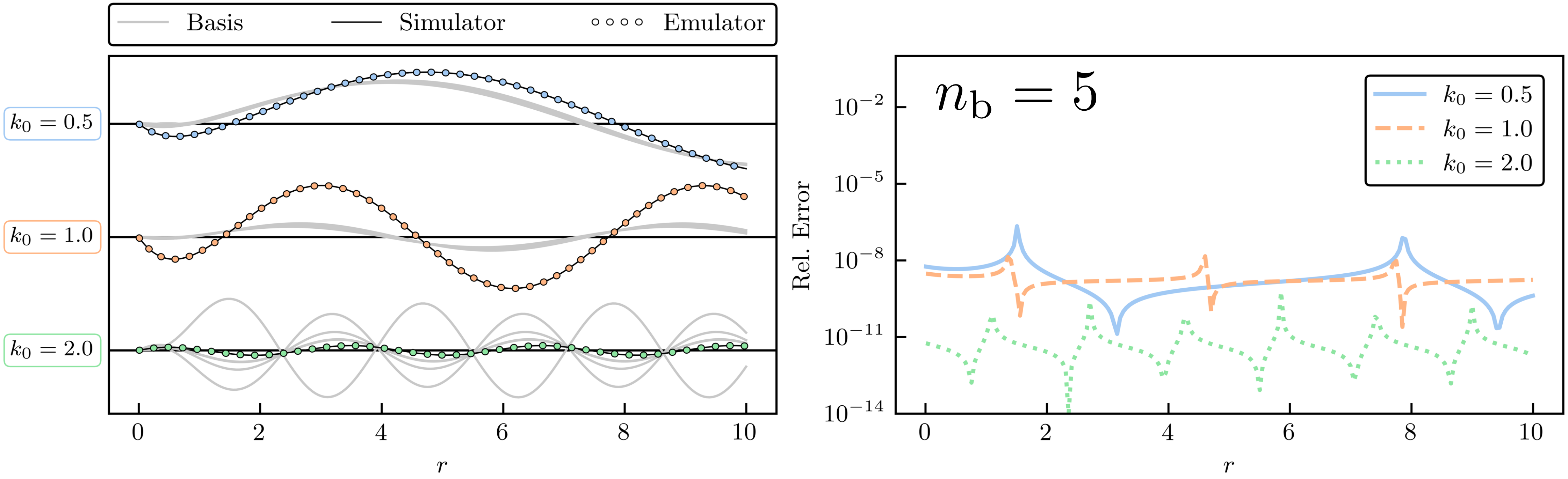

Alberto Garcia

Origin emulators

$$\int_\Omega d\Omega\,\zeta D(\psi) + \int_\Gamma d\Gamma\,\bar{\zeta} B(\psi) = 0$$

$$\int_\Omega d\Omega\,\zeta (H - E) + \int_\Gamma d\Gamma\,\bar{\zeta}[(r\psi)' - 1] = 0$$

$$\langle\zeta|H - E|\psi\rangle + \bar{\zeta}[(r\psi)' - 1]|_{r=0} = 0$$

Choose test functions

$$\zeta \to \psi_i, \quad \bar{\zeta} \to \bar{\zeta} \text{ such that } \bar{\zeta}(0) = 1$$

$$\langle\psi_i|H - E|\psi_j\rangle\beta_j + \bar{\zeta}(0)\Big[\sum_j \beta_j (r\psi_j)'(0) - 1\Big] = 0$$

$$\langle\psi_i|H - E|\psi_j\rangle\beta_j + \sum_j \beta_j - 1 = 0$$

Origin emulator (in coordinate space)

- Non-variational-based emulator
- Snapshots are composed of the boundary conditions

$$(r\psi) = 0,\ (r\psi)'(0) = 1 \quad \rightarrow \quad \langle \psi_i | H - E | \psi_j \rangle \beta_j + \sum_j \beta_j - 1 = 0$$

C. Drischler, ajg et al., Front. Phys. ***10*** *92931 (2023)*

- Sum of Gaussians potential:

$$V(r, \boldsymbol{\theta}) = \theta_1 \exp(-\kappa_1 r^2) + \theta_2 \exp(-\kappa_2 r^2) \quad (\ell = 0) \qquad \{\theta_1, \theta_2\} \in [-5, 5]\,\mathrm{MeV}$$

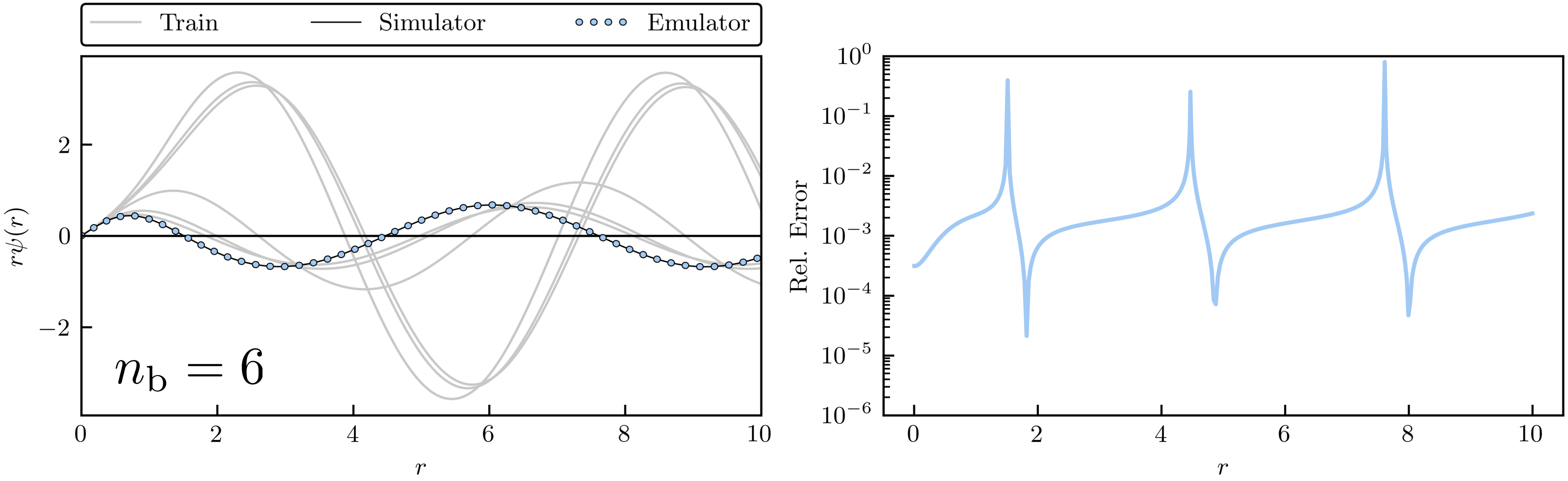

Alberto Garcia

Results for NVP emulator - Extrapolation

- Here: Extrapolation results for NVP
- Cross marks best-fit value for V0s

- Potential:

$$V_{^1S_0}(r) \equiv V_{0R}e^{-\kappa_R r^2} + V_{0s}e^{-\kappa_s r^2}$$

- Only vary V_{0s}

- Train with two repulsive parameter sets
- Extrapolate to attractive potentials

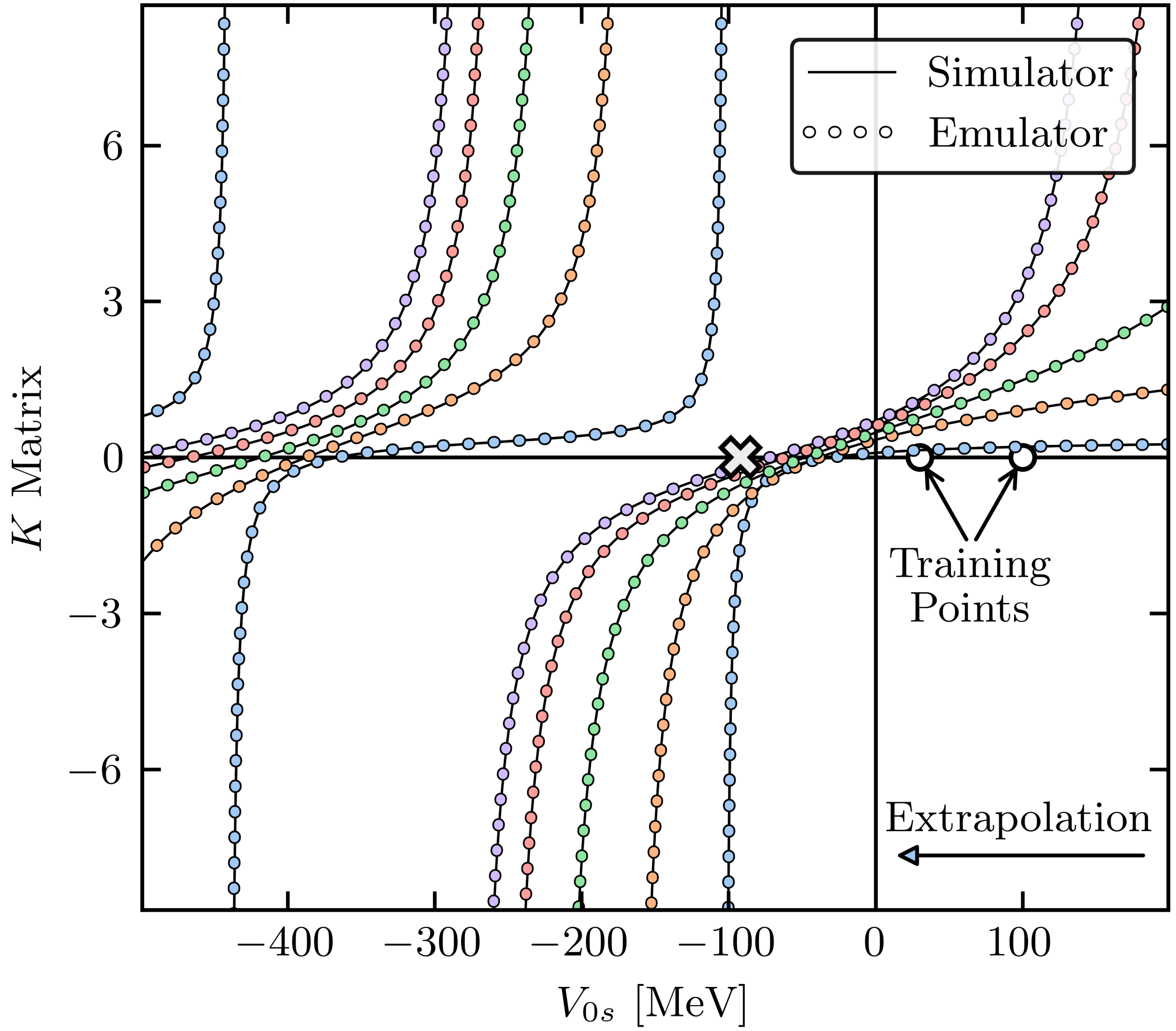

J.A. Melendez, ajg et al., Phys. Lett. B 821, 136608 (2021)

Results for NVP emulator with Coulomb

- Problematic for LS equation since it is a long-range interaction
- Solution: cut off potential at short distance $r = r_c$, emulate with new potential, and match conditions with emulated solution to obtain phase shifts
- Matching: finding phase shifts with respect to the Coulomb wave functions
- Here: proton-alpha scattering with non-local potential in s-wave

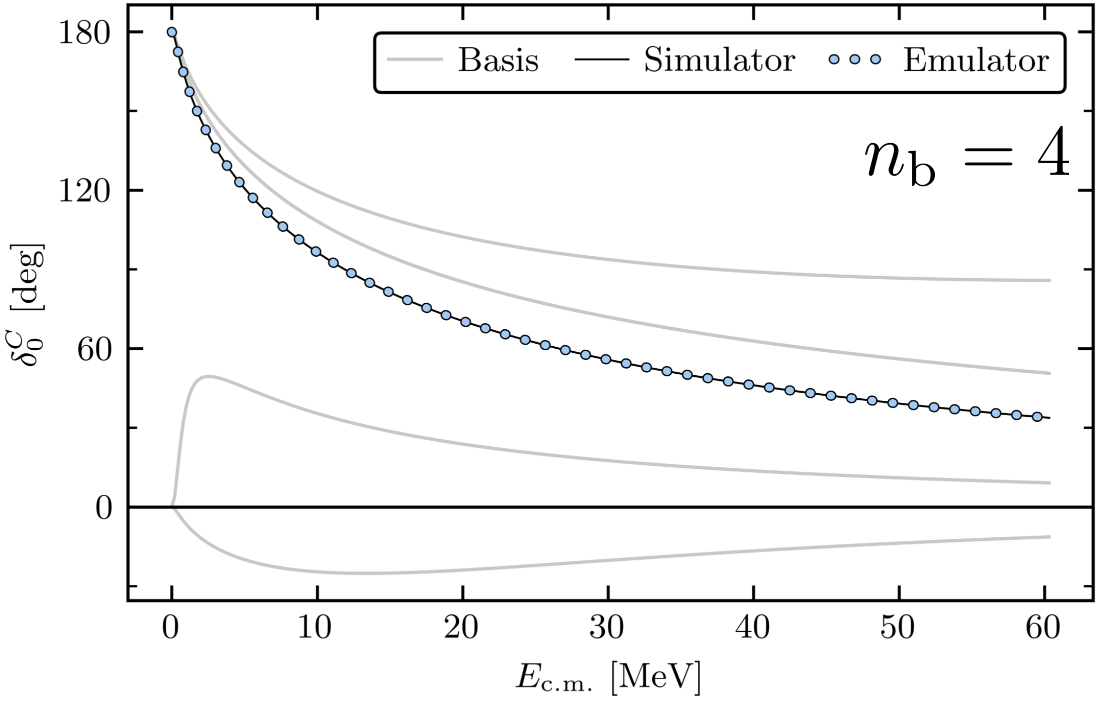

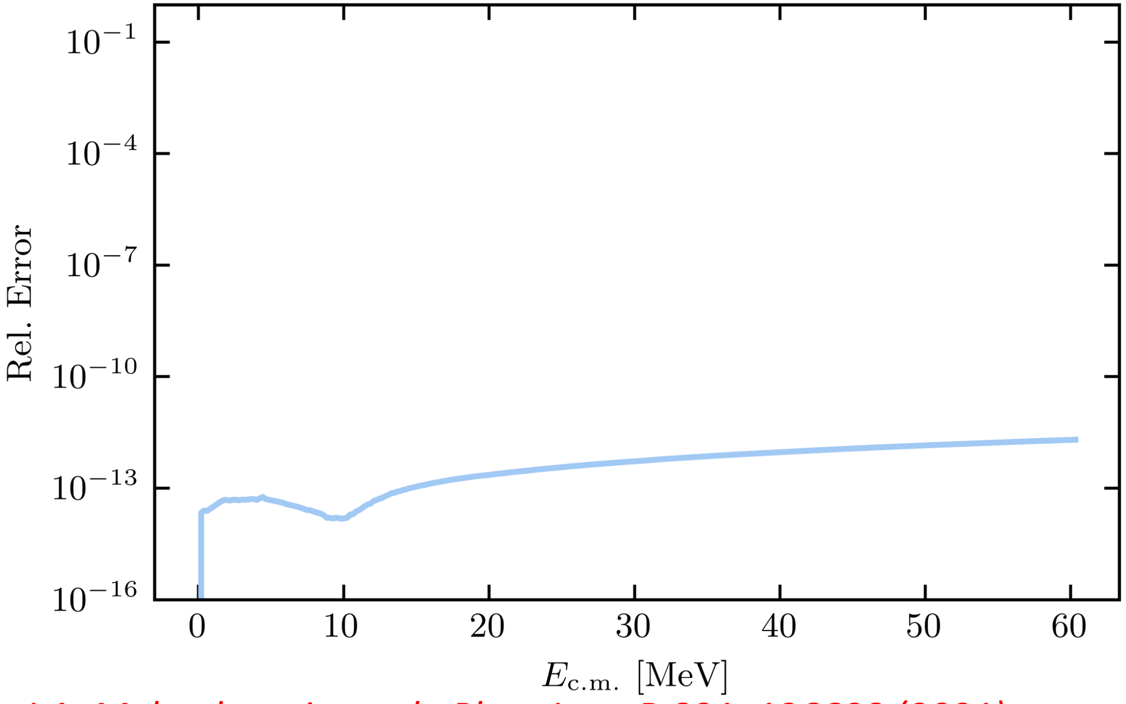

J.A. Melendez, ajg et al., Phys. Lett. B 821, 136608 (2021)

Alberto Garcia

Results for NVP emulator - Gradients

- Emulate gradients using NVP
- Useful for optimization and sampling algorithms that require gradients
- Examples: Newton's method, Gradient Descent

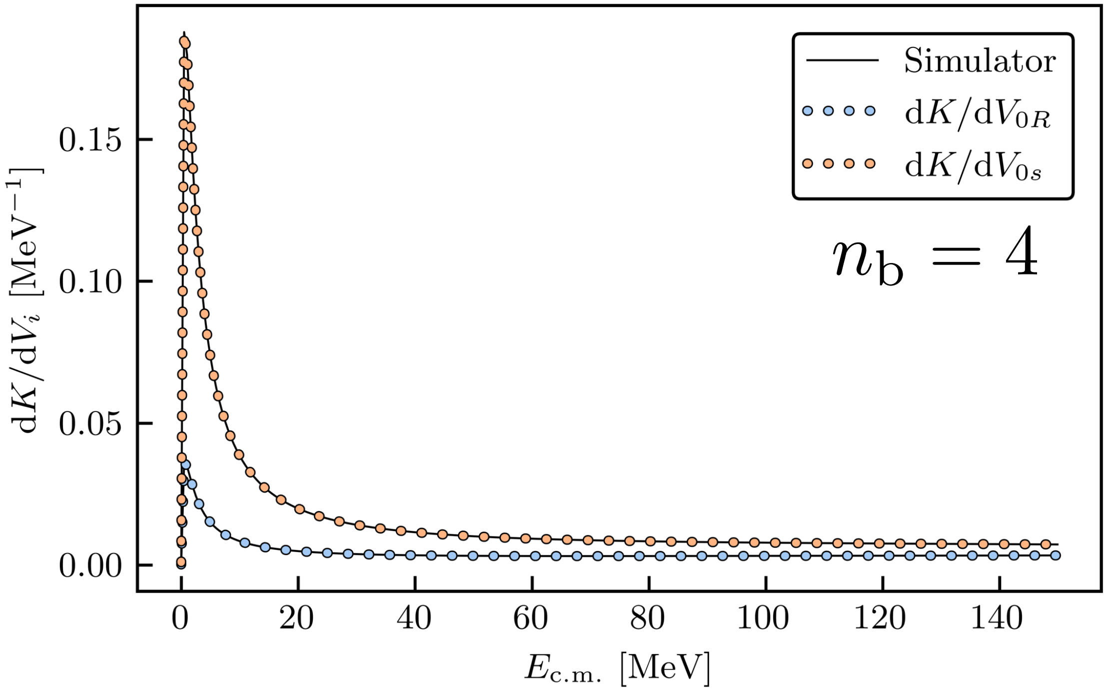

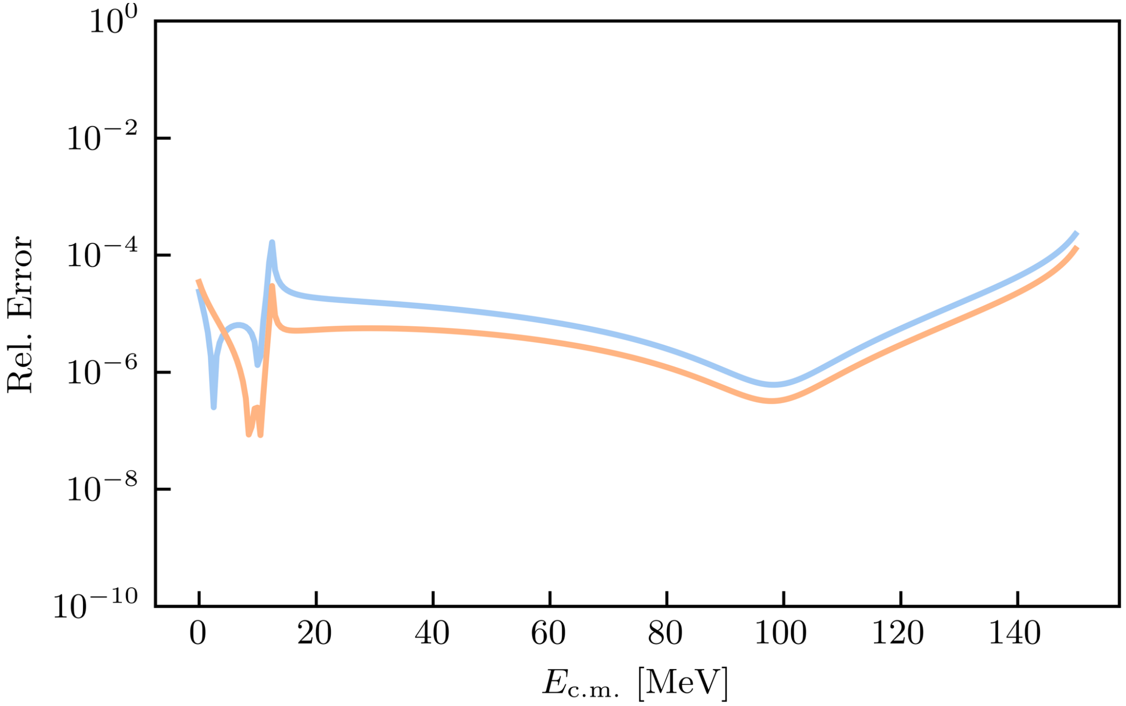

J.A. Melendez, ajg et al., Phys. Lett. B 821, 136608 (2021)

Alberto Garcia

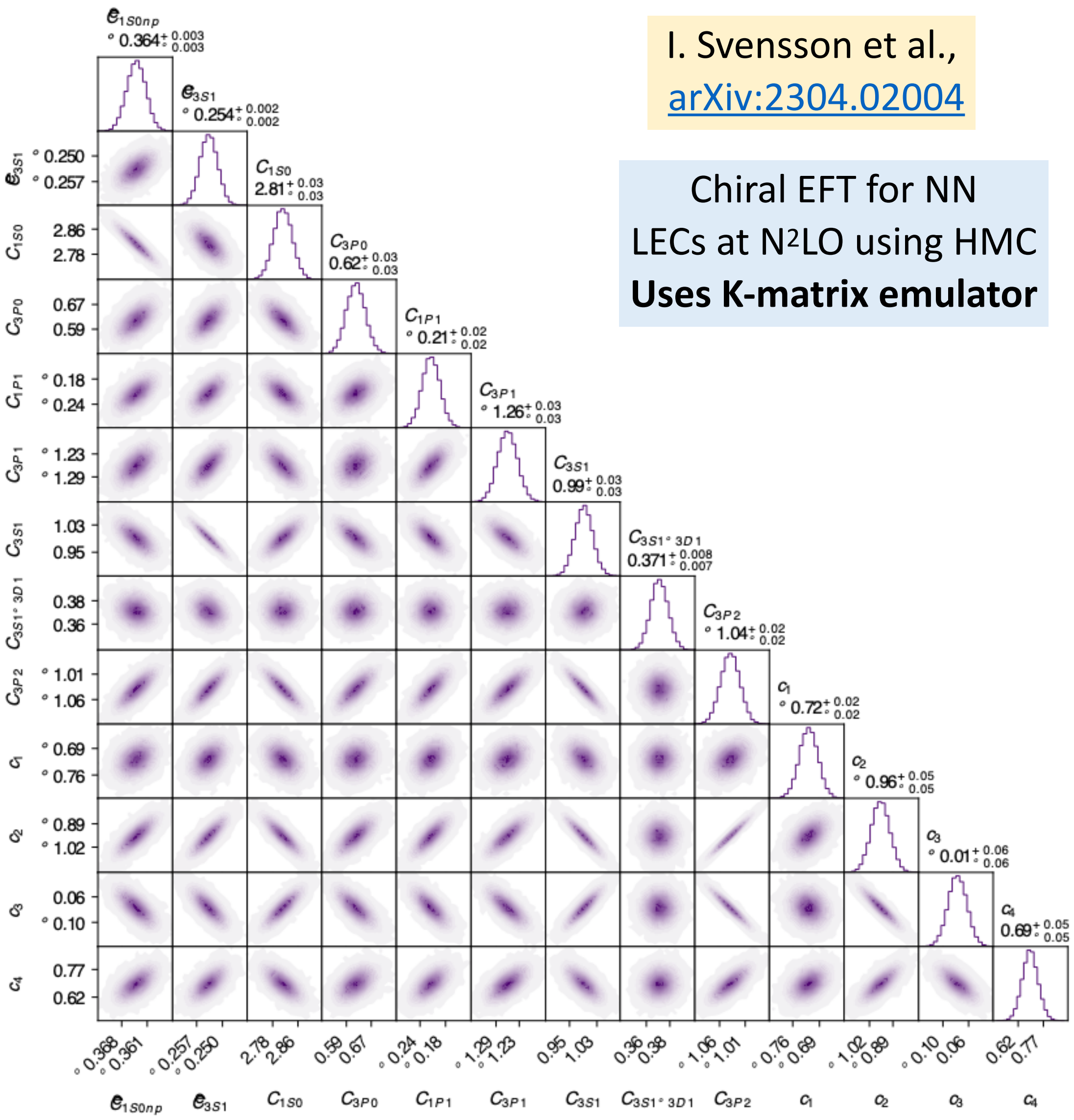

I. Svensson et al., arXiv:2304.02004

Chiral EFT for NN
LECs at N²LO using HMC
Uses K-matrix emulator

KVP emulator in coordinate space

R.J. Furnstahl, ajg et al., *Phys. Lett. B* **809**, 135719 (2020)
C. Drischler, ajg et al., *Front. Phys.* **10** 92931 (2023)

Implementation:

Snapshots

$$|\widetilde{\psi}^{\ell}\rangle \equiv \sum_{i=1}^{n_{\mathrm{b}}} \beta_i |\psi_i^{\ell}\rangle$$

Basis weights

$$\Delta\widetilde{U}^{\ell}_{ij}(\boldsymbol{\theta}) = \frac{2\mu k_0}{\det \boldsymbol{u}} \left[\langle \psi_i^{\ell} | \widehat{V}(\boldsymbol{\theta}) - \widehat{V}_j | \psi_j^{\ell}\rangle + (i \leftrightarrow j)\right]$$

$$\mathcal{L}^{\ell}[\vec{\beta}\,] = \beta_i L^{\ell}_{E,i} - \frac{1}{2}\beta_i \Delta\widetilde{U}^{\ell}_{ij}\beta_j$$

Coordinate space:

$$\langle \boldsymbol{r} | \psi_E(\boldsymbol{\theta_i})\rangle = \frac{u_E^{\ell,(i)}(r)}{r} Y_{\ell m}(\Omega_r) \quad \rightarrow \quad u_E^{\ell}(r) \underset{r\to\infty}{\longrightarrow} \frac{1}{k_0}\sin\left(k_0 r - \frac{\ell\pi}{2}\right) + L_E^{\ell}\cos\left(k_0 r - \frac{\ell\pi}{2}\right)$$

$$\Delta\widetilde{U}^{\ell}_{ij}(\boldsymbol{\theta}) = \int_0^{\infty} dr \left[u_i^{\ell}(r;E)\, V^{\ell}_{\boldsymbol{\theta},j}(r)\, u_j^{\ell}(r;E) + (i \leftrightarrow j)\right],$$

$$V^{\ell}_{\boldsymbol{\theta},j}(r) \equiv \frac{2\mu k_0}{\det \boldsymbol{u}}\left[V^{\ell}(r;\boldsymbol{\theta}) - V^{\ell}_j(r)\right]$$

Alberto Garcia

Results for a complex potential

R.J. Furnstahl, ajg et al., *Phys. Lett. B* **809**, 135719 (2020)

- Application of emulator to complex potentials → used for nuclear reactions

- Here: Wood-Saxon optical potential

$$V(r) = V_0 f(r, R_R, a_R) + iW_0 f(r, R_I, a_I)$$

$$f(r, R, a) = (1 + \exp\{(r-R)/a\})^{-1}$$

- Emulate the K matrix

$$L_E^\ell \to K_E^\ell$$

- Optimal values:

$$V_0 = -100\,\text{MeV},\ W_0 = -10\,\text{MeV}$$

- Parameter set:

$$\boldsymbol{\theta}_i = \{V_0, W_0\} \quad \text{vary } \pm 50\%$$

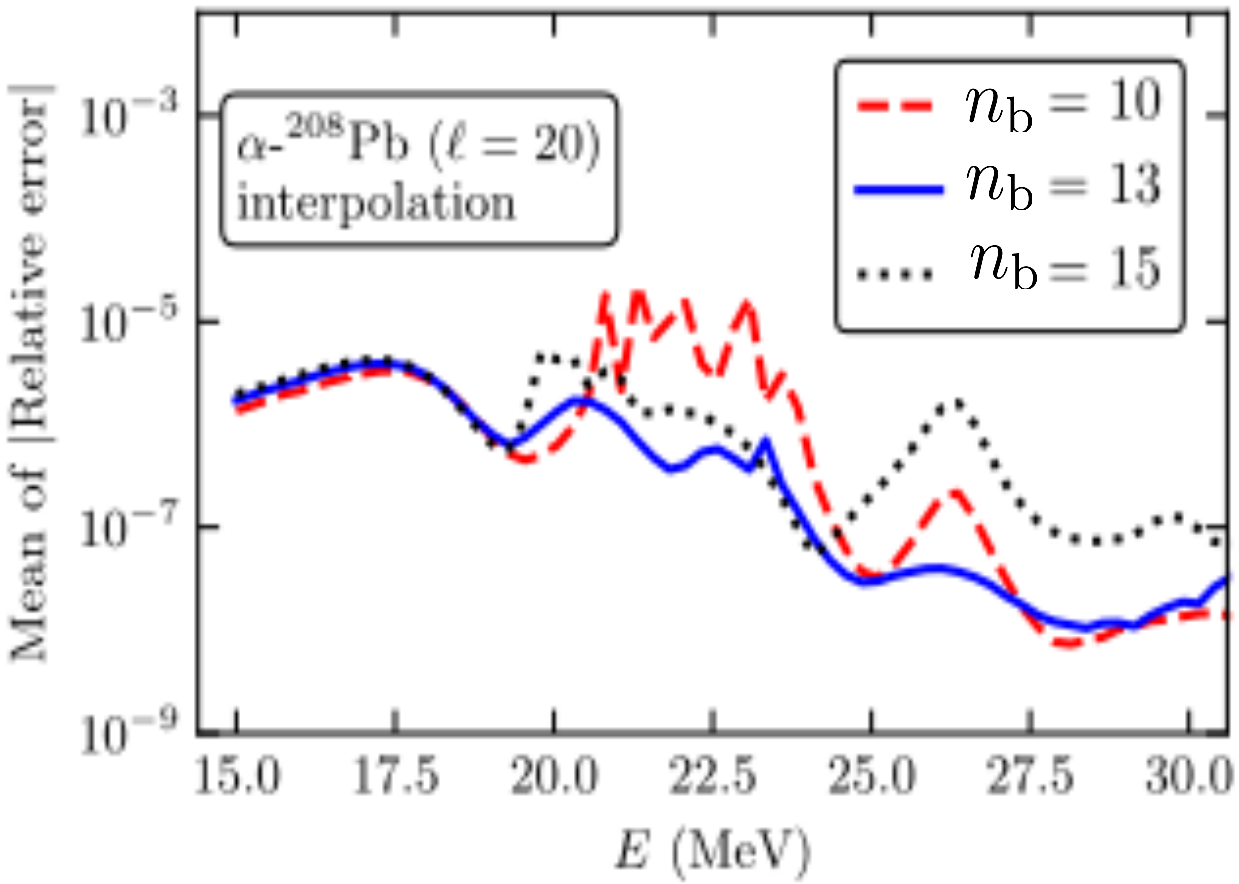

- 200 sampled parameter sets!

Alberto Garcia

R.J. Furnstahl, ajg et al., Phys. Lett. B ***809****, 135719 (2020)*

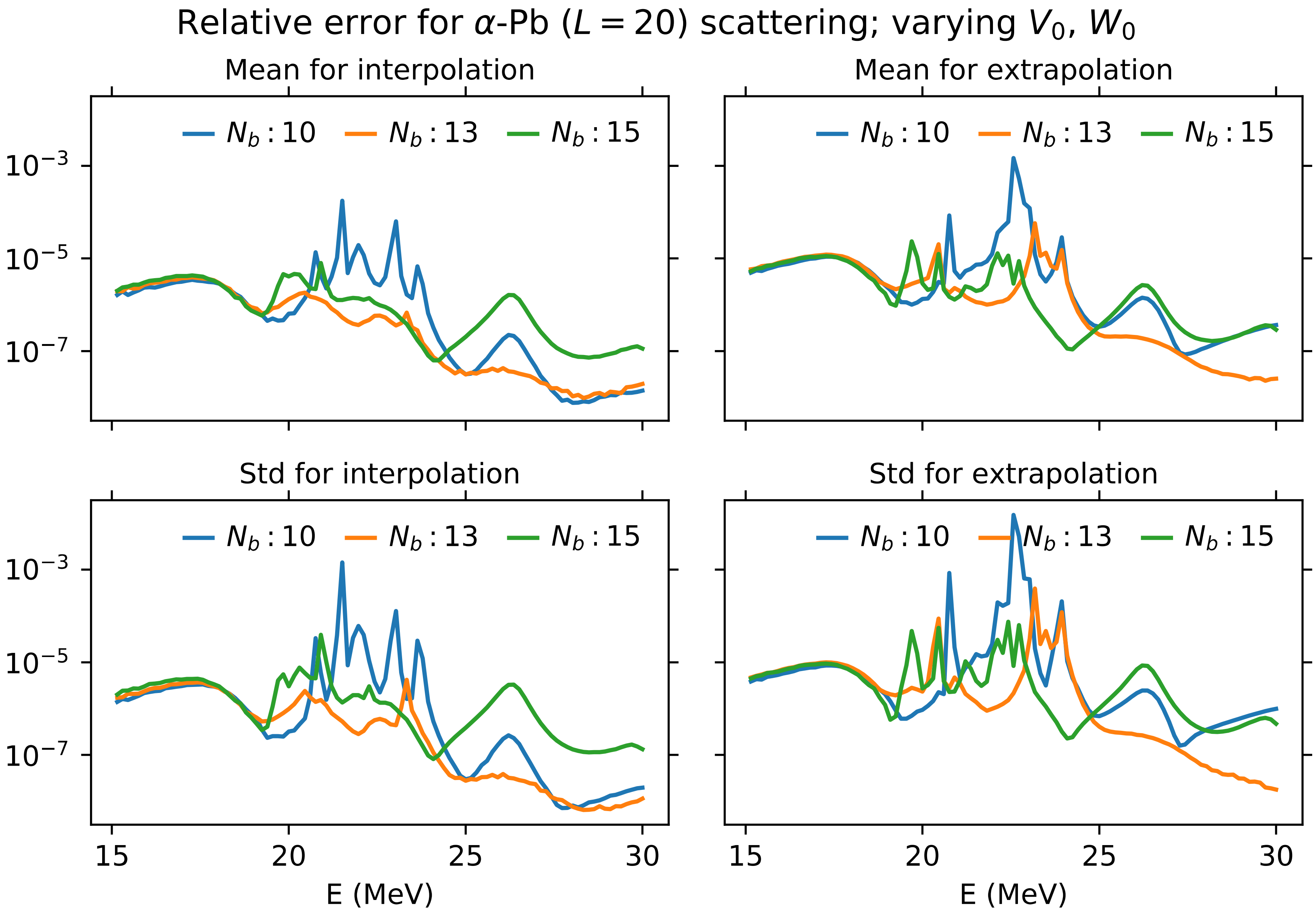

Alberto Garcia

R.J. Furnstahl, ajg et al., Phys. Lett. B **809**, 135719 (2020)

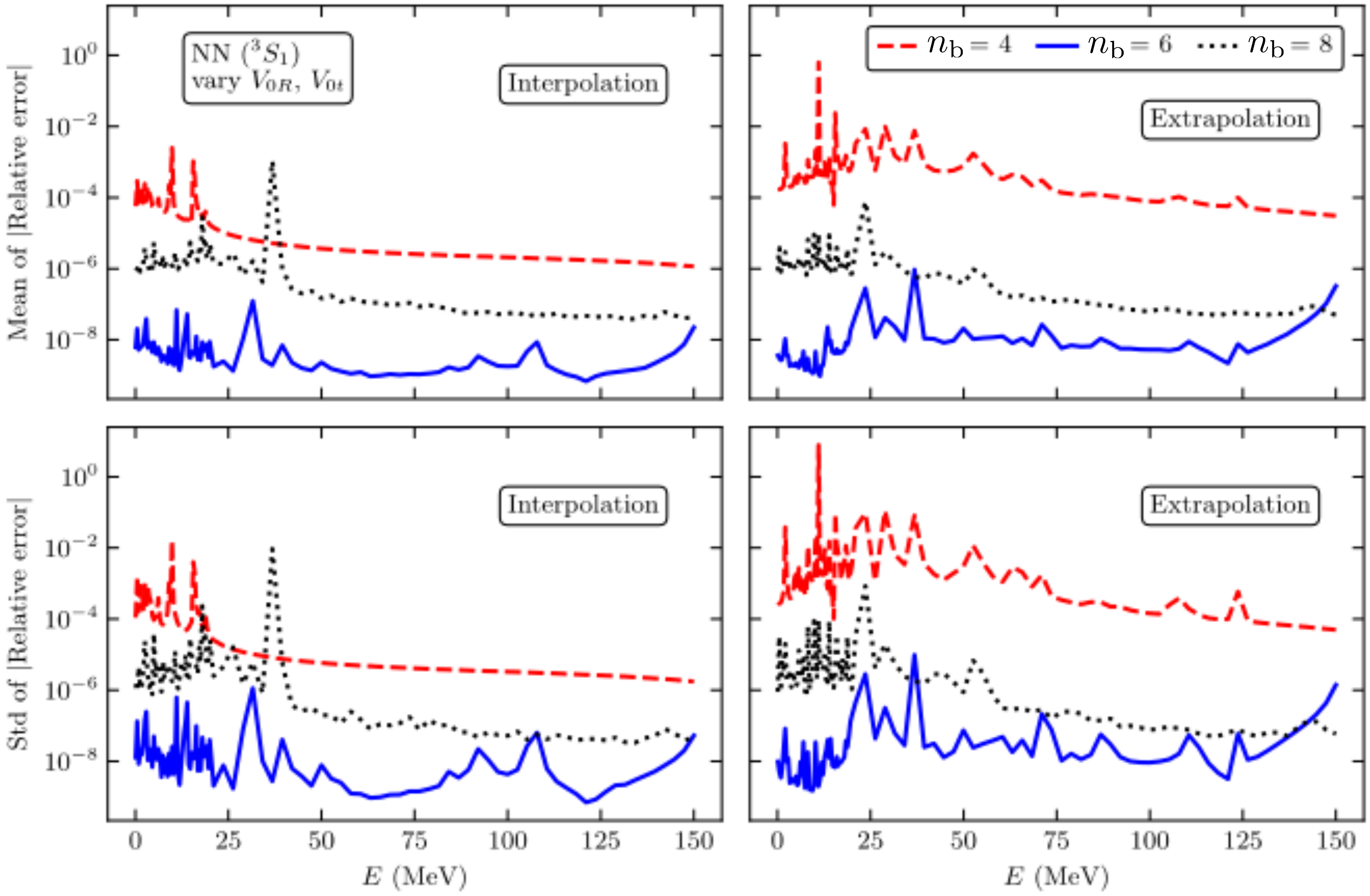

Alberto Garcia

R.J. Furnstahl, ajg et al., Phys. Lett. B **809**, 135719 (2020)

- Nonlocal potential
- Here:

  proton-alpha scattering in s-channel

- Emulate the K matrix

  $L_E^\ell \to K_E^\ell$

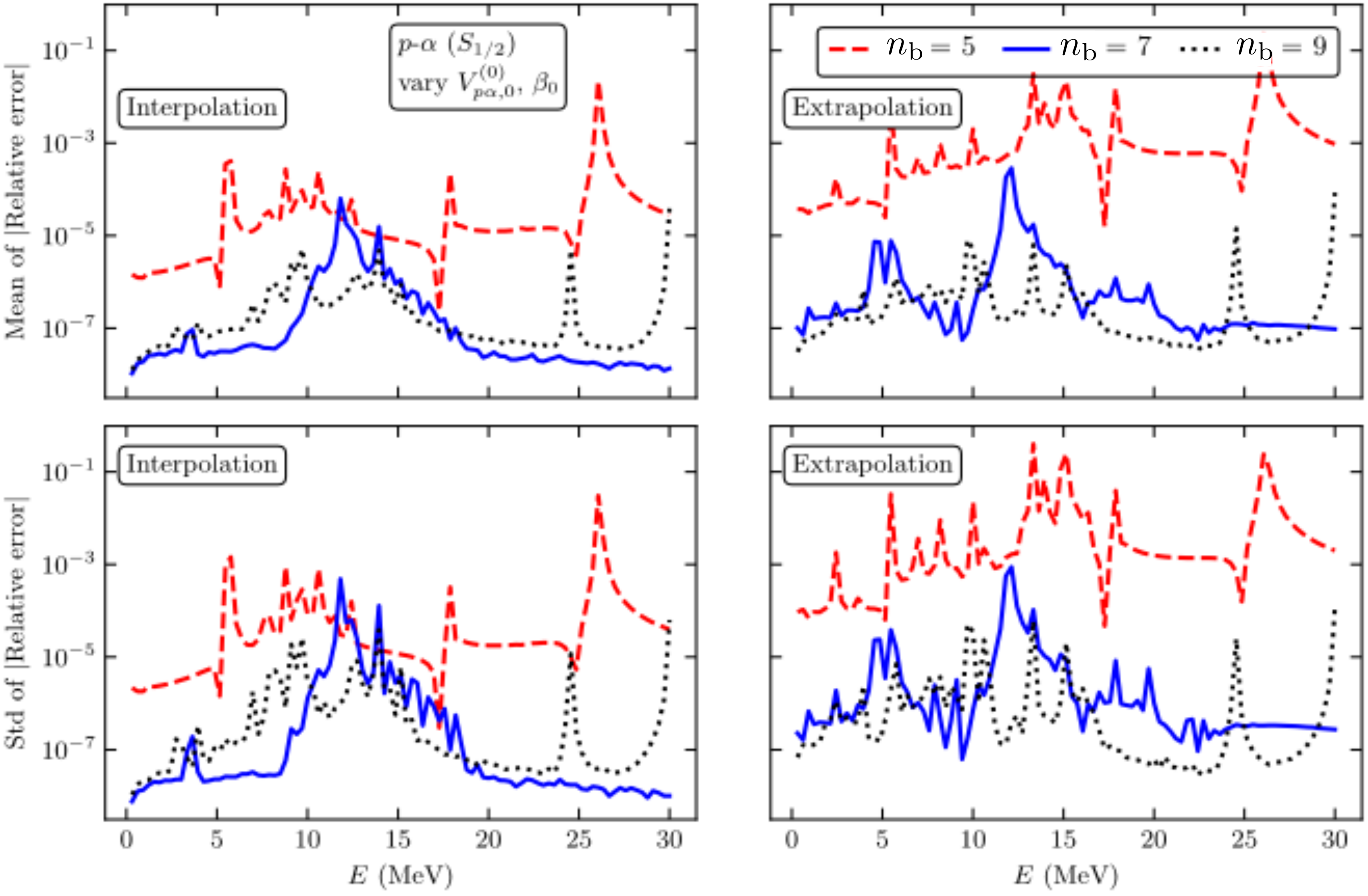

- Nonlocal potential
- Here: proton-alpha scattering in p-channel
- Emulate the K matrix

$$L_E^\ell \rightarrow K_E^\ell$$

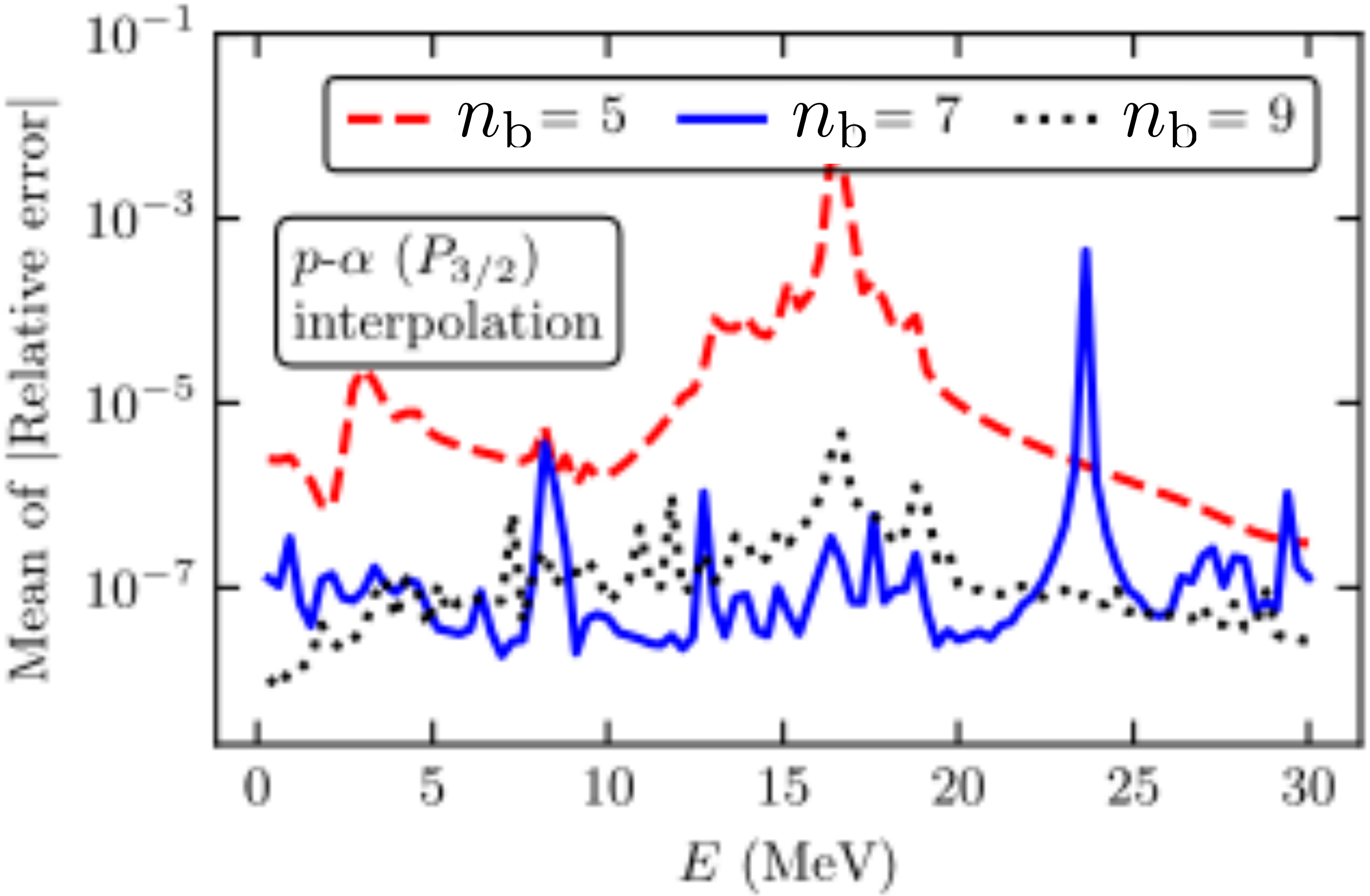

R.J. Furnstahl, ajg et al., Phys. Lett. B **809**, 135719 (2020)

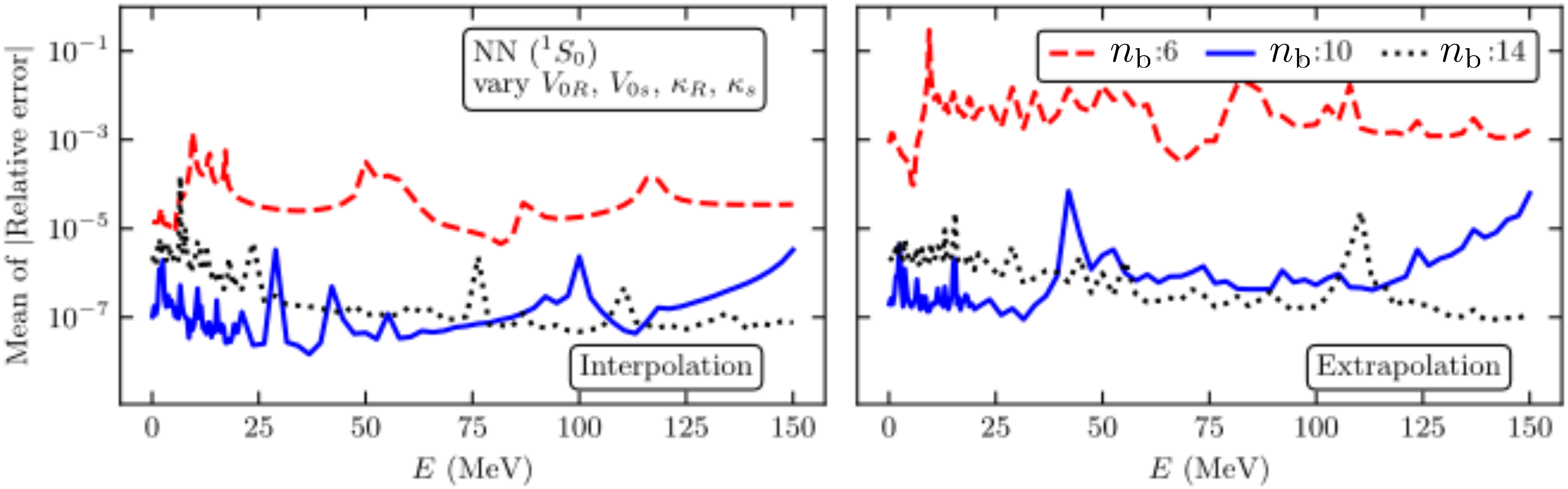

Alberto Garcia

KVP emulator in momentum space

*ajg et al., Phys. Rev. C **107**, 054001 (2023)*

Implementation:

Snapshots

$$|\widetilde{\psi}^s\rangle \equiv \sum_{i=1}^{n_\mathrm{b}} \beta_i |\psi_i^s\rangle$$

Basis weights

$$\Delta\widetilde{U}_{ij}^{ss'}(\boldsymbol{\theta}) = \frac{2\mu k_0}{\det \boldsymbol{u}} \left[\langle \psi_i^s | \widehat{V}(\boldsymbol{\theta}) - \widehat{V}_j | \psi_j^{s'}\rangle + (i \leftrightarrow j)\right]$$

$$\mathcal{L}^{ss'}[\vec{\beta}] = \beta_i L_{E,i}^{ss'} - \frac{1}{2}\beta_i \Delta\widetilde{U}_{ij}^{ss'} \beta_j$$

Momentum space:

For coordinate space implementation:
*R.J. Furnstahl, ajg et al., Phys. Lett. B **809**, 135719 (2020)*
*C. Drischler, ajg et al., Front. Phys. **10** 92931 (2023)*

$$\psi^{st}(k;k_0) = \frac{1}{k^2}\delta(k-k_0)\delta^{st} + \frac{2}{\pi}\mathbb{P}\frac{K^{st}(k,k_0)/k_0}{k^2-k_0^2}$$

$$\Delta\widetilde{U}_{ij}^{ss'}(\boldsymbol{\theta}) = \int_0^\infty\int_0^\infty dk\, dp\, k^2 p^2 \left[\psi_i^{ts}(k) V_{\boldsymbol{\theta},j}^{tt'}(k,p)\psi_j^{t's'}(p) + (i \leftrightarrow j)\right],$$

$$V_{\boldsymbol{\theta},j}^{tt'}(k,p) \equiv \frac{2\mu k_0}{\det \boldsymbol{u}}\left[V^{tt'}(k,p;\boldsymbol{\theta}) - V_j^{tt'}(k,p)\right]$$

Alberto Garcia

Chiral EFT potentials for NN scattering

P. Reinert et al., Eur. Phys. J B **54**, 86 (2018)

- Here: semi-local momentum-space regularized potential
- Affine dependence on the low-energy couplings (LECs):

$$V(\boldsymbol{\theta}) = V^0 + \boxed{\boldsymbol{\theta}} \cdot \boldsymbol{V}^1$$
$$\Delta\widetilde{U}(\boldsymbol{\theta}) = \Delta\widetilde{U}^0 + \boxed{\boldsymbol{\theta}} \cdot \boldsymbol{\Delta\widetilde{U}}^1$$

→ only calculate matrix elements once!

- Emulate neutron-proton (np) observables at multiple cutoffs

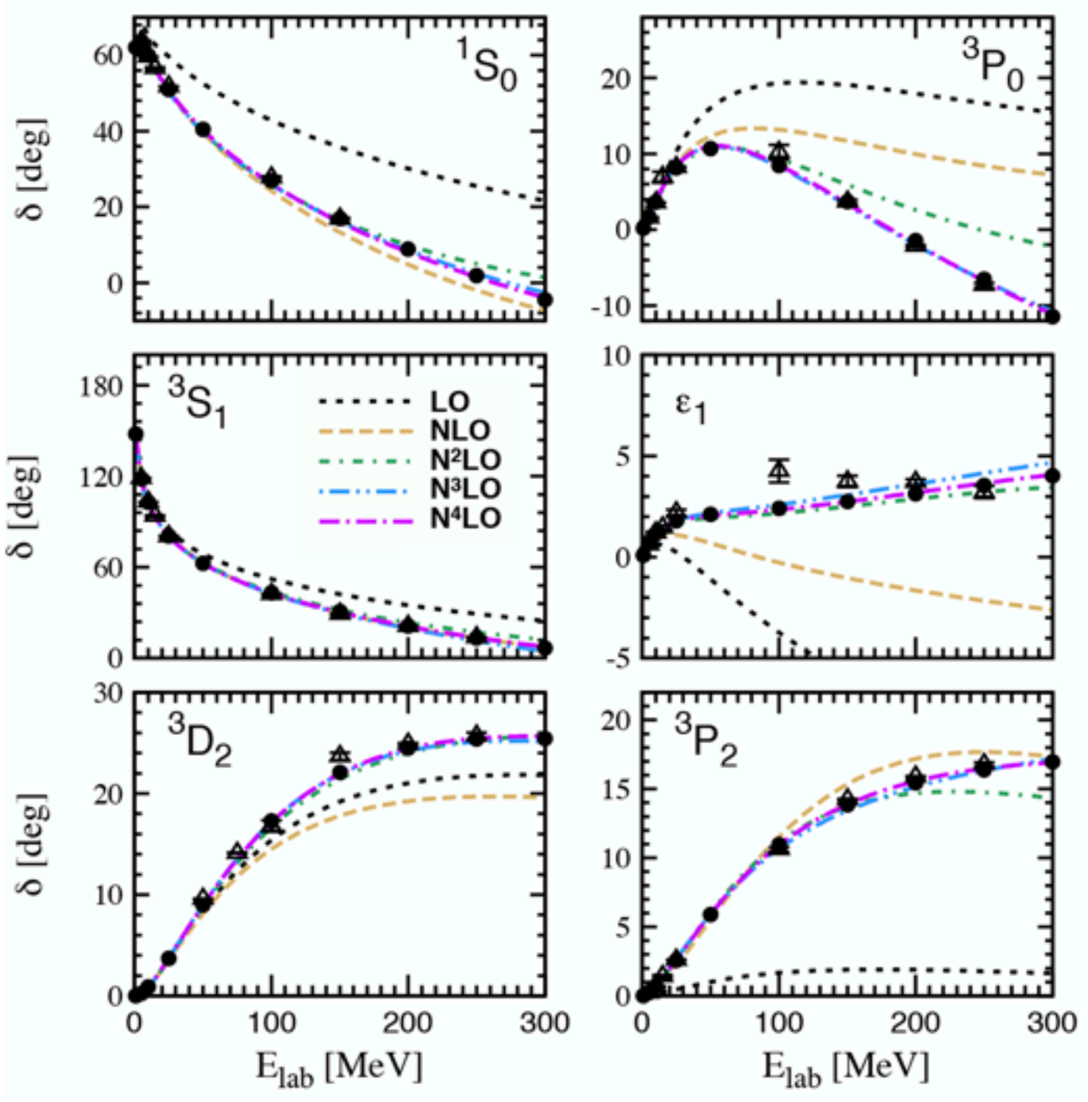

Alberto Garcia

Results for 1S0 channel

*ajg et al., Phys. Rev. C **107**, 054001 (2023)*

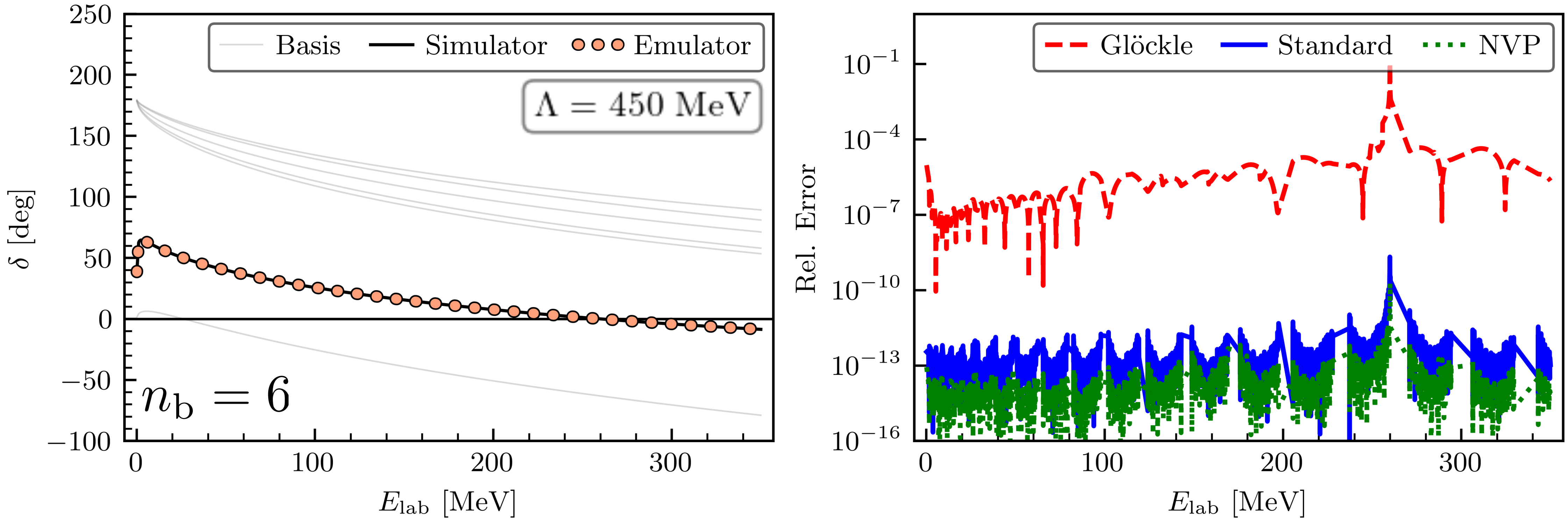

- Three parameters → $n_\mathrm{b} = 6$
- Parameters sampled using Latin-hypercube sampling (LHS)
- Glöckle spline interpolation:

$$\sum_k f(k) S_k(k_0) \to f(k_0)$$

Emulation of coupled channels

- Depends on the Petrov-Galerkin formalism

ajg et al., Phys. Rev. C ***107****, 054001 (2023)*

$$\Delta\widetilde{U} = \begin{pmatrix} \Delta\widetilde{U}^{00} & \Delta\widetilde{U}^{01} \\ \Delta\widetilde{U}^{10} & \Delta\widetilde{U}^{11} \end{pmatrix} \qquad \Delta\widetilde{U}_{ij}^{ss'} = \int_0^\infty \int_0^\infty dk\, dp\, k^2 p^2 \left[\Delta u_{ij}^{ss'} + (i \leftrightarrow j)\right]$$

$$\begin{aligned}
\Delta u_{ij}^{00} &= \psi_i^{00}(V_{\boldsymbol{\theta},j}^{00}\psi_j^{00} + V_{\boldsymbol{\theta},j}^{01}\psi_j^{10}) + \psi_i^{10}(V_{\boldsymbol{\theta},j}^{10}\psi_j^{00} + V_{\boldsymbol{\theta},j}^{11}\psi_j^{10}) \\
\Delta u_{ij}^{01} &= \psi_i^{00}(V_{\boldsymbol{\theta},j}^{00}\psi_j^{01} + V_{\boldsymbol{\theta},j}^{01}\psi_j^{11}) + \psi_i^{10}(V_{\boldsymbol{\theta},j}^{10}\psi_j^{01} + V_{\boldsymbol{\theta},j}^{11}\psi_j^{11}) \\
\Delta u_{ij}^{10} &= \psi_i^{01}(V_{\boldsymbol{\theta},j}^{00}\psi_j^{00} + V_{\boldsymbol{\theta},j}^{01}\psi_j^{10}) + \psi_i^{11}(V_{\boldsymbol{\theta},j}^{10}\psi_j^{00} + V_{\boldsymbol{\theta},j}^{11}\psi_j^{10}) \\
\Delta u_{ij}^{11} &= \psi_i^{01}(V_{\boldsymbol{\theta},j}^{00}\psi_j^{01} + V_{\boldsymbol{\theta},j}^{01}\psi_j^{11}) + \psi_i^{11}(V_{\boldsymbol{\theta},j}^{10}\psi_j^{01} + V_{\boldsymbol{\theta},j}^{11}\psi_j^{11})
\end{aligned}$$

Results for coupled channels

ajg et al., Phys. Rev. C ***107****, 054001 (2023)*

- Six non-redundant LECs → $n_\mathrm{b} = 12$
- Parameters sampled using Latin-hypercube sampling (LHS) $\boldsymbol{\theta}_i \in [-5, 5]$
- Glöckle spline interpolation:

$$\sum_k f(k) S_k(k_0) \rightarrow f(k_0)$$

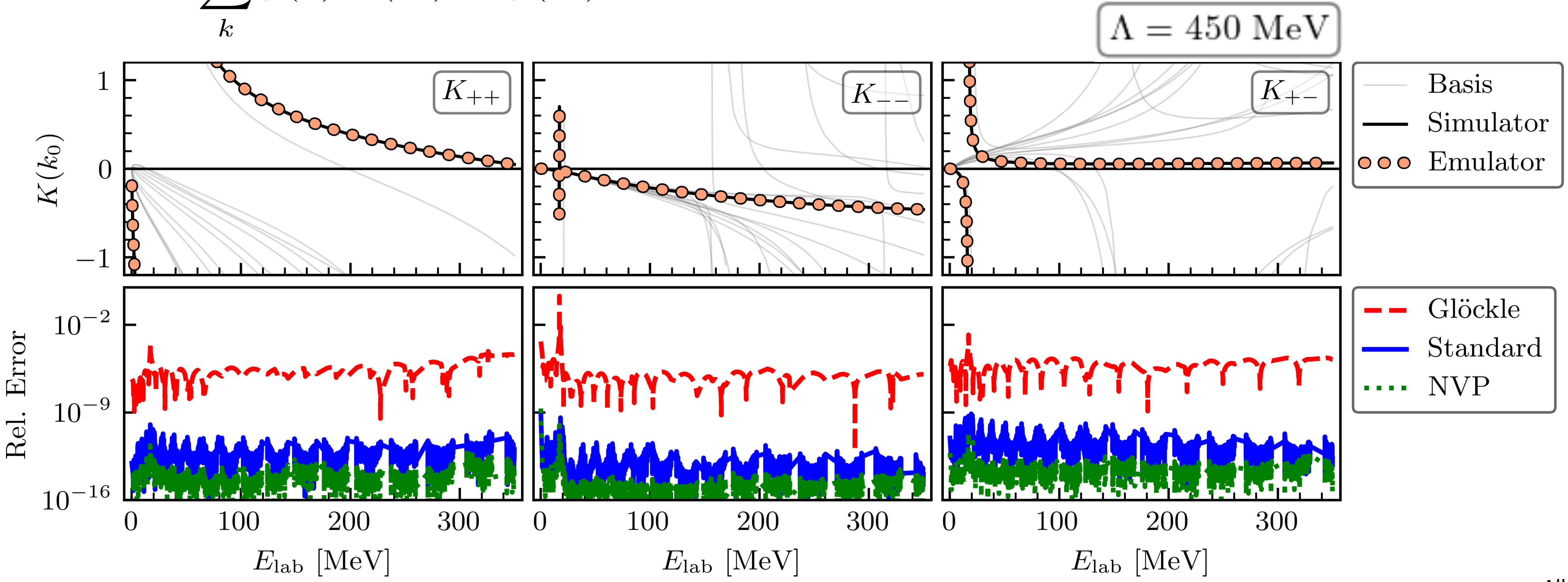

Alberto Garcia

Total cross section emulation

*ajg et al., Phys. Rev. C **107**, 054001 (2023)*

- Partial waves up to $j = 20$
- Used LHS to sample 500 parameter sets in an interval of [-5, 5]

- Errors negligible compared to other uncertainties
- Speed is highly implementation-dependent!
- Consistent for $\Lambda = 400 - 550\,\mathrm{MeV}$

- Different cutoff!

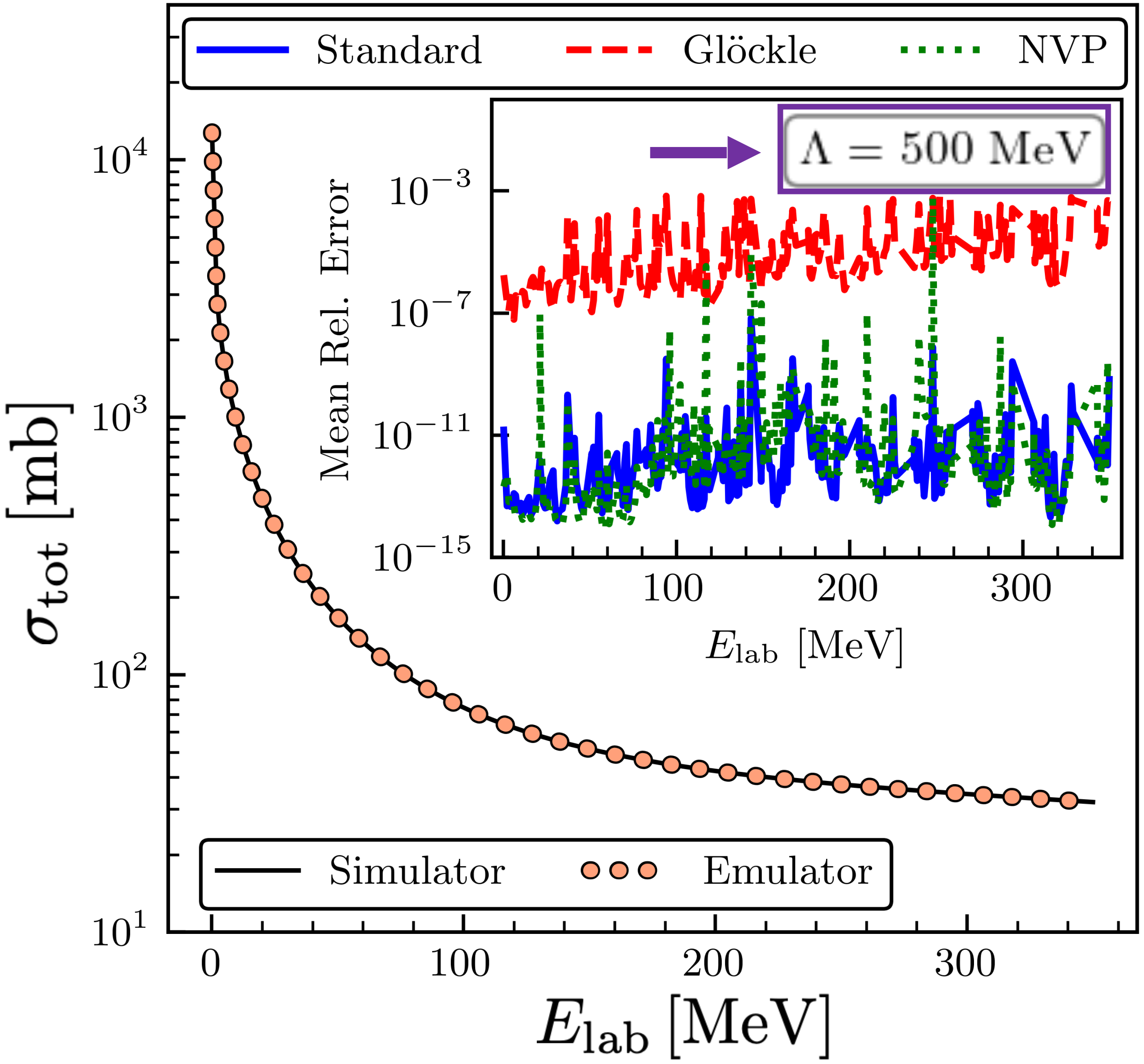

Alberto Garcia

Total cross section emulation w/ anomalies

- Partial waves up to $j = 20$
- Used LHS to sample 500 parameter sets in an interval of [-5, 5]
- Glöckle spline interpolation:

$$\sum_k f(k) S_k(k_0) \to f(k_0)$$

- Errors negligible compared to other uncertainties
- Speed is highly implementation-dependent!
- Consistent for $\Lambda = 400 - 550\,\mathrm{MeV}$

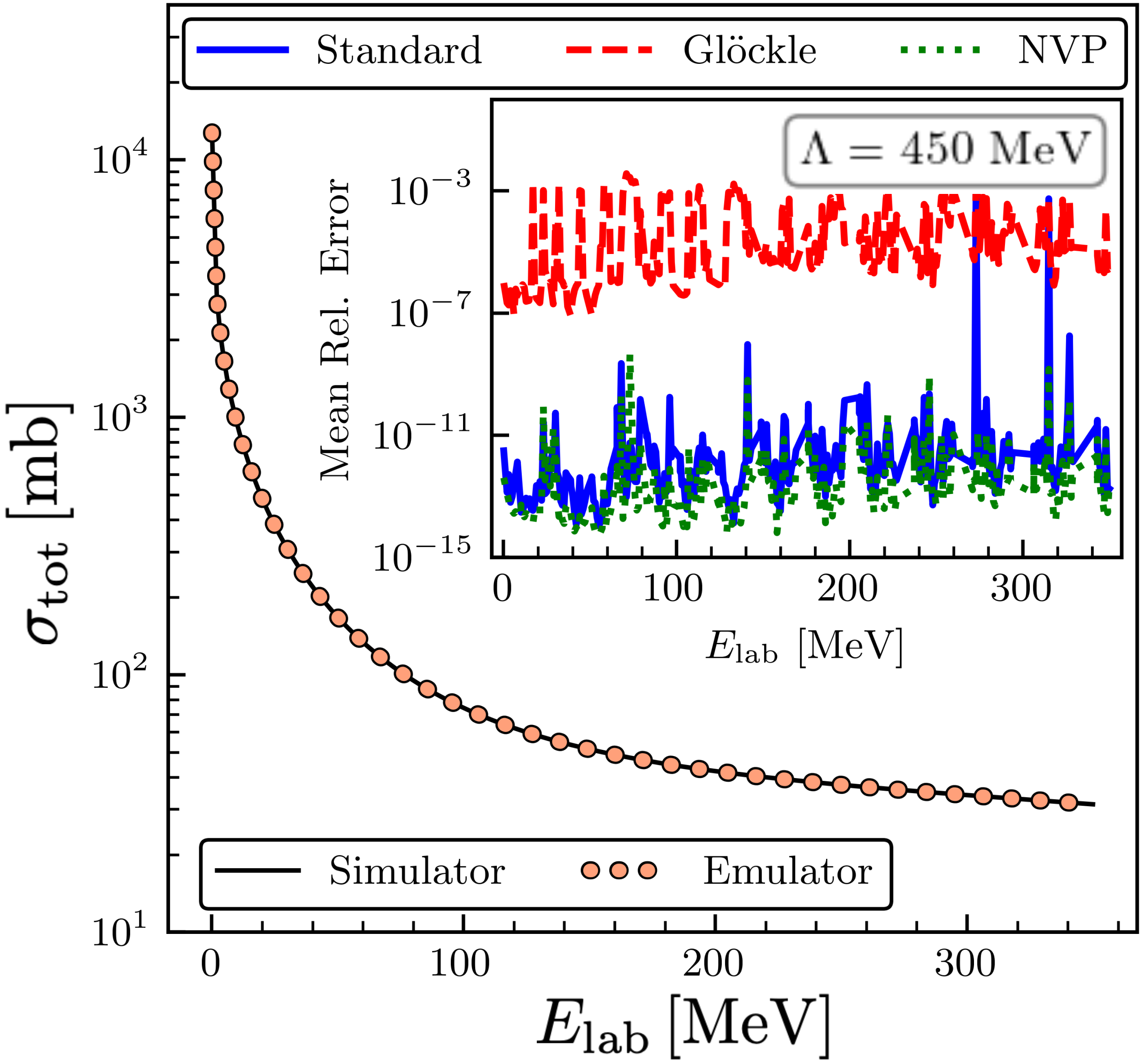

*ajg et al., Phys. Rev. C **107**, 054001 (2023)*

Table of spin observables emulation

Basis size	E [MeV]	$\mathrm{d}\sigma/\mathrm{d}\Omega$ Std.	$\mathrm{d}\sigma/\mathrm{d}\Omega$ Glöckle	D Std.	D Glöckle	A_y Std.	A_y Glöckle	A_{yy} Std.	A_{yy} Glöckle	A Std.	A Glöckle
$n_b = n_a$	5	-1.2	-1.2	-0.93	-0.93	-0.46	-0.46	-0.72	-0.72	-0.78	-0.78
	100	-0.73	-0.73	-0.47	-0.47	-0.12	-0.12	-0.20	-0.20	-0.28	-0.28
	200	-0.54	-0.64	-0.30	-0.30	-0.028	-0.028	-0.035	-0.035	-0.12	-0.12
	300	-0.49	-0.49	-0.24	-0.24	-0.066	-0.066	-0.037	-0.037	-0.043	-0.043
$n_b = 2n_a$	5	-10	-7.0	-8.8	-6.1	-8.8	-5.6	-8.5	-5.8	-8.3	-5.9
	100	-12	-6.3	-11	-5.1	-10	-4.9	-10	-4.9	-11	-5.3
	200	-10	-4.0	-8.8	-3.2	-7.8	-2.7	-8.4	-2.9	-8.0	-3.0
	300	-12	-4.9	-11	-4.0	-11	-3.9	-9.9	-3.8	-11	-3.9
$n_b = 4n_a$	5	-10	-7.3	-8.8	-6.4	-8.8	-6.1	-8.5	-6.4	-8.3	-6.1
	100	-13	-6.5	-12	-5.3	-11	-5.1	-11	-5.0	-11	-5.4
	200	-10	-4.4	-9.3	-3.6	-8.5	-3.0	-8.8	-3.3	-8.8	-3.3
	300	-12	-5.1	-11	-4.0	-10	-4.1	-10	-3.8	-11	-4.0

$\Lambda = 450\ \mathrm{MeV}$

- Angle-averaged relative errors (base-10 logarithm)
- Different basis size
- Consistent for $\Lambda = 400 - 550\,\mathrm{MeV}$

ajg et al., Phys. Rev. C ***107****, 054001 (2023)*

Neural networks

- Different types of networks:
  - Supervised learning
    - Desired output already known
  - Unsupervised learning
    - Desired output unknown

- Key to neural networks
  - Layers transform the inputs using a series of mathematical operations
  - Learns how to map the inputs to the outputs

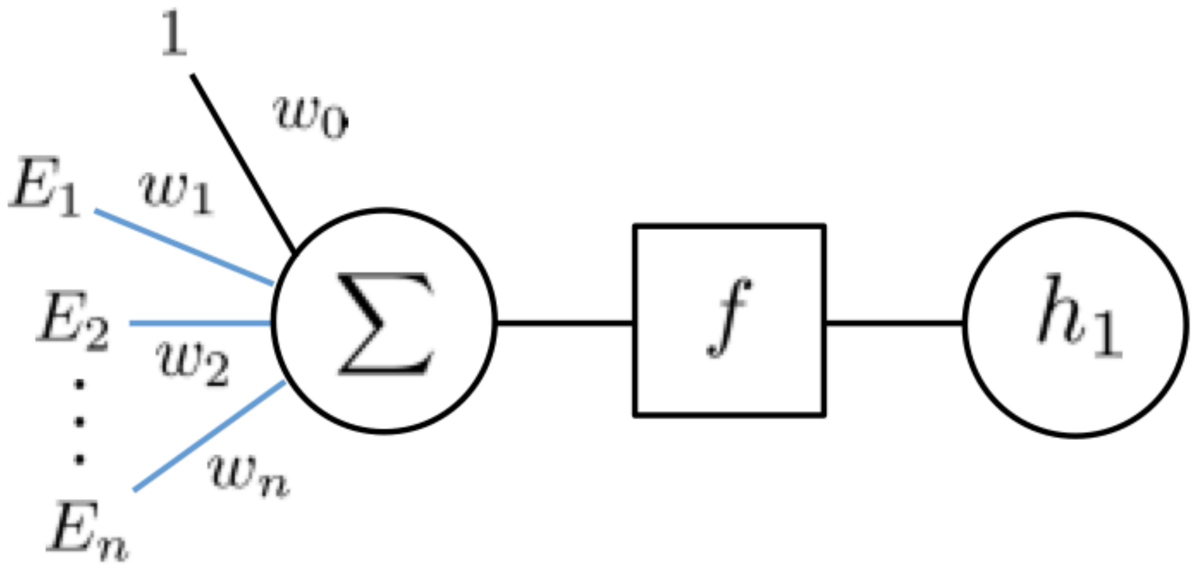

How do neural networks work

- Input data is split into train, validation, and test sets
- Further split into training and target inputs
- Hidden layers are responsible for learning the patterns found in the data set
- Output gives us what the network thinks the target inputs are given the data set
- Determine how close the prediction is by calculating the loss function
- If condition is not met, the weights are fine-tuned in backpropagation

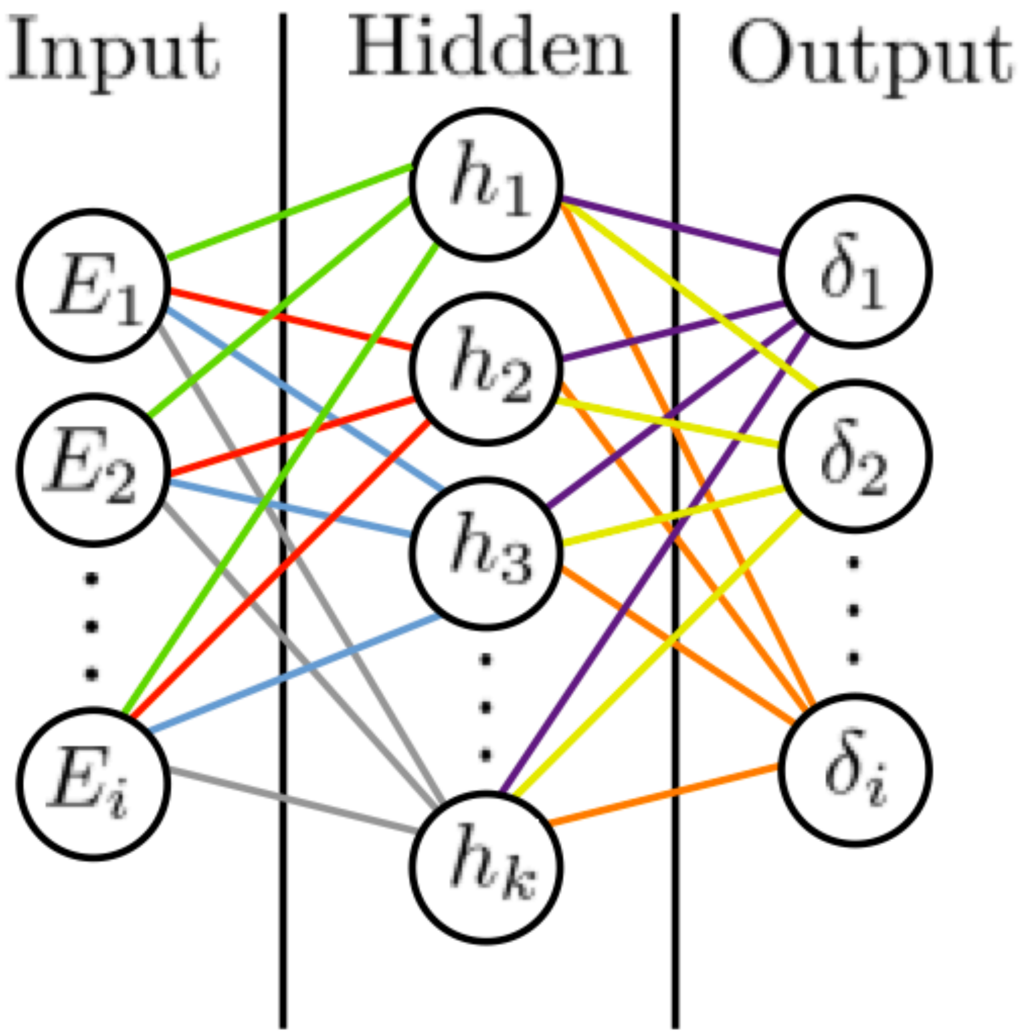

Alberto Garcia

Basics of training

$$\vec{x} = (1, x_1, x_2, ..., x_n)$$
$$\hat{\vec{y}} = (\hat{y}_1, \hat{y}_2, ..., \hat{y}_n)$$

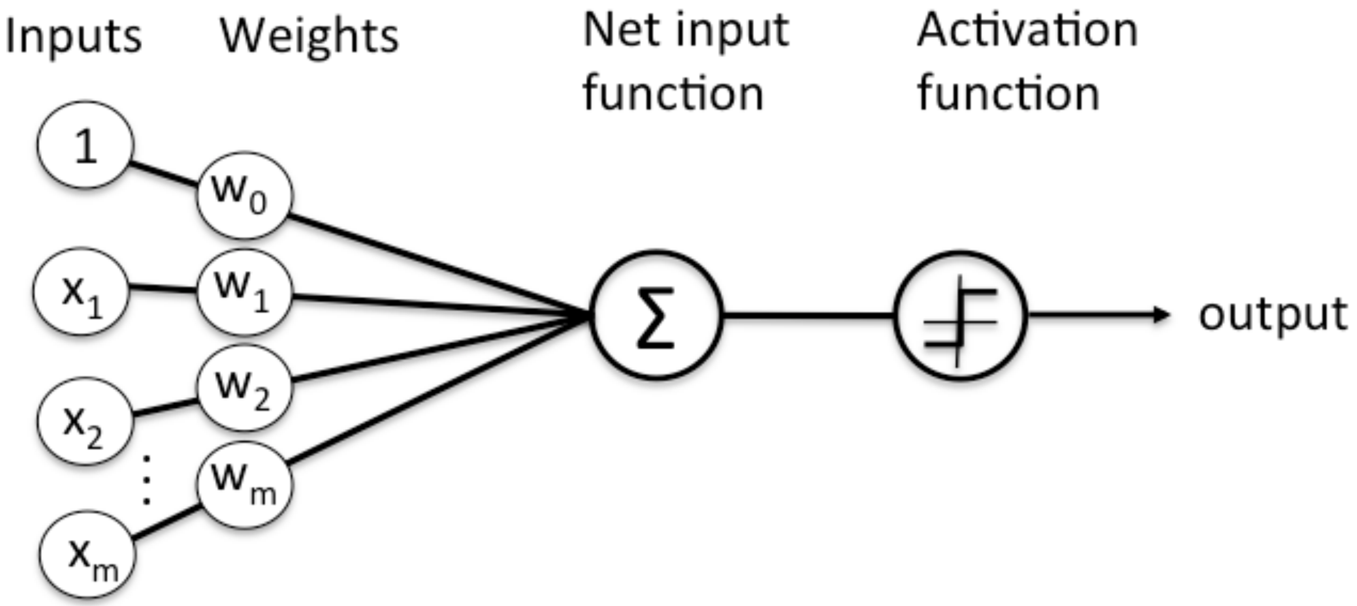

1) $$w_0 + \vec{w} \cdot \vec{x} = w_0 + w_1 x_1 + w_2 x_2 + ... + w_n x_n$$

2) $$y = f(w_0 + \vec{w} \cdot \vec{x})$$

3) $$\mathrm{L}(\hat{y}, y)$$

Alberto Garcia

Training process

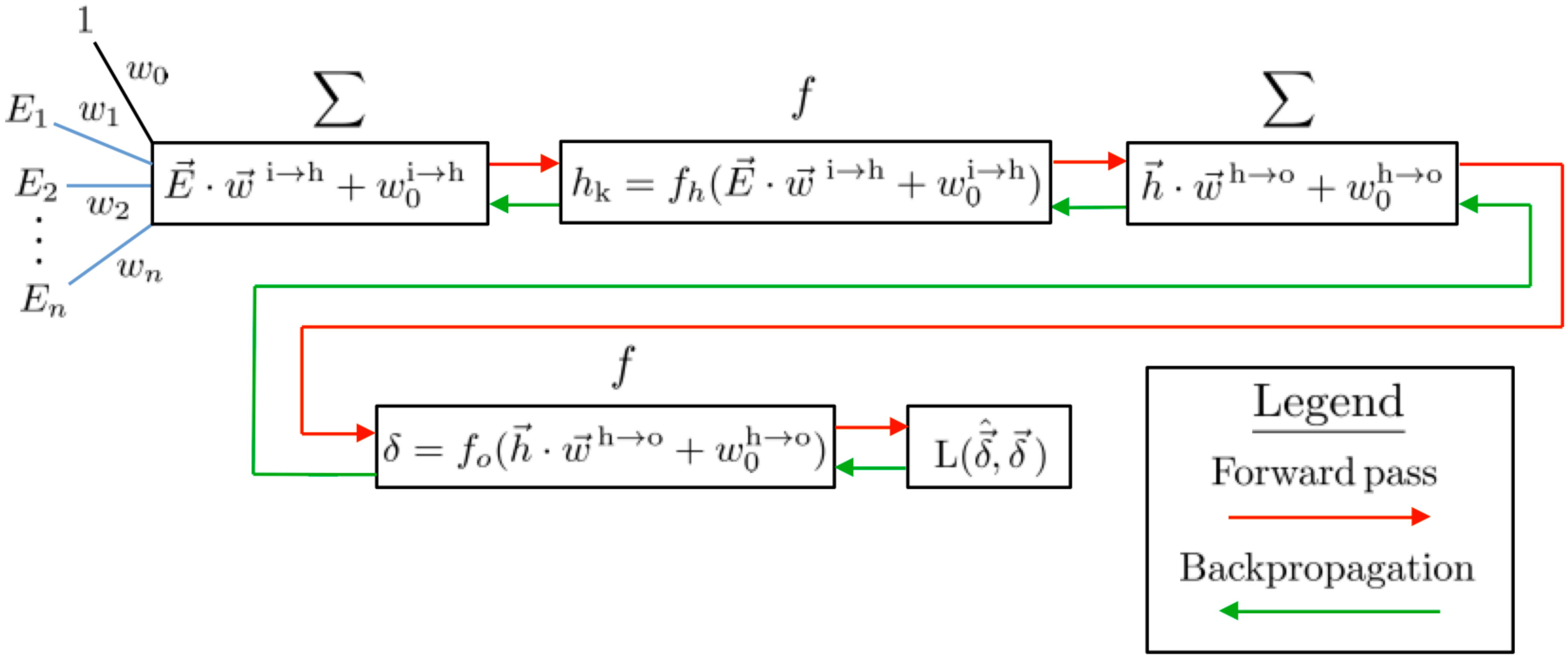

Alberto Garcia

Different components: initializer

- Used to initialize the weights
- Randomly sample weights from some distribution
- Most common method is Glorot Uniform
- Glorot initialization maintains the same smooth distribution throughout the training process due to normalization

Activation functions

- Used to initialize the weights
- Randomly sample weights from some distribution
- Glorot initialization maintains the same smooth distribution throughout training process due to normalization

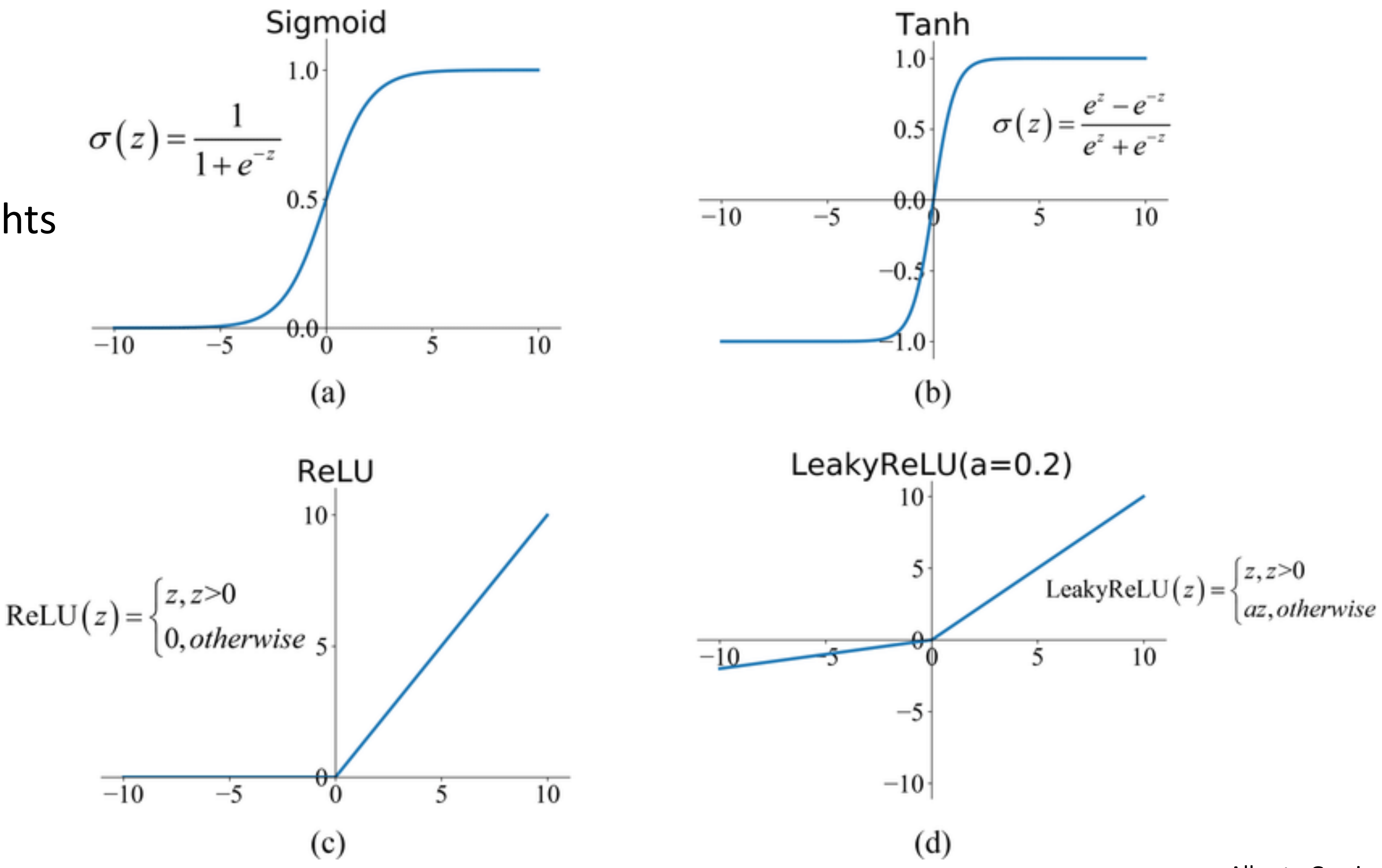

Alberto Garcia

Different components: activation function

- ReLU pros:
  - Prevents vanishing gradients since derivative is 0 or 1
  - Computationally more efficient
  - Better convergence performance

- ReLU cons:
  - Outputs are unconstrained and can cause issues
  - Dying ReLU problem: too many activations are below zero which can limit learning
  - Can be prevented using leaky ReLU

Different components: loss function

- Used to calculate the error between prediction and target

- Here: mean-square-error (MSE)

$$L_{\text{MSE}} = \sum_{i=1}^{N} \frac{(\hat{y}_i - y_i)^2}{N},$$

- Plane: predictions
- Red dots: target inputs
- Goal is to minimize distance between the red dots and plane

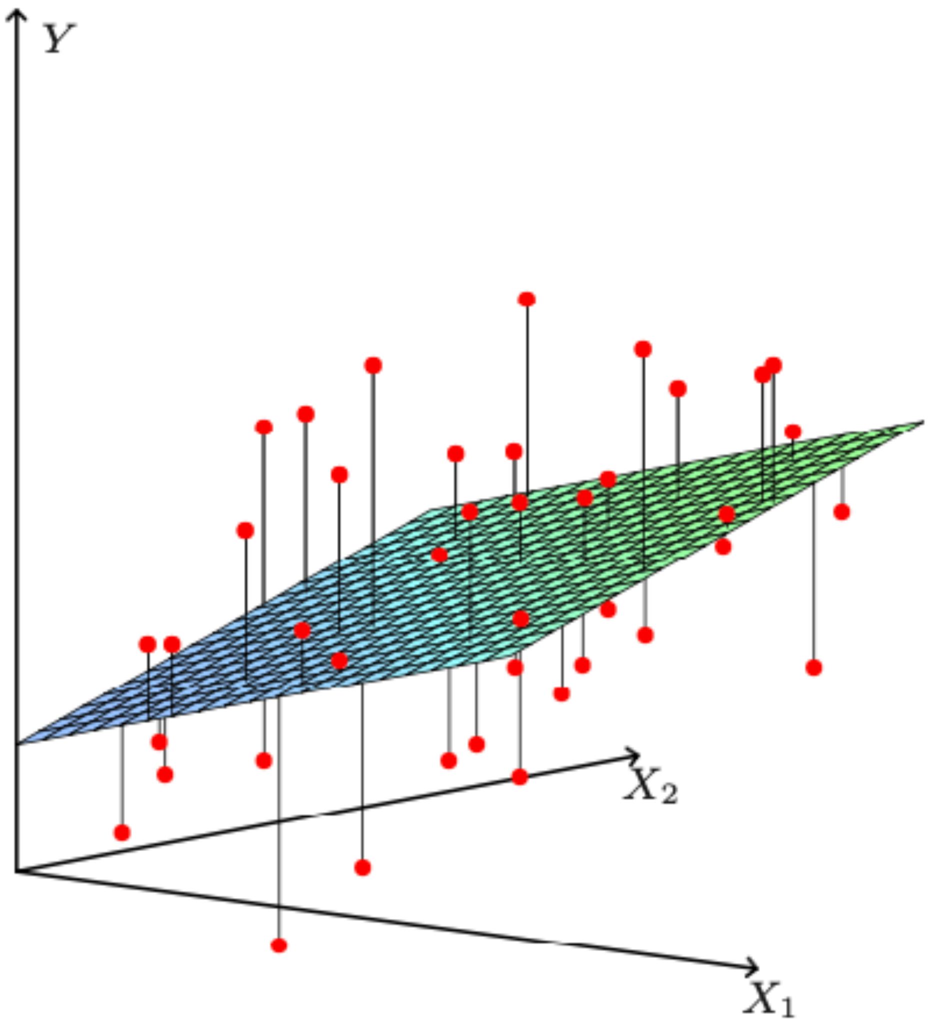

Different components: optimizer

- Algorithm used to minimize the loss
- Learning rate is used to scale gradients
  - Prevents weights from changing too fast

- Common optimizers:
  - Stochastic gradient descent (SGD)
  - ADAM

- SGD: adjusts all parameters with same learning rate
  - Slower convergence, but can perform better on unseen data
- ADAM: each parameter has own learning rate
  - May converge too rapidly and fall into non-ideal minimum

Backpropagation

- Weights get adjusted by an optimization algorithm in such a way as to minimize the loss

- Derivative of the loss function with respect to every weight in the current layer is calculated, multiplied by the learning rate, and subtracted from the corresponding weights

- New weights are passed to the next layer

- Process continues until all the weights in the network are adjusted

- Network undergoes a forward pass and recalculates a training and validation loss

- Process is repeated until a desired accuracy has been reached or until the model is trained as many times as the user chooses